

Journal of

ELECTROANALYTICAL CHEMISTRY

*International Journal Dealing with all Aspects
of Electroanalytical Chemistry,
Including Fundamental Electrochemistry*

EDITORIAL BOARD:

- J. O'M. BOCKRIS (Philadelphia, Pa.)
B. BREYER (Sydney)
G. CHARLOT (Paris)
B. E. CONWAY (Ottawa)
P. DELAHAY (Baton Rouge, La.)
A. N. FRUMKIN (Moscow)
L. GIERST (Brussels)
M. ISHIBASHI (Kyoto)
W. KEMULA (Warsaw)
H. L. KIES (Delft)
J. J. LINGANE (Cambridge, Mass.)
G. W. C. MILNER (Harwell)
J. E. PAGE (London)
R. PARSONS (Bristol)
C. N. REILLEY (Chapel Hill, N.C.)
G. SEMERANO (Padua)
M. VON STACKELBERG (Bonn)
I. TACHI (Kyoto)
P. ZUMAN (Prague)

E L S E V I E R

GENERAL INFORMATION

See also Suggestions and Instructions to Authors which will be sent free, on request to the Publishers.

Types of contributions

- (a) Original research work not previously published in other periodicals.
- (b) Reviews on recent developments in various fields.
- (c) Short communications.
- (d) Bibliographical notes and book reviews.

Languages

Papers will be published in English, French or German.

Submission of papers

Papers should be sent to one of the following Editors:

Professor J. O'M. BOCKRIS, John Harrison Laboratory of Chemistry,
University of Pennsylvania, Philadelphia 4, Pa., U.S.A.

Dr. R. PARSONS, Department of Chemistry,
The University, Bristol 8, England.

Professor C. N. REILLEY, Department of Chemistry,
University of North Carolina, Chapel Hill, N.C., U.S.A.

Authors should preferably submit two copies in double-spaced typing on pages of uniform size. Legends for figures should be typed on a separate page. The figures should be in a form suitable for reproduction, drawn in Indian ink on drawing paper or tracing paper, with lettering etc. in thin pencil. The sheets of drawing or tracing paper should preferably be of the same dimensions as those on which the article is typed. Photographs should be submitted as clear black and white prints on glossy paper.

All references should be given at the end of the paper. They should be numbered and the numbers should appear in the text at the appropriate places.

A summary of 50 to 200 words should be included.

Reprints

Twenty-five reprints will be supplied free of charge. Additional reprints can be ordered at quoted prices. They must be ordered on order forms which are sent together with the proofs.

Publication

The *Journal of Electroanalytical Chemistry* appears monthly and has six issues per volume and two volumes per year, each of approx. 500 pages.

Subscription price (post free): £ 10.15.0 or \$ 30.00 or Dfl. 108.00 per year; £ 5.7.6 or \$ 15.00 or Dfl. 54.00 per volume.

Additional cost for copies by air mail available on request.

For advertising rates apply to the publishers:

Subscriptions

Subscriptions should be sent to:

ELSEVIER PUBLISHING COMPANY, P.O. Box 211, Amsterdam, The Netherlands.

SUMMARIES OF PAPERS PUBLISHED IN
JOURNAL OF ELECTROANALYTICAL CHEMISTRY

Vol. 7, No. 5, May 1964

EFFECTS OF WORKING-ELECTRODE POTENTIAL ON THE
RATES AND EXTENTS OF CONTROLLED-POTENTIAL
ELECTROLYSES

The effects of working-electrode potential on the rate of a controlled-potential electrolysis and on the quantity of electricity that eventually accumulates are discussed. In particular, it is proven that electrolysis at any potential where an appreciable current flows on a totally irreversible wave must proceed to virtual completion, and experimental confirmation of this prediction is given for the reduction of hydrogen ion on mercury electrodes.

L. MEITES,

J. Electroanal. Chem., 7 (1964) 337-342.

THE ADSORPTION OF HYDROXYL IONS AT THE
MERCURY-SOLUTION INTERFACE AND THE ANODIC
DOUBLE-LAYER CAPACITY IN FLUORIDE SOLUTIONS

The specific adsorption of hydroxyl ions on a mercury electrode from aqueous solutions at 25° has been investigated by measuring the capacity of the electrical double layer as a function of concentration. The virtual absence of specifically adsorbed ions is demonstrated by comparison with the predictions of diffuse-layer theory. The nature of the rapid increase of capacity on positive polarisation is considered in the light of the measurements, and its relevance to the anodic capacity in fluoride solutions is discussed.

R. PAYNE,

J. Electroanal. Chem., 7 (1964) 343-358.

POLAROGRAPHY OF HYDROGEN PEROXIDE IN
LANTHANUM NITRATE SOLUTIONS

The reduction of hydrogen peroxide at the D.M.E. is catalyzed in lanthanum salt solutions. In 0.01 M $\text{La}(\text{NO}_3)_3$ it has been shown that a cathodic hydrogen peroxide current appears at +0.2 V vs. S.C.E., followed by a depression in the current which extends to the main hydrogen peroxide wave at -0.3 V. Experiments on suspensions of lanthanum hydroxide in lanthanum nitrate-hydrogen peroxide solutions have shown that the reduction current at potentials more oxidizing than -0.3 V increased upon contact with the solid, while the height of the normal wave decreased. Filtration of these mixtures and tests with potassium permanganate and nitric acid on the filtrate indicated that the species responsible for the reduction current was soluble, oxidizable, and unstable to acid. Mercury in contact with the lanthanum nitrate-hydrogen peroxide test solution led to the more rapid production of this species along with the evolution of oxygen. A soluble complex between lanthanum ion and hydrogen peroxide, formed under mildly alkaline conditions, is postulated as the species being reduced. The suppression of the catalytic current in the potential range +0.1 to -0.2 V is interpreted as the result of adsorption of insoluble lanthanum hydroxide or polymeric lanthanum hydroxy-complexes on the D.M.E. Current-time curves consistent with this explanation have been obtained.

M. T. HENNE AND J. W. COLLAT, *

J. Electroanal. Chem., 7 (1964) 359-367.

GENERAL PROPERTIES OF CHRONOPOTENTIOMETRIC METHODS IN CYLINDRICAL AND SPHERICAL DIFFUSION

General mathematical relations are given for theoretical chronopotentiometric transition times on spherical or cylindrical electrodes in the case of diffusion-controlled systems.

In this way, it is possible to obtain current density values which have to be imposed at these electrodes in order to compensate fully or partly the different terms expressing the non-linear character of the diffusion field.

H. D. HURWITZ,

J. Electroanal. Chem., 7 (1964) 368-381.

MEASUREMENT OF HYDROGEN ADSORPTION BY THE MULTIPULSE POTENTIODYNAMIC (MPP) METHOD

By means of the MPP method, it is possible to study hydrogen adsorption on an extremely reproducible platinum surface under well-defined conditions of mass-transport. Non-repetitive linear potential-time sweeps of speeds up to 2000 V/sec result in readily-interpretable current-time traces. The addition of chloride ion to the solution is shown quantitatively not to affect the amount of hydrogen deposited at 0.0 or 0.06 V.

S. GILMAN,

J. Electroanal. Chem., 7 (1964) 382-391.

COMPARISON OF ALTERNATING VOLTAGE POLAROGRAPHY WITH ALTERNATING CURRENT POLAROGRAPHY

It has been shown that the a.v. polarograph provides much better calibration curves than does the a.c. polarograph. The concentration range amenable to analysis is greatly extended, and useful results are obtainable at higher frequencies. The convenience and rapidity of a.v. polarography are the same as with the simplest type of a.c. polarograph.

The circuit arrangement in a.v. polarography is not particularly critical. While for absolute precision, various parts of the circuit need to have impedances so high that the cell impedance is by comparison negligible, the results are not greatly affected if this condition is not rigorously met. By contrast, the impedance of the measuring circuit in a.c. polarography is a critical matter — for instance, it is necessary to use as small a voltage-dropping resistance as possible, and even a decrease from 100 to 10 Ω in this value improves the performance considerably; this makes necessary higher amplification, and it is one illustration of the advantage of a.v. polarography that no amplification at all is required when using readily available vacuum-tube millivoltmeters.

Comparison of the results with theory demonstrated that the a.v. polarograph gives information that can be quantitatively interpreted in terms of the electrode processes occurring. In a.c. polarography, this can be done only with a more elaborate arrangement in which the cell voltage is continuously monitored, making the investigation considerably more time-consuming and laborious.

H. H. BAUER AND D. C. S. FOO,

J. Electroanal. Chem., 7 (1964) 392-397.

AN AUTOMATIC AMPEROMETRIC METHOD FOR THE
SPECIFIC ENZYMATIC DETERMINATION OF GALACTOSE

An automatic enzymatic method is described for the determination of galactose. The method is based on the catalysis by galactose oxidase of the oxidation of galactose. Hydrogen peroxide produced by the enzymatic reaction rapidly oxidizes iodide to iodine in the presence of Mo(VI).

The formation of iodine is detected amperometrically. Automatic control equipment provides direct read-out of the time required for a definite amount of iodine to be produced. The reciprocal of the measured time interval when plotted against the galactose concentration provides a linear working curve.

Automatic results for samples show relative standard deviations of about 2% over a range of 50-500 p.p.m. galactose.

H. L. PARDUE AND C. S. FRINGS,

J. Electroanal. Chem., 7 (1964) 398-402.

KINETIC PARAMETERS FROM IRREVERSIBLE
POLAROGRAPHIC WAVES IN PRESENCE OF
MASS TRANSFER POLARIZATION

Modified forms of general rate equations applicable for quasi-reversible (partially irreversible) polarographic single waves (purely cathodic or anodic) have been derived. These equations have been applied to calculate the formal kinetic parameters, using experimental data for V^{3+} - V^{2+} reaction obtained by polarography. The application of the above equations to totally irreversible polarographic waves has also been shown using polarographic data for the Ni^{2+} - Ni reaction.

S. SATHYANARAYANA,

J. Electroanal. Chem., 7 (1964) 403-413.

REPORT.
GORDON RESEARCH CONFERENCE ON ELECTRO-
CHEMISTRY, SANTA BARBARA, CALIFORNIA

R. P. BUCK,

J. Electroanal. Chem., 7 (1964) 414-415.

EFFECTS OF WORKING-ELECTRODE POTENTIAL ON THE RATES AND EXTENTS OF CONTROLLED-POTENTIAL ELECTROLYSES

LOUIS MEITES

Department of Chemistry, Polytechnic Institute of Brooklyn, Brooklyn, N.Y. (U.S.A.)

(Received January 26th, 1964)

INTRODUCTION

There are gross disagreements among the results of those who have investigated the rates and extents of controlled-potential electrolyses at potentials not on the plateau of the wave of the substance involved in the half-reaction occurring at the working electrode. ROGERS AND MERRITT¹ studied the relation between the working-electrode potential and the fraction of cadmium or thallos ion that undergoes reversible reduction to the metal amalgam; their potentiocoulograms obeyed the predictions of the Nernst equation, but they found that times of the order of 8–9 h were required for the attainment of equilibrium. Both MOROS² and the writer³, however, found that equilibrium in the reduction of cadmium ion was reached in only about 40 min.

For totally irreversible processes (such as the reduction of trichloroacetate⁴) it has been stated⁵ that, although both the initial current and the rate at which it decays decrease as the potential moves from the plateau of the wave toward its foot, there is no effect of potential on the quantity of electricity ultimately consumed, so that the reduction is quantitative if it occurs at all. Of the large number of totally irreversible processes recently investigated by SANTHANAM⁶, however, not one obeyed this prediction; in nearly every case the measured quantity of electricity decreased as the potential of the working electrode moved farther away from the plateau.

In a number of methods recently devised⁷ for the chronocoulometric evaluation of the rate constants of chemical reactions occurring during controlled-potential electrolyses, the calculations involve one or more electrolytic rate constants. In the application of these methods as well as in the resolution of the above discrepancies, a knowledge of the theoretical effects of potential on the rate constants and ultimate extents of controlled-potential electrolyses is essential. Some important general equations relevant to these problems are derived and discussed below.

GENERAL EQUATIONS

We shall consider the half-reaction



where β_O^* and β_R^* are the first-order rate constants of the forward and backward processes, respectively, at the particular working-electrode potential employed. The

asterisks denote potential-dependent values; omission of the asterisk denotes the limiting value attained on the plateau of the wave of the substance specified by the subscript. The rate of consumption of O at any instant is given by

$$-\frac{dC_O}{dt} = \beta_O^* C_O - \beta_R^* C_R (V_R/V_O) \quad (2)$$

where each C denotes a concentration (most conveniently in mmoles/l) in the bulk of the phase containing the substance in question, the volume of that phase being denoted by V for the i 'th species (and being most conveniently given in l). The volume ratio in the second term on the right-hand side serves to relate the rate of depletion of R in the phase containing it to the corresponding rate of increase of the concentration of O in its own phase. Material conservation requires that

$$V_O C_O + V_R C_R = V_O C_O^\circ + V_R C_R^\circ = N \quad (3)$$

where the C° 's are the respective initial concentrations and N is the total number of millimoles of material present. Equations (2) and (3) would have to be modified by introducing a numerical coefficient if the stoichiometry of the reaction were different from that expressed by eqn. (1). Combining them gives

$$-\frac{dC_O}{dt} = -\frac{\beta_R^* N}{V_O} + (\beta_O^* + \beta_R^*) C_O \quad (4)$$

whence

$$C_O = C_O^\circ e^{-(\beta_O^* + \beta_R^*)t} + \frac{\beta_R^* N}{(\beta_O^* + \beta_R^*) V_O} [1 - e^{-(\beta_O^* + \beta_R^*)t}] \quad (5)$$

Meanwhile the current i (in mF/sec) is given by

$$i = -n V_O \frac{dC_O}{dt} = n V_R \frac{dC_R}{dt} \quad (6)$$

and eqns. (4)–(6) yield

$$i = n(\beta_O^* V_O C_O^\circ - \beta_R^* V_R C_R^\circ) e^{-(\beta_O^* + \beta_R^*)t} \quad (7)$$

If the solution initially contains only O (so that $N = V_O C_O^\circ$), this becomes

$$i = \beta_O^* n V_O C_O^\circ e^{-(\beta_O^* + \beta_R^*)t} = i^\circ e^{-(\beta_O^* + \beta_R^*)t} \quad (8)$$

but whether R is initially present or not it is apparent from eqn. (7) that

$$\frac{d(\ln i)}{dt} = -(\beta_O^* + \beta_R^*) \quad (9)$$

Equations (5) and (9) show that the quantity $(\beta_O^* + \beta_R^*)$ is the effective rate constant for the electrolytic process.

Another convenient description of the current may be obtained by combining eqns. (2) and (6) to yield

$$i = \beta_O^* n V_O C_O - \beta_R^* n V_R C_R \quad (10)$$

When O alone is present initially, Nernst diffusion-layer theory gives^{8,9}

$$i = n D_O A (C_O - C_{O,o}) / \delta_O \quad (11)$$

where δ_o is the hypothetical thickness of the diffusion layer, $C_{O,o}$ is the concentration of O at the electrode-solution interface, D_o is the diffusion coefficient of O, and A is the electrode area. Comparing this with the first term on the right-hand side of eqn. (10), one sees that

$$\beta_{O^*} = \frac{D_o A}{V_o \delta_o} \left(\frac{C_o - C_{O,o}}{C_o} \right) = \beta_o \left(\frac{C_o - C_{O,o}}{C_o} \right) = \beta_o \frac{i_o}{i_{O,l}} \quad (12)$$

where $i_{O,l}$ is the limiting current attained on the plateau of the wave of O. Similarly,

$$\beta_{R^*} = \beta_R \left(\frac{C_R - C_{R,o}}{C_R} \right) = \beta_R \frac{i_R}{i_{R,l}} \quad (13)$$

That is, the ratio of β^* to β is governed by the same ratio of concentration gradients that governs the ratio of the current to the limiting current. These equations permit convenient predictions of β^* -values from, and convenient correlations of measured values with, voltammetric data.

One need only integrate eqn. (7) to obtain an expression for the total quantity of electricity consumed in the electrolysis:

$$Q_\infty = \int_0^\infty i dt = n \left(V_o C_{O^o} - \frac{N}{1 + (\beta_{O^*}/\beta_{R^*})} \right) \quad (14)$$

With the aid of the Nernst equation it is readily shown that

$$\beta_{O^*}/\beta_{R^*} = e^{nF(E^{o'} - E)/RT} \quad (15)$$

where $E^{o'}$ is the formal potential of the O-R couple under the conditions employed. Combining this with eqn. (14) yields a description of the final equilibrium

$$E = E^{o'} - \frac{RT}{nF} \ln \frac{nV_R C_{R^o} + Q_\infty}{nV_O C_{O^o} - Q_\infty} \quad (16)$$

which is equivalent to the expressions given previously¹⁻³.

The following paragraphs summarize some important special forms of these general equations.

TOTALLY IRREVERSIBLE REACTIONS

At potentials where O is reduced to R at a significant rate, the rate of oxidation of R is negligibly small — that is, $\beta_{R^*} \approx 0$ — if the half-reaction is totally irreversible. Equation (14) then becomes at once

$$Q_\infty = nV_O C_{O^o} \quad (17)$$

which shows that, as was previously stated^{4,5}, the reduction of O must proceed to completion if sufficient time is allowed. Similarly, the oxidation of R must proceed to completion if the potential is positive enough to cause it to occur at a significant rate, so that $\beta_{O^*} \approx 0$. Because there are many data (of which those of SANTHANAM⁶ are cited merely as the most recent and the most numerous) in the literature that do not appear to confirm this prediction, it has been examined experimentally in a case in which ambiguity is hardly possible: the reduction of hydrogen ion from potassium chloride solutions. Replicate aliquots of a standard solution of hydrochloric

acid were mixed with replicate aliquots of 1.00 *F* potassium chloride and electrolyzed at mercury cathodes, the electrolysis potential being varied among successive electrolyses while all other conditions were maintained as nearly constant as possible. The pH during the electrolysis was monitored with the aid of glass and calomel electrodes in the working-electrode compartment of the double-diaphragm cell¹⁰ employed. The initial pH was always 2.11 ± 0.03 . In the electrolyses at the more positive potentials the integrator stopped when the pH had risen to 6.6 ± 0.4 , which corresponds to at least 99.99% complete reduction; at a few of the most negative potentials, small corrections were necessary for a continuous faradaic background current. These were applied as described by MEITES AND MOROS¹¹, and their accuracies were confirmed by correlating the steady final current in each electrolysis with the rate of appearance of hydroxyl ion indicated by the readings of the pH meter. As is shown by Table 1, the values of Q_∞ were constant to better than $\pm 0.15\%$ even though the values of β^* varied about fifty-fold over the range of potentials employed.

TABLE 1

EFFECTS OF WORKING-ELECTRODE POTENTIAL ON THE RATE AND EXTENT OF REDUCTION OF HYDROGEN ION

Each solution contained 0.5263 mmole of hydrochloric acid in 105 ± 0.5 ml of 1.0 *F* potassium chloride. The values of β^* were obtained from the chronocoulometric equation of GELB AND MEITES⁷.

$E_{w.e.}$ (V vs. Ag/AgCl(s), KCl(s))	$10^3 \beta_{H^+}^*$ (sec ⁻¹)	Q_∞ (mF)
-1.39	0.278	0.5255
-1.42	0.470	0.5271
-1.45	0.809	0.5260
-1.48	1.35	0.5272
-1.51	2.10	0.5254
-1.54	3.30	0.5271
-1.57	4.91	0.5258
-1.60	6.64	0.5248
-1.63	8.21	0.5250
-1.67	9.86	0.5263
-1.70	10.75	0.5273
-1.73	12.45	0.5265
-1.76	12.24	0.5267
-1.79	12.35	0.5266
		Mean: 0.5263 ± 0.0007

In view of these results, variations of Q_∞ with potential for a totally irreversible process must be attributed either to failure to prolong the electrolysis sufficiently [eqn. (9) shows that the time required to reach any given degree of completion is inversely proportional to β_0^* , as is otherwise obvious], to errors in integrating the small currents involved, or to the existence of side reactions.

An alternative description of the current obtained from the reduction of O when the half-reaction is totally irreversible is^{9,12}

$$i = nAC_{O,O} k_{s,h} e^{\alpha n_a F(E^{O'} - E)/RT} \quad (18)$$

where α is the transfer coefficient and n_a the number of electrons involved in the rate-determining step. Combining eqns. (8), (12), and (18) gives

$$\frac{i}{\beta_{O^*}} - \frac{i}{\beta_O} = \frac{V}{A k_{s,h}} e^{-\alpha n_a F(E^{O'} - E)/RT} \quad (19)$$

which may also be written

$$E = \left(E^{O'} + \frac{RT}{\alpha n_a F} \ln \frac{A k_{s,h}}{V_O \beta_O} \right) - \frac{RT}{\alpha n_a F} \ln \frac{\beta_{O^*}}{\beta_O - \beta_{O^*}} \quad (20)$$

For the data in Table I, a plot of E vs. $\log \beta_{O^*}/(\beta_O - \beta_{O^*})$ was found to be linear and to have a slope of 0.126 V, whence $\alpha n_a = 0.47$. This is in acceptable agreement with the literature value, 0.50–0.51, for the reduction of hydrogen ion from dilute acidic solutions¹³.

REVERSIBLE REACTIONS

In this case the relation between Q_∞ and working-electrode potential stated by eqn. (16) has been so closely confirmed by experiment^{1-3,14} that further discussion of it is unnecessary.

The variation of current with time is described by eqn. (8), in which both β^{*} 's will have finite values unless the electrolysis is carried out at a potential on one or the other of the plateaus. If, at any potential on the rising part of the wave, one has

$$\beta_{O^*}/\beta_O = x \quad (21)$$

one must also have

$$\beta_{R^*}/\beta_R = 1 - x \quad (22)$$

That is, the half-wave potential of O is the same as that of R, the quarter-wave potential of O is the same as the three-quarter-wave potential of R, and so on. Hence eqn. (7) becomes

$$i = n[x \beta_O V_O C_{O^0} - (1 - x) \beta_R V_R C_{R^0}] e^{-[x\beta_O + (1-x)\beta_R]t} \quad (23)$$

from which another description of the equilibrium state is readily deduced:

$$\frac{x}{1-x} = \frac{nF}{RT} e^{(E^{O'} - E)} = \frac{\beta_R V_R C_R}{\beta_O V_O C_O} \quad (24)$$

These equations show that the rate of the electrolysis increases with decreasing proportion at equilibrium of the species having the larger value of β . For reductions of metal ions to metal amalgams, β_R is almost always larger than β_O , and consequently the current should decay more rapidly as the potential becomes more positive. In the reduction of a metal ion to another of lower oxidation state, however, and also in reversible organic reductions like those of quinones, β_O and β_R are usually approximately equal; if they are exactly equal, the rate of the electrolysis will be independent of potential, and plots of $\log i$ [or of $\log(-i)$ if the initial current is anodic] vs. time at different potentials will all be parallel. No explanation can be found in these equations for the very long times required for the attainment of equilibrium in the experiments of ROGERS AND MERRITT¹.

Cases intermediate between the extremes discussed here are easily amenable to predictions based on the current-potential curves obtained with separate solutions of O and R under identical experimental conditions.

SUMMARY

The effects of working-electrode potential on the rate of a controlled-potential electrolysis and on the quantity of electricity that eventually accumulates are discussed. In particular, it is proven that electrolysis at any potential where an appreciable current flows on a totally irreversible wave must proceed to virtual completion, and experimental confirmation of this prediction is given for the reduction of hydrogen ion on mercury electrodes.

REFERENCES

- 1 L. B. ROGERS AND C. MERRITT, JR., *J. Electrochem. Soc.*, 100 (1952) 131.
- 2 S. A. MOROS, *Ph.D. Thesis*, Polytechnic Institute of Brooklyn, 1961.
- 3 L. MEITES, *Physical Methods of Organic Chemistry*, (Vol. I of *Technique of Organic Chemistry*, edited by A. WEISSBERGER), Interscience Publishers, Inc., New York, 3rd ed., 1960, p. 3306.
- 4 T. MEITES AND L. MEITES, *Anal. Chem.*, 27 (1955) 1531.
- 5 L. MEITES, *Physical Methods of Organic Chemistry*, (Vol. I of *Technique of Organic Chemistry*, edited by A. WEISSBERGER), Interscience Publishers, Inc., New York, 3rd ed., 1960, p. 3307.
- 6 K. S. V. SANTHANAM, *Ph.D. Thesis*, Sri Venkateswara University, 1963.
- 7 R. I. GELB AND L. MEITES, *J. Phys. Chem.*, 68 (1964) 630.
- 8 J. J. LINGANE, *Electroanalytical Chemistry*, Interscience Publishers, Inc., New York, 1953, p. 193.
- 9 C. N. REILLEY, *Treatise on Analytical Chemistry*, (edited by I. M. KOLTHOFF AND P. J. ELVING), Part I, Vol. 4, Interscience Publishers, Inc., New York, 1963, pp. 2173-7.
- 10 L. MEITES, *Anal. Chem.*, 27 (1955) 1116.
- 11 L. MEITES AND S. A. MOROS, *Anal. Chem.*, 31 (1959) 23.
- 12 P. DELAHAY, *New Instrumental Methods in Electrochemistry*, Interscience Publishers, Inc., New York, 1954, p. 35.
- 13 R. PARSONS, *Handbook of Electrochemical Constants*, Butterworths Scientific Publications, London, 1959, pp. 95-6.
- 14 Y. ISRAEL, *Ph.D. Thesis*, Polytechnic Institute of Brooklyn, 1964.

J. Electroanal. Chem., 7 (1964) 337-342

THE ADSORPTION OF HYDROXYL IONS AT THE MERCURY-SOLUTION INTERFACE AND THE ANODIC DOUBLE-LAYER CAPACITY IN FLUORIDE SOLUTIONS

R. PAYNE*

Department of Physical Chemistry, University of Bristol (England)

(Received February 17th, 1964)

INTRODUCTION

The hydroxyl ion is usually regarded as anomalous in its electrocapillary behaviour showing little or no specific adsorption at the electrocapillary maximum (e.c.m.) yet apparently strongly adsorbed at small positive polarisations¹. The experimental evidence for this conclusion is the sharp rise of the capacity curve at positive potentials close to the e.c.m. which is similar to the behaviour of systems in which the anion is known to be strongly adsorbed. This is somewhat surprising in view of the close similarity of the thermodynamic properties of hydroxyl and fluoride ions which are little adsorbed in this range of polarisation². However, consideration of the potential of the mercury-mercuric oxide electrode shows that the capacity must rise to a high value at a comparatively negative potential in a hydroxide solution because of the reversible discharge of hydroxyl ions which introduces a large pseudo-capacity, and it is possible that this is the effect observed. It is therefore of considerable interest to determine the extent to which hydroxyl ions are adsorbed close to the limit of polarisation, both with regard to the general connection between anion adsorption and the anodic reaction, and the possibility that hydroxyl ion adsorption may be responsible for the ultimate rise of the anodic capacity in systems, notably fluoride solutions³, where the anion is not appreciably adsorbed.

EXPERIMENTAL

Seven different concentrations of sodium hydroxide in water, ranging from ~ 0.01 – $1 M$, were studied. The capacity at a dropping mercury electrode was measured with a precision of 0.1% by an a.c. bridge method at a frequency of 1 kc using the apparatus and technique previously described^{4,5}. Potentials were measured with respect to a pair of hydrogen electrodes in the same solution with a precision of 1 mV. Solutions were prepared by volumetric dilution of a stock solution which was carefully analysed by volumetric titration against individually weighed amounts of potassium hydrogen phthalate.

Capillaries were drawn from 1-mm bore pyrex capillary tubing. Suitable capillaries

* Present address: Space Physics Laboratory (Energetics Branch), USAF Cambridge Research Laboratories, L. G. Hanscom Field, Bedford, Mass., U.S.A.

were selected by measurement of the drop-time (10–12 sec) and the flow rate (0.3–0.5 mg sec⁻¹) under a head of mercury of ~ 80 cm. Selected capillaries were siliconed before use. Boiling nitric acid was first drawn through to prepare the surface. The capillary was washed with equilibrium water and dried under vacuum and then siliconed by momentarily drawing through dimethyl dichlorosilane vapour. The tip was re-cut before use to permit wetting of the end face and thereby prevent suspension of the drop from the outer circumference of the capillary which otherwise occurs. A single capillary was used for all the measurements to avoid internal inconsistency due to variation of the capillary characteristics. The cathodic minimum capacity was measured as a function of concentration in a single experiment by the technique of replacing the solution, leaving the dropping electrode permanently set up so that discrepancies between measured mercury flow-rates in individual experiments were eliminated. Individual flow rates for each concentration were, however, also measured as a routine procedure and gave values of the capacity minimum which were always within 0.1% of the "smoothed" values.

Mercury was purified by prolonged treatment with dilute nitric acid followed by washing and finally three distillations *in vacuo*. Equilibrium water was prepared by distillation of ordinary distilled water from alkaline permanganate. A.R. sodium hydroxide pellets were used directly from a freshly-opened bottle without further purification. No evidence of electro-reducible or organic impurity was found during the measurements.

Solutions were de-aerated by bubbling with oxygen-free nitrogen, filtered and pre-saturated with equilibrium water. The mercury flow-rate was measured by weighing the mercury delivered in a time interval measured by a stop-watch checked against a crystal-controlled oscillator. The potential of the e.c.m. was measured for each solution by the method of the streaming mercury electrode⁶. All measurements were carried out in a water thermostat controlled to $\pm 0.05^\circ$.

RESULTS

The concentration dependence of the capacity in sodium hydroxide solutions in water at 25° is shown in Fig. 1. The results are plotted on the experimental E^- scale (reference electrode reversible to the anion¹). Values for the cathodic capacity minimum together with the e.c.m. potentials are recorded in Table 1.

The pronounced minimum in the capacity close to the e.c.m. in the more dilute solutions is due to the minimum in the diffuse-layer capacity.

The results were integrated using an Elliot 803 computer to give the potential, capacity, interfacial tension γ and the function $\xi^- = \gamma + q_m E^-$, all interpolated at integral values of q_m , the surface charge density. Preliminary analysis of the results showed that the maximum positive charge attainable in this system is only $\sim 6\mu\text{C cm}^{-2}$ owing to the onset of the anodic reaction at a potential of ~ 0.8 V with respect to the hydrogen electrode in the same solution at all concentrations (Fig. 1). The coincidence of the capacity curves on the positive branch indicates that the curve is shifting in the negative direction by the full amount, $(RT/F) \ln a_{\pm}$, that the reference electrode potential changes, as would be expected if the steeply-rising anodic capacity is the start of the pseudo-capacity peak associated with the electrode reaction. That this is so is confirmed by the simultaneous sharp increase in the series resistance observed at 0.8 V.

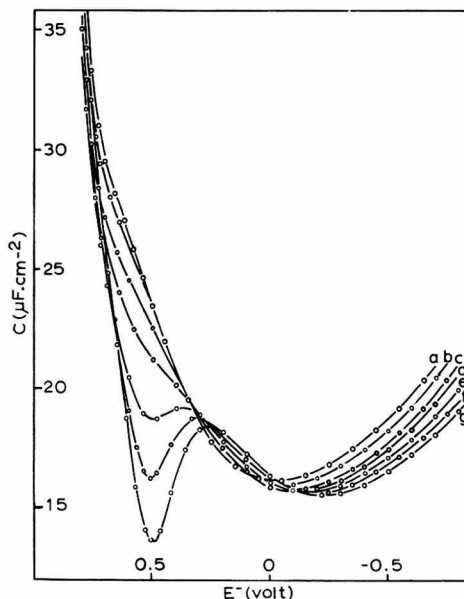


Fig. 1. Capacity vs. potential for aqueous sodium hydroxide solutions at 25°. (a), 1.089 *M*; (b), 0.5445 *M*; (c), 0.2178 *M*; (d), 0.1089 *M*; (e), 0.04356 *M*; (f), 0.02718 *M*; (g), 0.01089 *M*. Potentials measured against a hydrogen electrode in the same solution.

TABLE I

POTENTIALS OF THE ELECTROCAPILLARY MAXIMUM AND VALUES OF THE CATHODIC MINIMUM FOR AQUEOUS SODIUM HYDROXIDE SOLUTIONS AT 25°

<i>c</i> (mole l ⁻¹)	<i>C</i> _{min} (μF cm ⁻²)	- <i>E</i> ⁻ e.c.m. (V)	-(<i>E</i> ⁻ e.c.m. - (<i>RT</i> / <i>F</i>) ln <i>a</i> [±])
0.01089	15.54	0.515	0.634
0.02178	15.61	0.532	0.634
0.04356	15.65	0.548	0.633
0.1089	15.68	0.568	0.632
0.2178	15.74	0.583	0.630
0.5445	15.91	0.602	0.627
1.089	16.14	0.620	0.627

Values of the function ξ^- computed from the integrated capacities using the measured e.c.m. potential to determine the first integration constant and the interfacial tension data of GOUY⁷ for the second integration constant, were plotted as a function of $z(RT/F) \ln a_{\pm}$ at constant positive values of q_m ; the slope of this plot is equal to the surface excess of cations ($\bar{\Gamma}^+$) in the double layer⁸,

$$\frac{F}{zRT} \left(\frac{\partial \xi^-}{\partial \ln a_{\pm}} \right)_{q_m} = \bar{\Gamma}^+ \quad (1)$$

It is evident from inspection of these curves that the cation is repelled at all positive values of q_m indicating that the anion is not appreciably adsorbed.

The theoretical variation of ξ^- with concentration was computed by assuming all the charge to be in the diffuse layer, *i.e.*, no specific adsorption. The charge due to

the cation (qa^+) was calculated from the equation²

$$qa^+ = 11.74\sqrt{c} (e^{-19.46\phi_2} - 1) \quad (2)$$

the potential ϕ_2 of the outer Helmholtz plane being given by the total diffuse-layer charge

$$qa = 11.74\sqrt{c} \sinh(19.46\phi_2). \quad (3)$$

qa^+ was then plotted against $2RT/F \ln a_{\pm}$ for each value of q_m and integrated numerically to give ξ^- . The experimental value for the lowest concentration was taken as the integration constant. The results are compared with the experimental points in

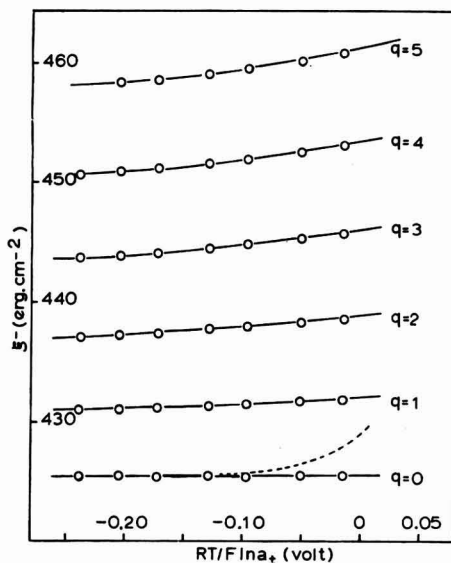


Fig. 2. Comparison of theoretical and experimental variation of the function ξ^- with concentration. Lines calculated from diffuse-layer theory assuming absence of specific adsorption. Points are experimental values.

Fig. 2. The agreement is excellent, the deviation being never more than 0.2 erg cm^{-2} . However it should be pointed out that the experimental values depend on the electrocapillary data of GOUY. According to GOUY the interfacial tension at the e.c.m. is independent of concentration in the range studied here, but this is in disagreement with the measurements of OLDFIELD⁹ who found a depression of 0.7 erg cm^{-2} at the e.c.m. in a unimolar solution. Both authors give values for other alkali hydroxides which are in close agreement with their respective sodium hydroxide data. The divergence however is not large and does not affect the conclusion that hydroxyl ions are not appreciably adsorbed even at the most positive values of q_m .

This conclusion was confirmed by examination of the ESIN AND MARKOV plots for the system. PARSONS¹⁰ has shown that the ESIN AND MARKOV coefficient can be used as a criterion of specific adsorption. It can be shown from diffuse-layer theory that

$$-\left(\frac{\partial q^-}{\partial q_m}\right)_c = \frac{1}{2} \exp \left[\sinh^{-1} \left(\frac{-qa}{2A} \right) \right] \left[1 + \left(\frac{qa}{2A} \right)^2 \right]^{-1} \quad (4)$$

providing specific adsorption is absent. q^- is the charge due to anions in the double layer and $A = 11.74\sqrt{c}$. $\partial q^-/\partial q_m$ is related to the potential E^+ by the thermodynamic equation

$$\frac{F}{2RT} \left(\frac{\partial E^+}{\partial \ln a_{\pm}} \right)_{q_m} = \left(\frac{\partial q^-}{\partial q_m} \right)_c \tag{5}$$

E^+ is the potential of the mercury electrode measured with respect to a reference electrode reversible to the cation. Integration of the right-hand side of eqn. (5) with respect to $\ln a_{\pm}$ gives the theoretical variation of E^+ with concentration. The integration has been performed graphically for positive values of q_m . The results are compared

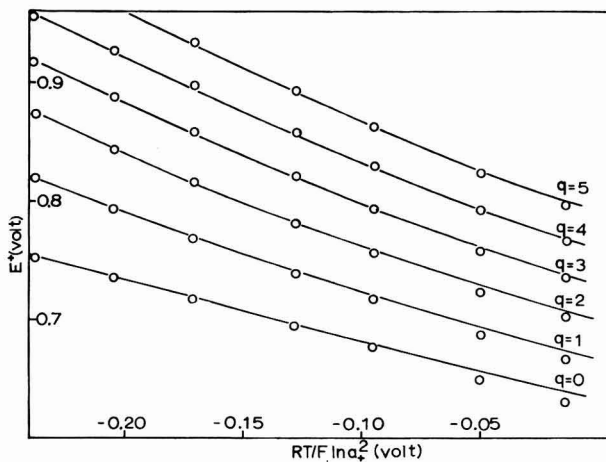


Fig. 3. Comparison of theoretical and experimental Esin and MARKOV plots. Lines calculated from diffuse-layer theory assuming absence of specific adsorption. Points are experimental values.

with the experimental values in Fig. 3, the value for the most dilute solution being taken as the integration constant. The agreement again is very satisfactory. The small divergencies that occur appear to be systematic at the higher concentrations but are greater, surprisingly, for the lower values of q_m . This is probably connected with the value assigned to the constant of integration.

The final test for specific adsorption of anions was a comparison of the measured capacities with values calculated from diffuse-layer theory assuming a concentration independent inner-layer capacity, *i.e.*, no specific adsorption. The inner-layer capacity, C^i , was determined from the experimental values for the most concentrated solution by subtracting the diffuse-layer capacity, calculated from the equation

$$C_a = 19.46(137.8c + q_m^2)^{1/2} \tag{6}$$

assuming a series combination of inner-layer and diffuse-layer capacities¹

$$\frac{1}{C} = \frac{1}{C^i} + \frac{1}{C_a} \tag{7}$$

The C^i values were then used together with C_d values for the lower concentrations, to calculate the total capacity in these solutions. The experimental and calculated capacities are compared in Fig. 4. The agreement is again satisfactory evidence that little specific adsorption occurs. It is difficult to assess the effect on a calculation of

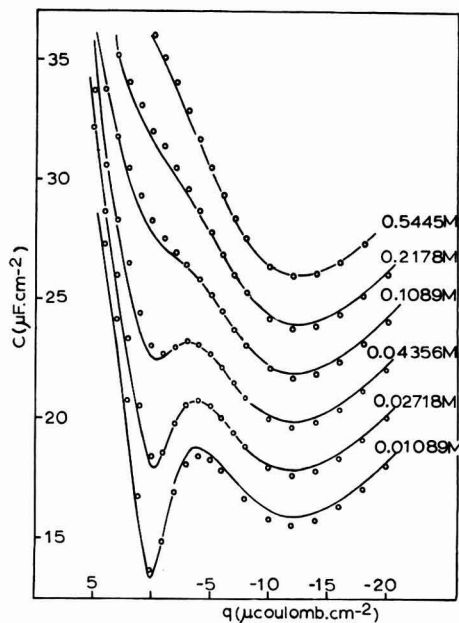


Fig. 4. Comparison of theoretical and experimental variation of the differential capacity with the charge. Lines calculated from diffuse-layer theory and capacity data for 1.089 *M* sodium hydroxide. Points are experimental values. Curves at higher concentrations are displaced upwards for clarity by $2 \mu\text{F cm}^{-2}$ per concentration.

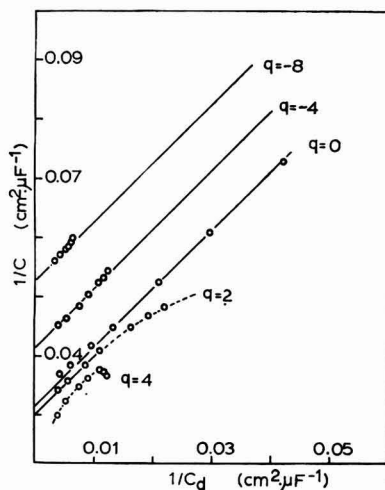


Fig. 5. Plot of reciprocal capacity *vs.* reciprocal diffuse-layer capacity calculated for a non-adsorbed electrolyte. Lines are drawn with unit slope.

this kind, of neglect of specific adsorption since both C^i and the additivity of τ/C^i and τ/C_a are simultaneously affected. A better method of utilising the capacity data as a criterion of specific adsorption has been suggested by PARSONS¹¹. If specific adsorption is absent, a plot of τ/C against τ/C_a should according to eqn. (7) be linear, of unit slope and intercept τ/C^i for a given value of q_m . Examples of this type of plot are given in Fig. 5. The lines are drawn with unit slope. At zero- and negative-values of q_m the agreement is reasonable although at the more extreme charges the points are necessarily cramped because C_a is large and its contribution little dependent on the concentration. For positive values of q_m , however, eqn. (7) clearly breaks down, indicating either defects in diffuse-layer theory or the assumption of the series combination of capacities or, more likely, some specific adsorption of anions. It is however interesting to note a slight, but significant, curvature of the plots for negative values of q_m where specific adsorption of anions is certainly negligible.

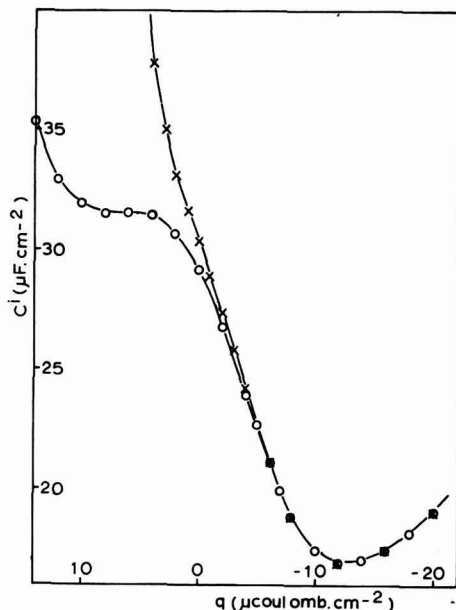


Fig. 6. Comparison of inner layer capacities for sodium hydroxide (x-x) and sodium fluoride solutions (o-o).

The inner-layer capacities for sodium hydroxide and sodium fluoride¹² are compared in Fig. 6. Again it is difficult to assess the importance of specific adsorption of hydroxyl ions in explaining the divergence of the curves on the positive side. It seems reasonable to suppose that the anodic reaction is immediately preceded by a sharp increase in specific adsorption and that this is largely responsible for the increase of the inner-layer capacity. An alternative explanation is an increase of dielectric constant or decrease in thickness accompanying the replacement of fluoride ions by hydroxyl ions, although this appears unlikely.

DISCUSSION

In spite of the close agreement of the experimental results with the predictions of diffuse-layer theory for a non-adsorbed electrolyte, there seems little doubt that some specific adsorption of hydroxyl ions occurs even at the e.c.m. This apparent contradiction is due to neglect of the electrolyte excluded from the inner layer implied in arbitrarily setting the boundary of the diffuse layer in the outer Helmholtz plane. This problem has been discussed by GRAHAME AND PARSONS¹³.

According to GOUY'S measurements the interfacial tension at the e.c.m. is independent of concentration, and the surface excess of electrically-neutral sodium hydroxide is therefore zero at the e.c.m. From the definition of surface excess it follows that the mean mole fraction of sodium hydroxide in the interface is identical with that in the bulk solution. However if the cation is assumed to be excluded from the inner region of the double layer it must automatically be positively adsorbed in the diffuse layer since the individual ionic surface excesses are zero. Consequently the anion is repelled from the diffuse layer and must therefore be compensatingly specifically adsorbed in the inner region. This is confirmed by the slight shift of the e.c.m. potential in the negative sense (Table I, column 4) and also by the capacity data. The close agreement with diffuse-layer theory is due to the accidental compensation of neglect of the inner layer and specific adsorption of anions. A theoretical variation of the interfacial tension with concentration at the e.c.m. has been calculated assuming an electrolyte-free inner layer of 4\AA -thickness. The surface deficiency was computed from the bulk concentration and integrated with respect to the solute chemical potential as before, to give the variation of γ with concentration. The result shown in Fig. 2 is a curve which rises quite sharply at the higher concentrations; in a unimolar solution the surface deficiency amounts to $\sim 4\ \mu\text{C cm}^{-2}$ and the increase in $\gamma_{\text{max}} \approx 2\ \text{erg cm}^{-2}$. This is qualitatively the kind of variation of γ_{max} with concentration observed for other electrolytes where the anion is non-adsorbed e.g., SO_4^{2-} , HPO_4^{2-} and HAsO_4^{2-} -ions⁷.

It has been suggested that the anodic rise of the capacity in fluoride solutions may be due to specific adsorption of hydroxyl ions³ and it is of interest to examine this suggestion in the light of the measurements. The anodic capacity, irrespective of the anion, invariably rises steeply as the potential approaches the reversible potential of the anodic reaction. This is to be expected in view of the pseudo-capacity associated with the reaction, which is of the order of $10^4\ \mu\text{F cm}^{-2}$ in a unimolar solution at 25° ¹⁴. The anodic process on mercury appears to be an intrinsically very rapid exchange as the reversibility of the common anion reversible reference electrode systems demonstrates. Consequently the process is wholly diffusion-controlled for the purpose of measurements at low audio frequencies so that the pseudo-capacity is fully developed. The close correlation between the anodic double-layer capacity and the charge-transfer process is also the reason for the correlation noted by GRAHAME¹⁵ between the potential of the rising capacity at which the capacity begins to rise steeply and the solubility of the corresponding mercurous salt which controls the reversible potential of the process.

In view of the large magnitude of the pseudo-capacity the rise of the double-layer capacity can be regarded approximately as asymptotic to the reversible potential of the anodic reaction so that the potential of the capacity rise should shift in the

negative direction by an amount $2.303 RT/F$ (59 mV) for a ten-fold increase in the anion activity, where this controls the potential of the anodic reaction. On the other hand specific adsorption of anions leads to a more rapid rise of the capacity so that the shift is more than 59 mV. This is because the shift is related to the ESIN AND MARKOV coefficient through the identity,

$$\left(\frac{\partial E}{\partial \ln a_{\pm}}\right)_C = \left(\frac{\partial E}{\partial \ln a_{\pm}}\right)_{q_m} - \left(\frac{\partial E}{\partial C}\right) \ln a_{\pm} \left(\frac{\partial C}{\partial \ln a_{\pm}}\right)_{q_m} \quad (8)$$

where E is the potential measured on a fixed scale and is here expressed as a function of the capacity, (C), and the mean ionic activity, (a_{\pm}). The first term on the right-hand side of eqn. (8) is the ESIN AND MARKOV coefficient which is greater than 59 mV where the anion is specifically adsorbed because of the discreteness of charge effect¹⁶. The second term in eqn. (8) is small since the first factor $(\partial E/\partial C)$ approaches zero when the capacity is rising steeply. For example, the product of both factors is ~ 5 mV for a unimolar potassium chloride solution¹³ when the capacity is $50 \mu\text{F cm}^{-2}$. In this case the anion is strongly adsorbed and the value of $(\partial E/\partial \ln a_{\pm})_C$ is approximately 90 mV.

For sodium fluoride solutions the situation is complicated by hydrolysis of the anion since hydrofluoric acid is comparatively weak (pK , 3.17). The question of hydroxyl ion adsorption therefore arises as a possible cause of the anodic rise of capacity. It is believed that this problem can be resolved by a detailed examination of the capacities in relation to salt concentration and pH.

In Figs. 7 and 8 are shown the anodic capacities for sodium hydroxide and sodium fluoride¹² solutions, respectively, plotted on an E^- scale. The potential for the reversible discharge of anions (which it should be noted is independent of concentration on this scale) is shown as a dotted line; the value for a hypothetical mercury-mer-

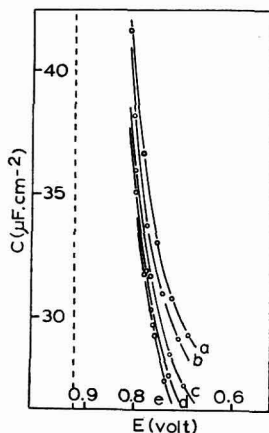


Fig. 7. Anodic capacities for sodium hydroxide solutions plotted against the potential measured with respect to an electrode reversible to the anion. The potential for reversible discharge of hydroxyl ions is shown as a dotted line. (a), 1.089 M ; (b), 0.5445 M ; (c), 0.2178 M ; (d), 0.1089 M ; (e), 0.04356 M .

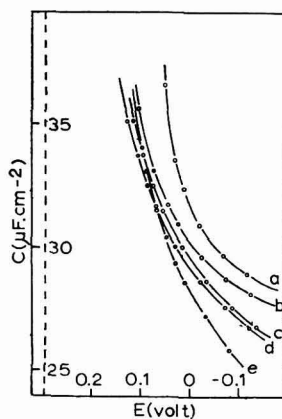


Fig. 8. Anodic capacities for sodium fluoride solutions plotted against the potential of a hypothetical electrode reversible to the fluoride ion (capacity data of GRAHAME¹²). The potential for reversible discharge of fluoride ions is shown as a dotted line. (a), 0.916 M ; (b), 0.66 M ; (c), 0.1 M ; (d), 0.01 M ; (e), 0.001 M .

curous fluoride electrode was calculated from thermodynamic data using a value of $-104.5 \text{ kcalmole}^{-1}$ for the standard free energy of formation of mercurous fluoride at 273°K ¹⁷. The curves for the hydroxide system converge and clearly approach the reversible potential, indicating firstly, that there is little specific adsorption and secondly, that the potential of the capacity rise is controlled by the hydroxyl ion activity. In the case of the fluoride system, the curves also converge with the notable exception of the most concentrated solution, again indicating that the potential of the capacity rise is responding to the anion concentration. This is confirmed by Fig. 9

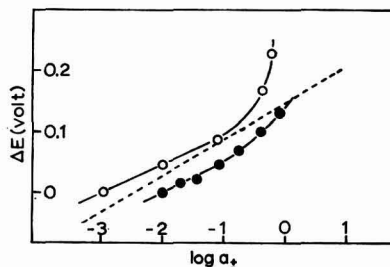


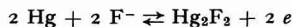
Fig. 9. The shift of potential (ΔE) measured at $C = 34 \mu\text{Fcm}^{-2}$ of the anodic capacity for sodium hydroxide ($\bullet-\bullet$) and sodium fluoride ($\circ-\circ$)¹² solutions plotted as a function of salt activity. The dotted line has a slope of 60 mV.

where the shift of the rising capacity along the potential axis (measured at $C = 31 \mu\text{Fcm}^{-2}$ against a fixed reference electrode) is plotted for both systems in the form of ΔE measured from the lowest concentration. Although the plots are curved, the lower concentration values lie close to the theoretical slope of 59 mV and there is obviously a close similarity between the behaviour of the two systems.

It is of interest at this point to consider the possible mechanism of fluoride ion discharge. As the capacities plotted in Fig. 8 show, the theoretical value of 0.30 V (*vs.* N.C.E.) for the standard potential of the mercury-mercurous fluoride electrode is entirely reasonable from the point of view of these measurements. However mercurous fluoride is very soluble in water and is rapidly hydrolysed according to the equation¹⁸



so that it appears that mercuric oxide is the ultimate product of the anodic reaction in both fluoride and hydroxide solutions. Nevertheless this does not eliminate the possibility that the fluoride ion concentration is controlling the potential of the discharge since the potential-determining stage may be fast discharge of fluoride ions,



followed by the slower hydrolysis reaction. The potential in this case would depend on the fluoride ion concentration as found.

It is now necessary to examine the capacity data for the fluoride solutions in relation to the variation of pH with concentration due to hydrolysis. The calculated variation is given in Table 2.

According to Fig. 9, the potential of the capacity rise shifts by ~ 220 mV over the whole range of concentration while the pH increases by only 1.37 units. The effect therefore appears to be too large to be explained by the variation of hydroxyl ion concentration. This is broadly confirmed by plotting the capacities against the po-

TABLE 2
THE VARIATION OF pH WITH CONCENTRATION OF
SODIUM FLUORIDE IN AQUEOUS SOLUTION

c (mole l^{-1})	pH
0.001	7.08
0.01	7.58
0.1	8.03
0.66	8.39
0.916	8.45

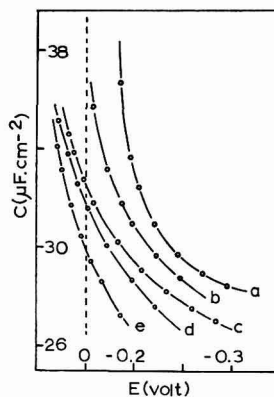
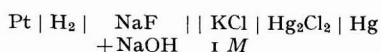


Fig. 10. The anodic capacity for sodium fluoride¹² solutions plotted against the potential measured with respect to an electrode reversible to hydroxyl ions. (a), 0.916 M; (b), 0.66 M; (c), 0.1 M; (d), 0.01 M; (e), 0.001 M.

tential measured with respect to a mercury-mercuric oxide electrode in the same solution (Fig. 10). There is obviously no reasonable relationship between the positions of the curves on this scale, and the reversible potential for hydroxyl ion discharge actually cuts the curves for the three lowest concentrations. Furthermore the pseudo-capacity associated with discharge of hydroxyl ions at a concentration of 10^{-6} mole l^{-1} (pH 8) could hardly be more than a fraction of the observed capacity, so that even if hydroxyl ion adsorption were considered responsible for the rising double-layer capacity, the very large pseudo-capacity found could hardly be due to their discharge. It seems reasonable to assume that the ion which is specifically adsorbed on extreme polarisation is also the ion which is ultimately involved in the charge-transfer process. At the same time it is doubtful whether adsorption equilibrium could be established during the lifetime of the drop at such low concentrations¹⁹.

Measurements of the double-layer capacity in aqueous tenth molar solutions of sodium fluoride with small additions of sodium hydroxide have recently been reported by AUSTIN AND PARSONS²⁰. It was found that the capacity was little affected by the added hydroxide below a nominal pH of 11 but that the potential of the anodic rise was shifted in the negative direction by ~ 150 mV by increase of the pH from 11 to 12. This odd behaviour is difficult to understand. However the measurements are open to criticism in as much as the hydroxide concentrations were only roughly adjusted and the pH was not measured. The measurements have therefore been repeated for the same nominal pH values, which were also determined from measurements of the e.m.f. of the cell,



The measured capacities are shown in Fig. 11 and are in approximate agreement with the earlier measurements, *i.e.*, the anodic capacity rise appears to be independent of the added hydroxide below nominal pH 10 and shifts almost discontinuously by

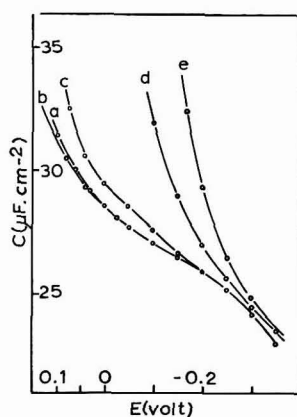


Fig. 11. The effect of added hydroxyl ions on the anodic capacity for 0.1 M sodium fluoride solution. Nominal pOH: (a), 6 (base solution); (b), 5; (c), 4; (d), 3; (e), 2.

TABLE 3

VALUES OF E.M.F. FOR THE CELL



AND CALCULATED pH VALUES

x (mole l^{-1})	E (V)	pH
0	0.776	8.33
10^{-5}	0.792	8.60
10^{-4}	0.792	8.60
10^{-3}	0.906	10.53
10^{-2}	0.979	11.76

~ 150 mV between pH 10 and 11. The reason for this odd behaviour is provided by the measured pH-values recorded in Table 3 which show that the pH is independent of the added hydroxide at the lower concentrations.

It seems clear that the hydroxyl ions are being removed, probably by neutralisation with dissolved carbon dioxide present in the water, so that the measured capacities may also be complicated by adsorption of bicarbonate ions.

DAMASKIN, NIKOLAEVA-FEDOROVICH AND FRUMKIN²¹ have reported measurements of the capacity in 0.9 M solutions of caesium fluoride and sodium fluoride which differ from GRAHAME's measurements in as much as the capacity variation is flat up to a potential of 0.25 V positive with respect to the normal calomel electrode,

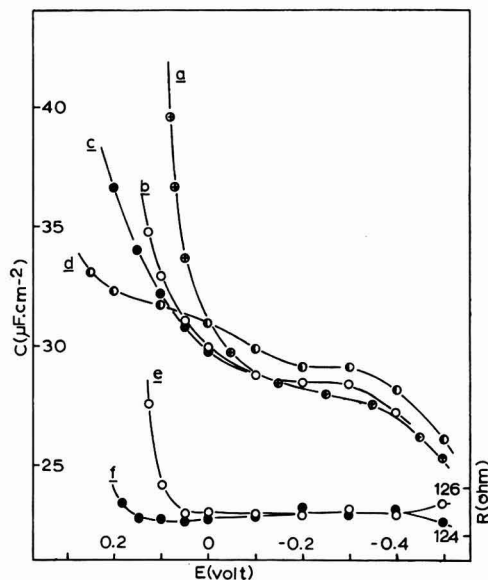


Fig. 12. Comparison of the anodic capacity for ~ 1 M sodium fluoride solutions. (a), GRAHAME¹²; (b), this work; (c), with added hydrofluoric acid; (d), DAMASKIN, NIKOLAEVA-FEDOROVICH AND FRUMKIN²¹; (e) and (f), series resistance corresponding to (b) and (c) respectively.

whereas GRAHAME's curves rise sharply at $E \approx 0.1$ V (Fig. 12). The reason for this discrepancy is still in dispute. The Russian workers have attributed the sharp capacity rise found by GRAHAME to specific adsorption of silicofluoride ions presumed to be present as an impurity resulting from attack of the glass by the fluoride solution; their solutions were prepared in teflon and palladium apparatus and were only in contact with glass during the actual measurements. This explanation however is not convincing for three reasons. In the first place we have never found any visible etching of pyrex vessels by sodium fluoride solutions even after standing for several months. Secondly we have regularly obtained results in close agreement with those of GRAHAME for tenth normal solutions. Although our solutions have also been purified in pyrex it is unlikely that identical amounts of impurity would result in each case. In any case we would expect trace impurities to remain in solution during

the recrystallisation of the fluoride. Thirdly GRAHAME has shown that the silicofluoride ion is not appreciably adsorbed from magnesium silicofluoride solutions so that it is unlikely to be adsorbed from dilute solutions in a concentrated fluoride base solution. In view of the relevance of this question to the interpretation of the capacity rise in fluoride solutions proposed above, we have conducted a number of simple experiments aimed at providing an alternative explanation. Although no firm conclusion is possible, a number of interesting observations have been made which we believe suggest an alternative explanation and which will now be described briefly.

There seems little doubt that the anodic capacity in sodium fluoride solutions left for long periods in pyrex glass increases as DAMASKIN *et al.* find, but we find no conclusive evidence that this is due to adsorption of silicofluoride ions. On the other hand a slow increase of pH has been noticed in such a solution and moreover the increased capacity vanishes if hydrofluoric acid is added to the solution. In Fig. 13 are shown the anodic capacity curves for a freshly-prepared tenth normal solution of sodium fluoride and an identical solution which had been stored in a pyrex flask for three months. Both solutions were prepared from the same sample of salt recrystallised in pyrex vessels. The fresh solution had the unexpectedly low pH of 6.9 which was attributed to the presence of dissolved carbon dioxide. The aged solution on the other hand had a pH of 8.5. The addition of hydrofluoric acid to this solution shifted the potential of the capacity rise in the positive direction by more than 50 mV while a similar but smaller effect was observed for the fresh solution.

A clue to the reason for this behaviour is provided by the corresponding variation of the series resistance which is also recorded in Fig. 13. For the fresh solution the

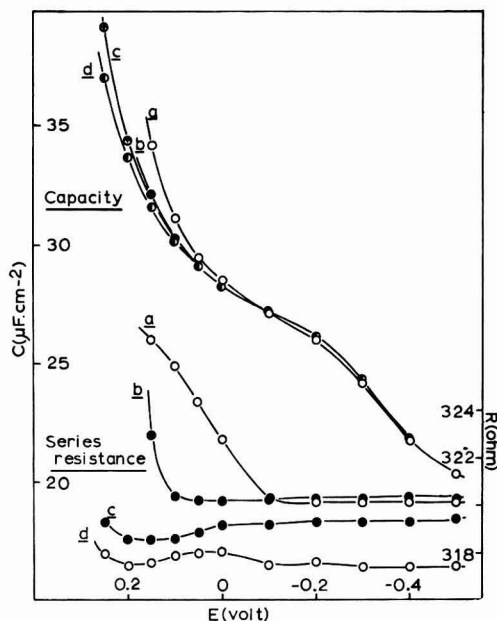
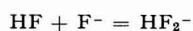


Fig. 13. The effect of added hydrofluoric acid on the anodic capacity and series resistance for 0.1 *M* sodium fluoride solution. (a), solution aged in glass; (b), fresh solution; (c), as (b) with added hydrofluoric acid; (d), as (a) with added hydrofluoric acid.

resistance curve is flat up to +0.1 V beyond which it rises steeply; this is the characteristic behaviour observed for an electrode approaching the potential of the fast anodic reaction and is accompanied by a corresponding sharp increase of anodic current. For the aged solution on the other hand the resistance increases more slowly over a wide range of potential starting at -0.1 V. The same effect has also been observed in the adsorption of iodide ions from dilute solutions ($\sim 10^{-2} M$) in a concentrated nitrate base solution where it is accompanied by frequency dependent capacities and is thought to be due to kinetic control of the adsorption process, *i.e.*, diffusion control. It seems likely therefore that the aged fluoride solution contains a low concentration of an unidentified impurity ion which is strongly specifically adsorbed. The resistance curves also show that this is removed by the addition of hydrofluoric acid and that the range of ideal polarisability is thereby extended up to +0.25 V as found by the Russian workers. It is not clear whether the effect is due to the change of pH or to the presence of free hydrofluoric acid. If it is a pH effect it seems reasonable to suppose that the impurity is hydroxide or carbonate which would be removed by acidification. If on the other hand the effect is due to the hydrofluoric acid rather than the change of pH it is possible that this is the result of conversion of the fluoride to bifluoride according to the equilibrium,



In any case it is difficult to reconcile these measurements with the assumption that silicofluoride etched out of the glass is the active agent particularly since hydrofluoric acid, which attacks glass rapidly, actually produces a *decrease* in the capacity.

The anodic capacity has also been measured for a 0.9 M solution prepared from A.R. sodium fluoride without further purification. The results are compared in Fig. 12 with the measurements of GRAHAME¹² for 0.916 M sodium fluoride prepared from salt recrystallised in glass and those of DAMASKIN *et al.*²¹ for a 0.9 M solution prepared in teflon and palladium apparatus. The series resistance is also recorded for the present work together with the effect of adding hydrofluoric acid to the solution. The disagreement between the three sets of data is in striking contrast with the high order of reproducibility characteristic of this type of measurement. The most obvious explanation of the discrepancy is that suggested by the Russian workers since contamination of a solution with capillary active anions usually (but not always) results in increased capacity in this region of polarisation. However DAMASKIN'S curve lies wholly above the other curves, except for the far anodic end, and moreover possesses a broad hump centred on $E \approx 0$ which is not explained. It may be significant that the capacity is systematically increased at the more negative potentials ($E \approx -0.3$ V) and decreased at the far anodic end in passing from GRAHAME'S measurements through ours to DAMASKIN'S, and that the same effect is produced by the addition of hydrofluoric acid as can be verified by inspection of Fig. 13. As before, the addition of the acid extends the range of ideal polarisability up to ~ 0.2 V and further additions increase this to ~ 0.25 V. Similar behaviour is found for unimolar solutions of ammonium fluoride.

A complete evaluation of these observations is not possible in the absence of a more precise knowledge of the composition of the solutions studied but we believe certain generalisations can be made. They are:

- (1) GRAHAME'S capacity measurements for sodium fluoride solutions are probably

correct with the possible exception of the most concentrated solutions. This belief is based on the reproducibility of the measurements for tenth molar solutions, and the conviction, supported by the variation of the series resistance and the concentration dependence of the anodic capacity, that the fluoride ion is responsible for the rising capacity and is ultimately discharged in the electrode reaction.

(2) The increased capacity observed in an aged fluoride solution is not due to silicofluoride ions but is due to specific adsorption of an unidentified impurity which is removed by acidification. Since the ageing appears to be accompanied by an increase in pH it is difficult to avoid the conclusion that the impurity is hydroxyl or carbonate ions.

(3) The discrepancies found between different measurements of the capacity for concentrated sodium fluoride solutions may be due to appreciable differences in the composition of solutions prepared by completely different methods.

I would like to thank Dr. R. PARSONS for the use of his computer programme and for making Professor GRAHAME's data available, and the D.S.I.R. for a Senior Research Fellowship at the University of Bristol during the tenure of which this work was carried out.

SUMMARY

The specific adsorption of hydroxyl ions on a mercury electrode from aqueous solutions at 25° has been investigated by measuring the capacity of the electrical double layer as a function of concentration. The virtual absence of specifically adsorbed ions is demonstrated by comparison with the predictions of diffuse-layer theory. The nature of the rapid increase of capacity on positive polarisation is considered in the light of the measurements, and its relevance to the anodic capacity in fluoride solutions is discussed.

REFERENCES

- 1 D. C. GRAHAME, *Chem. Rev.*, 41 (1947) 441.
- 2 D. C. GRAHAME, *J. Am. Chem. Soc.*, 76 (1954) 4819.
- 3 R. J. WATTS-TOBIN, *Phil. Mag.*, 6 (1961) 133.
- 4 R. PAYNE, *Thesis*, London, 1962.
- 5 G. J. HILLS AND R. PAYNE, to be published.
- 6 D. C. GRAHAME, E. H. COFFIN, J. I. CUMMINGS AND M. A. POTH, *J. Am. Chem. Soc.*, 74 (1952) 1207.
- 7 G. GOUY, *Ann. Chim. Phys.*, 29 (1903) 145.
- 8 R. PARSONS, *Trans. Faraday Soc.*, 51 (1955) 1518.
- 9 L. F. OLDFIELD, *Thesis*, London, 1951.
- 10 R. PARSONS, *Proc. Intern. Congr. Surface Activity*, 2nd, London, 3 (1957) 38.
- 11 R. PARSONS, private communication.
- 12 D. C. GRAHAME, *O.N.R. Report No. 14*, 1954.
- 13 D. C. GRAHAME AND R. PARSONS, *J. Am. Chem. Soc.*, 83 (1961) 1291.
- 14 J. E. B. RANGLES, *Discussions Faraday Soc.*, 1 (1947) 11.
- 15 D. C. GRAHAME, M. A. POTH AND J. I. CUMMINGS, *J. Am. Chem. Soc.*, 74 (1952) 4422.
- 16 R. PARSONS, *Modern Aspects of Electrochemistry*, Butterworth, London, 1954, p. 161.
- 17 G. G. KOERBER AND T. DE VRIES, *J. Am. Chem. Soc.*, 74 (1952) 5008.
- 18 P. J. DURRANT AND B. DURRANT, *Introduction to Advanced Inorganic Chemistry*, Longmans, London, 1962, p. 485.
- 19 R. PAYNE, unpublished work.
- 20 M. J. AUSTIN AND R. PARSONS, *Proc. Chem. Soc.*, (1961) 239.
- 21 B. B. DAMASKIN, N. V. NIKOLAEVA-FEDOROVICH AND A. N. FRUMKIN, *Dokl. Akad. Nauk SSSR*, 121 (1958) 129.

POLAROGRAPHY OF HYDROGEN PEROXIDE IN LANTHANUM
NITRATE SOLUTIONS*

MARY T. HENNE** AND JUSTIN W. COLLAT

Department of Chemistry, The Ohio State University, Columbus 10, Ohio (U.S.A.)

(Received February 6th, 1964)

INTRODUCTION

The reduction of hydrogen peroxide at the dropping mercury electrode (D.M.E.) has long been known to produce a much drawn-out polarographic wave centered at about -0.9 V *vs.* S.C.E. which is unaffected by changes of supporting electrolyte and is independent of hydrogen ion concentration between pH 2 and 11.5^{1,2}. The reduction wave of this powerful oxidant can be shifted to more positive potentials by the addition of various catalysts to the solution. For example, kinetic currents for hydrogen peroxide reduction have been investigated by BRDIČKA AND WIESNER³, for the case of ferrihem catalysis, and by KOLTHOFF AND PARRY for the case of ferric ion catalysis⁴, both of which effects are explainable in terms of the electroreduction of the catalyst and the oxidation in its reduced form by hydrogen peroxide. Molybdate, vanadate, and tungstate have also been shown by KOLTHOFF AND PARRY to catalyze hydrogen peroxide reduction through the formation of peroxy compounds which are easily reduced at the D.M.E.⁵.

Catalysis was also observed in air-saturated solutions of heavy-metal cations by STRNAD⁶. An increase of the first oxygen wave in the presence of iron(II), cobalt(II), nickel(II) and in particular by lead(II) was reported, which must be explained by further reduction of hydrogen peroxide formed at the surface of the D.M.E. in the presence of the added ions.

We report here the polarographic behavior of hydrogen peroxide in the presence of lanthanum ion, which causes the reduction wave to appear at potentials up to 0.8 V more positive than normal. The results indicate a mechanism of catalysis which depends on the properties of lanthanum ion to form (i) an insoluble hydroxide on the D.M.E. as the nearby solution becomes alkaline, and (ii) a soluble reducible complex with hydrogen peroxide under alkaline conditions.

EXPERIMENTAL

Polarograms were recorded with a Sargent Model XII recording polarograph supplemented by a Rubicon Model B potentiometer for measuring applied voltages. The

* Presented at the 140th Meeting of the American Chemical Society, Chicago, September 1961.

** Taken from the dissertation of Mary T. Henne, presented to the Graduate School of The Ohio State University in partial fulfillment of the requirements for the Ph.D. degree, June 1963.

cell, which was very similar to that described by DIEHL *et al.*⁷, permitted de-aeration of the sample solution in the absence of mercury in a separate side compartment. The mercury pool or the saturated calomel electrode was used as a non-polarizable electrode. On some occasions the mercury pool was used in nitrate solutions where its potential was not strictly defined. This departure from the usual technique was necessary to obviate the use of agar which is needed in a conventional H-cell. Experiments performed with this arrangement were used only to show the shapes of waves and not to obtain potential data.

Current-time curves were recorded photographically from a Tektronix Model 502 oscilloscope fed by the output of a Keithley Model 610 electrometer. The current-measuring function of the latter instrument was used for measuring currents in the cell circuit, the applied voltage of which was furnished by a 100 Ω helipot, (Beckman Instrument Company). The voltage drop in the circuit caused by the electrometer was ordinarily only about 10 mV, and never more than 30 mV. Applied voltages were corrected for this voltage drop.

Lanthanum salt solutions were prepared by igniting pure lanthanum oxide, (Lindsay Chemical Co.), for 6 h at about 900°, treating the residue with the stoichiometric amount of acid to yield the desired solution, and filtering off any excess. Stock 0.1 M lanthanum perchlorate, nitrate, and chloride solutions prepared daily according to this procedure had constant, reproducible pH values of 8.0, 7.6, and 7.5 respectively, and the catalytic effects observed with them could always be reproduced. Upon aging, the stock solutions deposited a fine white precipitate and were discarded.

Before each experiment the cell was cleaned by an acid rinse according to a rigidly standardized procedure⁸, which was found to contribute to reproducibility. Test solutions were mixed just prior to use and were de-aerated in the absence of mercury in the side compartment of the cell by passing nitrogen through them for 15 min. Polarograms were recorded immediately upon transfer of the de-aerated test solution from the side compartment of the cell to the electrolysis compartment. By this means a polarogram could be obtained within, at most, 10 min of bringing the solution into contact with mercury. The term "minimum contact time" is used herein to describe such an interval before electrolysis. In experiments where the test solution was separated from the S.C.E. anode by means of a potassium nitrate-agar bridge, the liquid-junction potential of the system was estimated by measuring the crossing potential of the D.M.E. in a quinhydrone-saturated buffer solution and comparing it with the theoretical. The correction of 20 mV obtained has been applied where $E_{d.e.}$ rather than applied voltage is indicated. Some experiments were conducted in the presence of 0.01% lauryl sulfonate, or gelatin, or 0.002% Triton X-100; the results, however, were not considered significant and generally these capillary active agents were not used. All polarographic experiments were performed at 25°.

Dissolved mercury was determined with dithizone reagent according to the procedure of SANDELL⁹.

RESULTS

The polarographic wave

The effect of lanthanum compounds on the polarographic wave of hydrogen peroxide is exemplified by the curves of Fig. 1. They show a pronounced positive potential

shift of the usual peroxide wave in addition to features which depend on the anion present in solution. We have concentrated our attention on the polarography of the lanthanum-hydrogen peroxide system in nitrate medium, because this system allows study of positive applied voltages and demonstrates an interesting current peak followed by a current minimum at positive potentials, see Fig. 1(b). This peak,

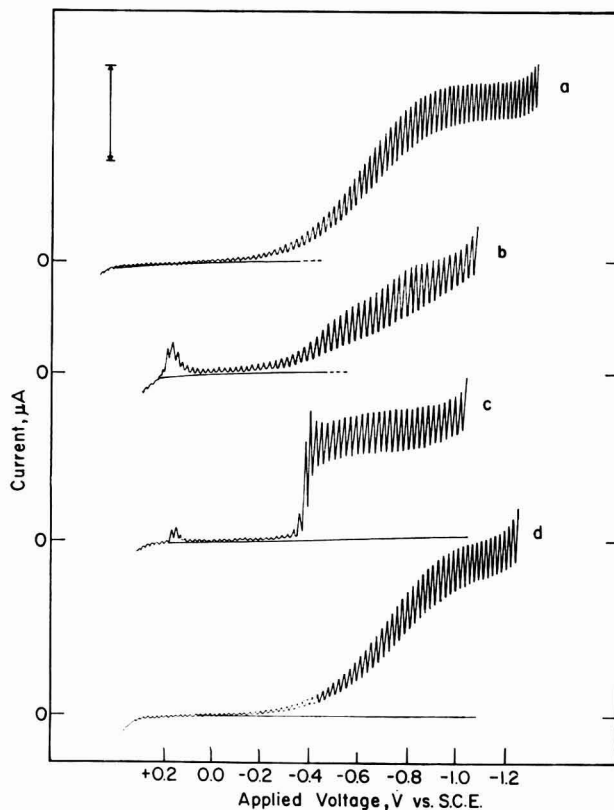


Fig. 1. Typical catalyzed reduction waves of hydrogen peroxide, $0.00041 M \text{H}_2\text{O}_2$ in all cases. (a), no $\text{La}(\text{NO}_3)_3$, $0.6 M \text{NaNO}_3$; (b), $0.05 M \text{La}(\text{NO}_3)_3$, $0.30 M \text{NaNO}_3$; (c), $0.01 M \text{La}(\text{NO}_3)_3$, $0.54 M \text{NaNO}_3$; (d), $0.01 M \text{La}(\text{NO}_3)_3$, $0.54 M \text{NH}_4\text{NO}_3$. The arrow represents $2 \mu\text{A}$.

which is probably the resultant of a peroxide reduction current and a large current suppressing effect of the reduction products, is found in solutions in which the lanthanum nitrate concentration is about $0.01 M$ or above and the hydrogen peroxide about $0.0004 M$ or above. Limiting currents measured at the positive current peak, ($+0.10$ to $+0.25 V$ vs. S.C.E.), and those measured where the wave reaches a current plateau, are proportional to the concentration of hydrogen peroxide. In an experiment where the lanthanum nitrate concentration was $0.01 M$ and the hydrogen peroxide, $0.0004 M$, with $0.54 M$ sodium nitrate as supporting electrolyte, variation of the height of the mercury reservoir produced a change in limiting current at $-0.6 V$

which obeyed the $h^{1/2}$ law, and virtually no change in the limiting current at the foot of the wave (-0.3 V).

Figure 1(d) shows an important specific effect of ammonium ion on the catalytic properties of lanthanum ion. When ammonium ion replaces sodium in the supporting electrolyte, the presence of lanthanum has no effect on the hydrogen peroxide wave. The acidity of the ammonium ion doubtless prevents the precipitation of lanthanum hydroxide at the surface of the D.M.E., a point to be discussed further. Here it should be noted that the catalytic activity of lanthanum cannot be wholly ascribed to the insoluble hydroxide which it yields, for zinc ion showed no catalytic properties towards hydrogen peroxide even though its hydroxide is less soluble than lanthanum hydroxide.

The role of lanthanum hydroxide

The importance of the age of lanthanum solutions in producing the catalytic effects described above, the fact that the solution at the surface of the mercury drop becomes alkaline during peroxide reduction in unbuffered media, and the specific effect of ammonium ion on the polarographic wave, indicated that solid lanthanum hydroxide or its hydroxy-complex precursors, $(\text{La}(\text{OH})_2^+ \text{ or } \text{La}(\text{OH})_2^+)$, might contribute to the reduction process. To test this hypothesis, known small amounts of sodium

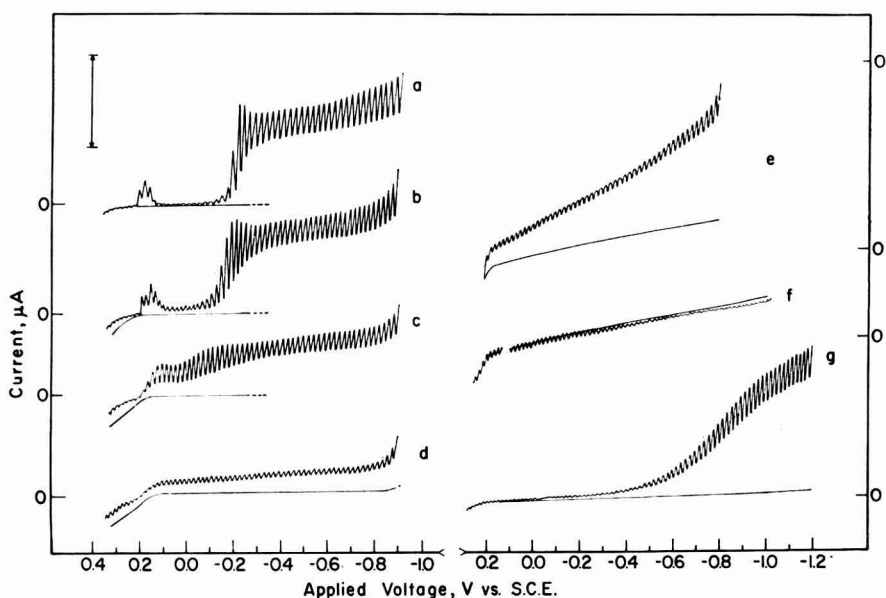


Fig. 2. The effect of solid $\text{La}(\text{OH})_3$ on the reduction process. (a), 0.00082 M H_2O_2 , 0.01 M $\text{La}(\text{NO}_3)_3$, 0.54 M NaNO_3 , no NaOH added; (b), as (a) with 0.02 g $\text{La}(\text{OH})_3$ per l; (c), as (a) with 0.05 g $\text{La}(\text{OH})_3$ per l; (d), as (a) with 0.10 g $\text{La}(\text{OH})_3$ per l. Solutions (a)–(d) were de-aerated 30 min out of contact with mercury and were polarographed after minimum contact time with mercury in the polarographic cell. (e), 0.00041 M H_2O_2 , 0.05 M $\text{La}(\text{NO}_3)_3$, 0.30 M NaNO_3 , 0.25 g $\text{La}(\text{OH})_3$ per l. Suspension stood for 48 h and was polarographed after minimum contact time. (f), Suspension of (e) after KMnO_4 treatment; (g), solution of (e) after pH lowered from 7.90 to 3.10 with HNO_3 . The arrow represents: 4 μA in (a), (b), (c) and (d); 0.4 μA in (e) and (f); 2 μA in (g).

hydroxide were added to lanthanum solutions containing hydrogen peroxide, and the suspensions formed were kept de-aerated and away from mercury for known times before being electrolyzed at the D.M.E. Polarograms of such suspensions showed an increase in the limiting current in the current minimum and a decrease in currents of the main reduction wave, both of which effects depended on the amount of solid in the suspension. This is shown in Fig. 2. All the features of the peroxide wave in the presence of lanthanum are absent. However, when a portion of this suspension was acidified to pH 3.1 with HNO_3 , the normal hydrogen peroxide wave observed in the absence of lanthanum returned. When a portion of the suspension was warmed with dilute excess KMnO_4 , with elimination of the excess solid by filtration, the small constant cathodic wave disappeared and the polarogram of the treated solutions was indistinguishable from the residual current curve. The polarographic properties of the test suspension were unaffected by removal of lanthanum hydroxide by filtration through a medium-porosity sintered-glass filter. Further polarographic study of suspensions of solid hydroxide in lanthanum nitrate-hydrogen peroxide mixtures showed that they lost oxygen at a slow but measurable rate until the mixture was 96 h old, after which the composition remained constant. After 6 days one mixture appeared unchanged. When a test suspension was brought in contact with mercury no significant oxidation of mercury occurred; over a 15 h period the concentration of mercury in such a solution, estimated polarographically, was less than 0.01 mM. We postulate a soluble complex of lanthanum and hydrogen peroxide formed in alkaline medium as the species responsible for the polarographic and chemical results described here. Investigation of the postulated species has shown that its reduction current: (i) increases with the amount of solid lanthanum hydroxide in suspension, (ii) is insensitive to the total amount of hydrogen peroxide in solution provided sufficient solid lanthanum hydroxide is present, (iii) varies directly with the lanthanum ion concentration up to 0.05 M, (iv) is unaffected by the concentration of sodium nitrate supporting electrolyte. Quantitative information on the reduction wave is limited by the fact that it is strongly affected by adsorption of lanthanum hydroxy-complexes or hydroxide on the D.M.E., a point to be discussed further. A qualitatively similar reduction wave was obtained in a sodium chloride supporting electrolyte, but no wave was observed in sodium perchlorate solution.

To ensure that the results were dependent on the presence of solid lanthanum hydroxide and not merely on aging of solution, experiments were performed which were identical to those already described except for the addition of sodium hydroxide. While decreases in the heights of the current peak at +0.2 V and the final peroxide wave were noted in aged solutions, there was no increase in the current minimum between these currents, as was clearly shown when the solid hydroxide was present, see Fig. 2(b). An exception to this behavior is the case when the concentration of lanthanum nitrate is high. In such a solution, [0.1 M $\text{La}(\text{NO}_3)_3$], lanthanum hydroxide precipitates on aging, and even a fresh solution doubtless contains some hydroxylated lanthanum species which react with hydrogen peroxide and account for an increase of current in the range of the current minimum.

The role of mercury

Experiments were performed to determine the effect of contact with mercury on the polarography of lanthanum nitrate-hydrogen peroxide test solutions. Figure 3

shows the result of a typical experiment. The growth of the limiting current in the current minimum range is taken as evidence of the accumulation of a decomposition product, and the pronounced change in the wave upon de-aeration with nitrogen is evidence that oxygen is produced as another decomposition product. When the

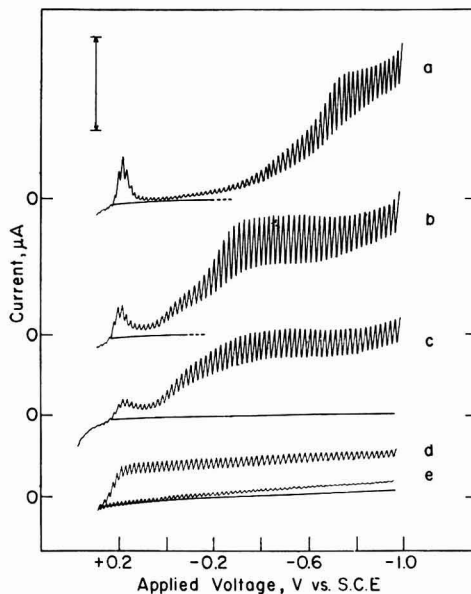


Fig. 3. The effect of mercury on $\text{La}(\text{NO}_3)_3\text{-H}_2\text{O}_2$ solutions, $0.00041 M \text{H}_2\text{O}_2$, $0.05 M \text{La}(\text{NO}_3)_3$, $0.30 M \text{NaNO}_3$. Time of contact with the mercury pool was: (a), minimum; (b) 1 h; (c), $2\frac{1}{2}$ h; (d) as (c) after 15 min de-aeration; (e), as (d) after KMnO_4 treatment. The arrow represents $2 \mu\text{A}$ in (a), (b) and (c) and $1 \mu\text{A}$ in (d) and (e).

de-aerated final product solution was treated with potassium permanganate, the limiting current decreased to 20% of its original value. It was shown by spectroscopic examination of this solution, as well as by use of dithizone reagent, that the remaining current was caused by a soluble mercury compound.

In separate experiments it was shown that lanthanum nitrate or mercury alone had little effect on the solution; thus 5% decomposition of hydrogen peroxide occurred in a $2\frac{1}{2}$ -h period in the presence of mercury alone and 17% decomposition occurred in this period in the presence of lanthanum nitrate alone, while virtually complete decomposition occurred in the presence of both.

When the concentration of lanthanum nitrate was lowered to $0.001 M$, the decomposition of H_2O_2 required 15 h, and the sole product of decomposition was oxygen. No mercury was found in this solution at the end of the lengthy period of contact, although oxygen from the decomposition was accumulating during this period. This shows that oxygen was not responsible for the dissolved mercury found in other test solutions. When the concentration of sodium nitrate was raised to $2 M$ and the concentration of lanthanum nitrate was kept at $0.05 M$, decomposition was slower than that illustrated in Fig. 3 and a larger proportion of the final limiting current was caused by dissolved mercury.

The current-time relation at single drops

Oscilloscopic recording of the current-time function at selected applied potentials was employed to give information on the process occurring during the life of a single drop. Results for a solution 0.01 M in $\text{La}(\text{NO}_3)_3$ and 0.0004 M H_2O_2 are shown in Fig. 4. The current-time curves obtained at the potential of the positive current peak are similar to those obtained in the region of the final wave, while those taken in the range of the current minimum are different, characterized by little or no current during the early part in the drop life and a gradual increase later. In cases where a substantial current flows [Fig. 4(b) and (e)-(h)] the trace for the first drop

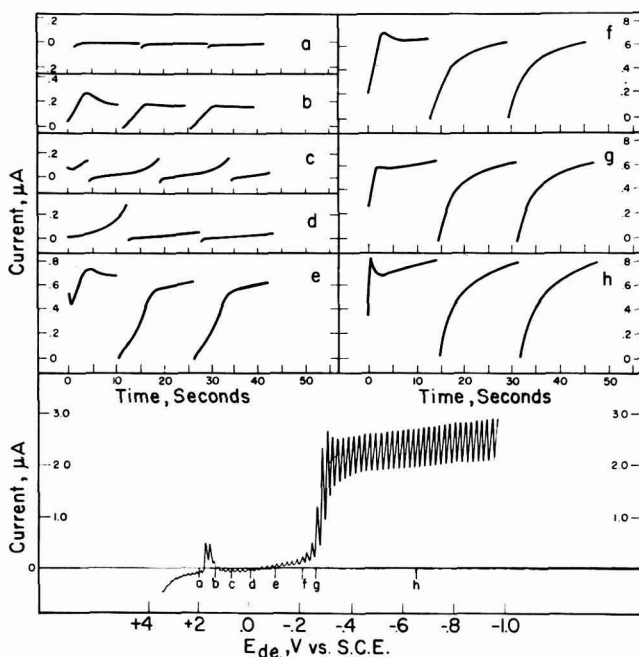


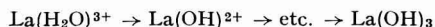
Fig. 4. Current-time curves for individual drops, 0.00041 M H_2O_2 , 0.01 M $\text{La}(\text{NO}_3)_3$, 0.54 M NaNO_3 . Bottom curve, conventional polarogram, open circuit drop time 0^e 5.9 sec; (a)-(h), current-time curves at the potentials indicated on the polarogram, open circuit drop time of 16.0 sec.

to which potential is applied has a maximum. We attribute the decrease in current which forms a maximum in these curves to the accumulation of colloidal lanthanum hydroxide in the neighborhood of the drop. This material covers the first drop within 1 or 2 sec of its formation, and subsequent drops from their inception. It was found that interruption of recording of current-time curves by stirring the solution with a stream of nitrogen restored the maximum to the first trace when the potential was again applied. Similar experiments on 0.001 M $\text{La}(\text{NO}_3)_3$ solution gave results qualitatively the same as those of Fig. 4, while experiments in 0.1 M $\text{La}(\text{NO}_3)_3$, in which decomposition of hydrogen peroxide is rapid, gave curves indicating almost linear growth of current with time over the entire potential range. When

ammonium nitrate was added to the test solution, all abnormal features of the individual current-time curves disappeared in agreement with the results of conventional polarography.

DISCUSSION

Our interpretation of the results reported here rests upon the chemistry of the lanthanum hydroxide-hydrogen peroxide-mercury system, and the special effect on limiting currents of adsorption of lanthanum hydroxy-complexes and lanthanum hydroxide on the D.M.E. The changes in the chemical nature of the test solutions which can be observed when lanthanum hydroxide is added to them, or when they are allowed to stand in contact with mercury for a long time suggest what happens, albeit to a slight degree, at the surface of a mercury drop in a fresh solution of hydrogen peroxide and lanthanum nitrate. Even when no electrolysis occurs at the D.M.E., slow oxidation of mercury with concomitant reduction of peroxide renders the drop surface alkaline. Upon polarization, the solution in the vicinity of the D.M.E. becomes more alkaline as the result of electrolytic reduction of hydrogen peroxide, which has been shown by KOLTHOFF AND PARRY⁴, to result in minute currents well before the main reduction wave. Thus, hydroxyl is available to shift the following reaction sequence to the right.



The existence of the intermediates shown in this sequence has been inferred from measurements of the solubility of lanthanum oxide by LEWIS¹⁰, who also suggested the existence of polynuclear complexes. The hydroxy-complexes of lanthanum are adsorbed on the surface of the D.M.E. to a degree exceeding the adsorption of lanthanum ion, or lanthanum hydroxide according to the interpretation of the differential capacitance measurements of DAMASKIN AND NIKOLAEVA-FEDOROVICH¹¹. The adsorbed material and suspended lanthanum hydroxide in the vicinity of the drop is available for reaction with hydrogen peroxide to form species in which a perhydroxyl group may be considered to have replaced a hydroxyl group. The formation of lanthanum peroxide, always under alkaline conditions, has been reported by CLEVE¹², MELIKOFF AND PISSARJEWSKY¹³, and MARKOV *et al.*¹⁴. We believe that a peroxy-complex or -compound with lanthanum is the species responsible for the waves we have observed at applied voltages between the mercury dissolution wave and the normal hydrogen peroxide wave. This is analogous to the behavior of the peroxy-complexes of molybdenum, vanadium or tungsten⁵. The current which results from the reduction of the lanthanum complex tends to be decreased by the accumulation of the adsorbed reaction product of lanthanum hydroxide on the surface of the D.M.E. The degree of adsorption of lanthanum hydroxide depends, in turn, on the nature of the anion present and the electrode potential. Thus, we observe a depression of the current after the first manifestation of a cathodic process at +0.2 V vs. S.C.E. This depression of current in the +0.1 V to -0.2 V region is less pronounced as the anion is replaced in the order ClO_4^- , NO_3^- , Cl^- , which is also the order of increasing adsorption of these ions on mercury. It is suggested that the less tenacious adsorption of nitrate permits a denser coverage of the electrode by the lanthanum hydroxide and results in a decreased current flow.

The complete absence of lanthanum catalysis in the presence of ammonium ion is a consequence of the acidity of the latter, which prevents the formation of the hydroxy complexes of lanthanum or the solid lanthanum hydroxide essential to the formation of the reducible complex.

SUMMARY

The reduction of hydrogen peroxide at the D.M.E. is catalyzed in lanthanum salt solutions. In 0.01 M $\text{La}(\text{NO}_3)_3$ it has been shown that a cathodic hydrogen peroxide current appears at +0.2 V vs. S.C.E., followed by a depression in the current which extends to the main hydrogen peroxide wave at -0.3 V. Experiments on suspensions of lanthanum hydroxide in lanthanum nitrate-hydrogen peroxide solutions have shown that the reduction current at potentials more oxidizing than -0.3 V increased upon contact with the solid, while the height of the normal wave decreased. Filtration of these mixtures and tests with potassium permanganate and nitric acid on the filtrate indicated that the species responsible for the reduction current was soluble, oxidizable, and unstable to acid. Mercury in contact with the lanthanum nitrate-hydrogen peroxide test solution led to the more rapid production of this species along with the evolution of oxygen. A soluble complex between lanthanum ion and hydrogen peroxide, formed under mildly alkaline conditions, is postulated as the species being reduced. The suppression of the catalytic current in the potential range +0.1 to -0.2 V is interpreted as the result of adsorption of insoluble lanthanum hydroxide or polymeric lanthanum hydroxy-complexes on the D.M.E. Current-time curves consistent with this explanation have been obtained.

REFERENCES

- 1 J. HEYROVSKÝ, *Casopis Československého Léčárnictva*, 7 (1927) 242; *C. A.*, 22 (1928) 4344.
- 2 I. M. KOLTHOFF AND C. S. MILLER, *J. Am. Chem. Soc.*, 63 (1941) 1013.
- 3 R. BRDIČKA AND K. WIESNER, *Collection Czech. Chem. Commun.*, 12 (1947) 39.
- 4 I. M. KOLTHOFF AND E. P. PARRY, *J. Am. Chem. Soc.*, 73 (1951) 3718.
- 5 I. M. KOLTHOFF AND E. P. PARRY, *J. Am. Chem. Soc.*, 73 (1951) 5315.
- 6 F. STRNAD, *Collection Czech. Chem. Commun.*, 11 (1939) 391.
- 7 H. DIEHL, J. I. MORRISON AND R. R. SEALOCK, *Experientia*, 7 (1951) 60.
- 8 M. T. HENNE, Dissertation, The Ohio State Univ., Columbus, Ohio, 1963.
- 9 E. B. SANDELL, *Colorimetric Determination of Traces of Metals*, Interscience, New York, 3rd ed., 1959, p. 626.
- 10 D. C. LEWIS, *Chem. & Ind. (London)*, (1957) 1238.
- 11 B. B. DAMASKIN AND N. V. NIKOLAEVA-FEDOROVICH, *Nauchn. Dokl. Vysšei Shkoly, Khim. Khim. Tekhnol.* (1959) No. 1, 43. *C. A.*, 53 13725h.
- 12 P. T. CLEVE, *Bull. Soc. Chim., France*, (2) 43 (1885) 53.
- 13 P. MELIKOFF AND L. PISSARJEWSKY, *Z. Anorg. Chem.*, 21 (1899) 70.
- 14 S. Z. MARKOV, L. V. LADEINOVA-SOBOLEVA AND A. M. CHERNYSHOVA, *Izv. Akad. Nauk SSSR, Otd. Khim. Nauk*, 11 (1961) 1933. Consultants' Bureau Engl. translation: *Bull. Acad. Sci. USSR, Div. Chem. Sci.*, (1961) 1805.

PROPRIÉTÉS GÉNÉRALES DES
MÉTHODES CHRONOPOTENTIOMÉTRIQUES EN RÉGIME DE
DIFFUSION CYLINDRIQUE ET SPHÉRIQUE
DÉTERMINATION DU COURANT COMPENSANT LES EFFETS LIÉS
AU CARACTÈRE NON LINÉAIRE DU MODE DE DIFFUSION

HENRI D. HURWITZ

Laboratoire de Chimie Analytique, Faculté des Sciences, Université Libre de Bruxelles (Belgique)

(Reçu le 8 février, 1964)

INTRODUCTION

De nombreuses méthodes chronopotentiométriques nouvelles, proposées par différents auteurs¹⁻⁹, se distinguent de la méthode galvanostatique¹⁰ par la forme du courant $i(t)$ imposé à l'électrode. Pour chacun des programmes $i(t)$ suggérés, les lois principales du transfert massique ont été établies après intégration des équations de Fick suivant des méthodes classiques dont celle des transformées de Laplace est la plus représentative. Les cas traités se sont d'autre part limités, dans leur majorité, aux processus simples de décharge directe en régime de diffusion linéaire. Assez récemment toutefois, MURRAY ET REILLEY¹¹ ont envisagé ces problèmes sous un aspect très général et ont pu de la sorte rendre compte simultanément des influences de la forme du courant $i(t)$, du mode de diffusion et du nombre d'espèces dépolarisantes. Dans leur travail, ces auteurs ont suivi un raisonnement en partie intuitif basé sur certaines propriétés d'additivité des flux mesurés à l'électrode. En procédant de cette manière, MURRAY ET REILLEY¹¹ ont défini des fonctions réponses $Z(0,t)$ (*true current impulse response function*) dont les formes mathématiques générales n'ont cependant pas été explicitées.

Le formalisme proposé par MURRAY ET REILLEY¹¹ présente de toute évidence un intérêt pratique appréciable puisqu'il permet d'obtenir, grâce à son caractère global, les solutions de différents systèmes sans qu'il soit nécessaire de recourir pour chacun d'eux aux équations différentielles de base. La méthode des transformées de Laplace fournit d'autre part une démonstration rigoureuse du concept de la fonction réponse¹² dont la formulation mathématique à l'aide d'une équation intégrale se trouve déjà mentionnée dans un travail de KAMBARA ET TACHI¹³. HERMAN ET BARD⁹ ont d'autre part justifié et illustré récemment certaines des propriétés caractéristiques de $Z(0,t)$ liées à l'expression de cette fonction en régime de diffusion linéaire.

En tenant compte de l'ensemble des résultats antérieurs, il nous a paru utile de dégager les formes générales de la fonction réponse valables pour un champ de diffusion sphérique ou cylindrique dans le cas d'un processus de décharge directe. Une telle détermination, en étant indépendante de l'allure du programme $i(t)$ permettrait d'envisager un certain nombre d'applications nouvelles dont quelques-unes pourraient être d'un grand intérêt pratique.

On sait en effet que les densités de courant, $i(t)$, généralement choisies ont la propriété de satisfaire, sur électrode plane, des expressions du type $a^0 = f(\tau)$ liant de manière simple le temps de transition mesuré τ à la concentration analytique au coeur de la solution, a^0 . Or ces relations directes ne sont plus conservées lorsque le système obéit à un mode de diffusion non linéaire¹⁴⁻²¹. Les expressions $a^0 = f(\tau)$ présentent alors un degré de complication qui les rend dans une large mesure impropres à l'emploi analytique. Il paraît donc utile, dans de telles conditions, de rechercher un programme $i(t)$ différent, permettant de restituer aux relations $a^0 = f(\tau)$ la forme simple qui les caractérise en régime de diffusion linéaire. Le problème ainsi posé consiste dès lors à évaluer une densité de courant susceptible de compenser l'ensemble des effets, sur $a^0 = f(\tau)$, liés à la symétrie non linéaire du champ de diffusion.

Du point de vue mathématique, on utilise dans ce travail la technique courante des transformées de Laplace²² ainsi que, dans leurs formes les plus classiques, les théorèmes y afférant. D'autre part, afin de simplifier la résolution des problèmes, on suppose que:

- (i) l'extension du champ de diffusion est semi-infinie;
- (ii) la solution n'est pas agitée (absence de convection);
- (iii) la composante d'apport par migration est annulée grâce à la présence d'un excès d'électrolyte support;
- (iv) la fraction du courant consommée par la charge capacitive de l'interphase peut être tenue pour négligeable;
- (v) l'état superficiel de l'électrode est parfaitement uniforme.

I. RÉGIME DE DIFFUSION LINÉAIRE

Lorsqu'une seule espèce A_1 , présente en solution, est déchargée, on obtient en appliquant la méthode des transformées de Laplace^{9,12,22},

$$Z_i^{i(t)}(0, t) \equiv \frac{1}{\sqrt{\pi}} \int_0^t \frac{i(t')}{(t-t')^{\frac{1}{2}}} dt' = n_1 F \sqrt{D_{A_1}} [a_1^0 - a_1(0, t, i(t))] \quad (1)$$

où D_{A_1} représente le coefficient de diffusion du dépolarisant unique A_1 ; n_1 , le nombre d'électrons échangés à l'électrode par particule; a_1^0 et $a_1(0, t, i(t))$ respectivement, la concentration de A_1 au coeur de la solution et à l'instant t à la surface de l'électrode. La densité du courant, $i(t)$, est choisie positive dans le sens de la décharge de A_1 . Par ailleurs on sait que $a_1(0, t, i(t))$ décroît en fonction du temps et s'annule au temps de transition $\tau_{1,1}$. Soit

$$Z_i^{i(t)}(0, \tau_{1,1}) \equiv \frac{1}{\sqrt{\pi}} \int_0^{\theta - \tau_{1,1}} \frac{i(t')}{(\theta - t')^{\frac{1}{2}}} dt' = n_1 F \sqrt{D_{A_1}} a_1^0 \quad (2)$$

Lorsque plusieurs espèces $A_1, A_2, \dots, A_p, \dots, A_n, \dots$ se déchargent à l'électrode, par $n_1, n_2, \dots, n_p, \dots, n_n, \dots$ électrons, à des tensions suffisamment distantes les unes des autres pour que l'on puisse observer sur le chronopotentiogramme des paliers distincts^{1,7,23,24} fournissant des temps de transition $\tau_{1,p}$ mesurables, on trouve^{9,13}

$$\begin{aligned} \frac{1}{\sqrt{\pi}} \int_0^{\theta - \sum_{p=1}^n \tau_{1,p}} \frac{i(t')}{(\theta - t')^{\frac{1}{2}}} dt' - \frac{1}{\sqrt{\pi}} \int_0^{\theta - \sum_{p=1}^{n-1} \tau_{1,p}} \frac{i(t')}{(\theta - t')^{\frac{1}{2}}} dt' &\equiv Z_i^{i(t)} \left(0, \sum_{p=1}^n \tau_{1,p} \right) - Z_i^{i(t)} \left(0, \sum_{p=1}^{n-1} \tau_{1,p} \right) = \\ &= a_n^0 n_n F \sqrt{D_{A_n}} \quad (3) \end{aligned}$$

où a_n^0 et D_{A_n} sont respectivement la concentration au coeur de la solution et le coefficient de diffusion de l'espèce A_n .

Il est enfin aisé de traiter le problème de la décharge de A_1 procédant par deux étapes consécutives^{1,24,25} (le cas de plus de deux étapes consécutives est trop exceptionnel pour mériter un développement particulier, mais cependant la généralisation est immédiate). La décharge des particules se poursuit alors à l'électrode jusqu'au temps de transition $\tau_{i,1}$ par l'intervention de la seule réaction



Au temps $\tau_{i,1}$ le courant est assuré simultanément par la décharge de B_1 produit depuis le début de la mesure



et par la réaction (4a). Il vient dès lors que

$$\frac{n_1 + n_2}{n_1} = \frac{Z_i^{(t)}(0, \tau_{i,1} + \tau_{i,2})}{Z_i^{(t)}(0, \tau_{i,1})} \quad (5)$$

où $\tau_{i,2}$ désigne le temps de transition caractéristique de (4b).

La résolution des intégrales $Z_i^{(t)}$ pour un grand nombre de fonctions $i(t)$ figure dans le travail de MURRAY ET REILLEY¹¹ ainsi que dans certains ouvrages classiques²² sur la conduction de la chaleur. On trouve⁶ de cette façon pour $i_i(t) = \varrho t^P$ ($P > -1$)

$$Z_i^{\varrho t^P}(0, t) \equiv \frac{\varrho P!}{(P + \frac{1}{2})!} t^{P+\frac{1}{2}} \quad (6)*$$

soit lorsque $P = 0$ (cas galvanostatique: $i_i(t) = i^0$)

$$Z_i^{i^0}(0, t) \equiv \frac{2 i^0}{\sqrt{\pi}} t^{\frac{1}{2}} \quad (7)$$

et lorsque $P = \frac{1}{2}$

$$Z_i^{\varrho t^{\frac{1}{2}}}(0, t) \equiv \frac{\varrho}{2} \sqrt{\pi} t \quad (8)$$

2. RÉGIME DE DIFFUSION SPHÉRIQUE

L'équation de Fick représentative de l'apport par diffusion sphérique du dépolarisant A_n est résolue en tenant compte des conditions initiales et limites

$$a_n(r, 0, i(t)) = a_n^0 = a_n(\infty, t, i(t)) \quad (9)$$

où r figure la distance comptée à partir du centre de l'électrode dont le rayon vaut r_0 .

(a) *Une seule substance présente en solution est déchargée.* A la condition (9) s'ajoute la valeur du flux à l'électrode

$$i(t) = n_1 F D_{A_1} \left(\frac{\partial a_1(r, t, i(t))}{\partial r} \right)_{r=r_0} \quad (10)$$

* $(P + \frac{1}{2})! = \sqrt{\pi} \frac{1 \cdot 3 \cdot 5 \dots (2P + 1)}{2^{P+1}}$

En régime galvanostatique ($i(t) = i^0$) le problème a été résolu successivement par RIUS, POLO ET LLOPIS¹⁴ et MAMANTOV ET DELAHAY¹⁵. Ces derniers auteurs ont obtenu la relation suivante, valable au plan de l'électrode ($r = r_0$)

$$r_0 \left[1 - \exp\left(\frac{D_{A_1} t}{r_0^2}\right) \operatorname{cfer} \sqrt{\frac{D_{A_1} t}{r_0^2}} \right] = \frac{n_1 F D_{A_1}}{i^0} [a_1^0 - a_1(r_0, t, i^0)] \quad (11)$$

où cfer désigne le complément de la fonction d'erreur. L'application du théorème de DUHAMEL²² à l'éqn. (11) fournit la valeur $[a_1^0 - a_1(r_0, t, i(t))]$ dans le cas général de la densité de courant $i(t)$. On obtient

$$\frac{r_0}{\sqrt{D_{A_1}}} \frac{\partial}{\partial \theta} \int_0^{\theta-t} i(t') \left[1 - \exp\left(\frac{D_{A_1}(\theta-t')}{r_0^2}\right) \operatorname{cfer} \left(\frac{D_{A_1}(\theta-t')}{r_0^2}\right)^{\frac{1}{2}} \right] dt' = n_1 F \sqrt{D_{A_1}} [a_1^0 - a_1(r_0, t, i(t))] \quad (12a)$$

soit encore

$$\begin{aligned} Z_{s,1}^{i(t)}(r_0, t) &\equiv \frac{1}{\sqrt{\pi}} \int_0^{\theta-t} \frac{i(t')}{(\theta-t')^{\frac{1}{2}}} dt' - \int_0^{\theta-t} i(t') \left(\frac{D_{A_1}}{r_0^2}\right)^{\frac{1}{2}} \exp\left(\frac{D_{A_1}(\theta-t')}{r_0^2}\right) \operatorname{cfer} \left(\frac{D_{A_1}(\theta-t')}{r_0^2}\right)^{\frac{1}{2}} dt' = \\ &= n_1 F \sqrt{D_{A_1}} [a_1^0 - a_1(r_0, t, i(t))] \quad (12b) \end{aligned}$$

On s'aperçoit, par comparaison avec l'éqn. (1), que la deuxième intégrale figurant dans le membre de gauche de l'éqn. (12b) tient compte des effets spécifiques liés à la symétrie non linéaire du champ de diffusion. Pour des valeurs $(D_{A_1} t / r_0^2)^{\frac{1}{2}} < 1$ on peut développer l'intégrand de ce dernier terme en série. Au temps $t = \tau_{s,1}$ correspondant par définition à la condition $a_1(r_0, \tau_{s,1}, i(t)) = 0$ il vient dès lors

$$Z_{s,1}^{i(t)}(r_0, \tau_{s,1}) = a_1^0 n_1 F \sqrt{D_{A_1}} \quad (13)$$

et

$$\begin{aligned} Z_{s,1}^{i(t)}(r_0, \tau_{s,1}) &\equiv \frac{1}{\sqrt{\pi}} \int_0^{\theta-\tau_{s,1}} i(t') \left\{ \frac{1}{(\theta-t')^{\frac{1}{2}}} - \sqrt{\pi} \left(\frac{D_{A_1}}{r_0^2}\right)^{\frac{1}{2}} + 2 \left(\frac{D_{A_1}}{r_0^2}\right) (\theta-t')^{\frac{1}{2}} - \right. \\ &\quad \left. - \sqrt{\pi} \left(\frac{D_{A_1}}{r_0^2}\right)^{\frac{1}{2}} (\theta-t') + \dots \right\} dt' \quad (14) \end{aligned}$$

(b) *Plusieurs constituants réagissent à l'électrode à des tensions suffisamment distantes pour que l'on puisse mesurer des temps de transition distincts.* Récemment, PETERS ET LINGANE¹⁸ ont étudié les systèmes en régime de diffusion non linéaire dans le cas galvanostatique. Ces auteurs ont utilisé une méthode basée sur le concept de la couche de diffusion différentielle^{13,26}. Il est possible de traiter par un procédé identique des systèmes soumis à un courant de forme $i(t)$. Dans ces conditions on définit l'extension $\delta_{s,p}$ de la couche de diffusion caractérisant l'espèce A_p par

$$\delta_{s,p} = \frac{a_p^0 - a_p(r_0, t, i(t))}{\left(\frac{\partial a_p(r, t, i(t))}{\partial r}\right)_{r=r_0}} \quad (15)$$

Dès lors par analogie avec ce qui existe en régime de diffusion linéaire, on admet que la forme de la fonction $\delta_{s,1}$ correspondant au système ne contenant qu'une seule espèce dépolarisante A_1 , se conserve pour l'extension $\delta_{s,n}$ relative au constituant A_n du système à plusieurs dépolarisants, pour autant que $t > \sum_{p=1}^{n-1} \tau_{s,p}$ où $\tau_{s,p}$ est le

temps de transition caractéristique de la décharge de A_p sur l'électrode sphérique. On détermine $\delta_{s,1}$ grâce aux éqns. (10) et (15) avec $p = 1$ ainsi que (12b). Il vient dès lors pour chaque espèce particulière A_n

$$\delta_{s,n} = \frac{\sqrt{D_{A_n}}}{i(t)} Z_{s,n}^{i(t)}(r_0, t) \quad \left(t > \sum_{p=1}^{n-1} \tau_{s,p} \right) \quad (16)$$

La valeur du flux à l'électrode est obtenue par la relation

$$i(t) = \sum_{p=1}^n n_p F D_{A_p} \left(\frac{\partial a_p(r, t, i(t))}{\partial r} \right)_{r=r_0} \quad (17)$$

En tenant compte des éqns. (15), (16) et (17), et pour un temps d'électrolyse $t = \sum_{p=1}^n \tau_{s,p}$ on trouve l'expression générale proposée par MURRAY ET REILLEY¹¹, soit

$$1 = \sum_{p=1}^n \frac{n_p F \sqrt{D_{A_p}} a_p^0}{Z_{s,p}^{i(t)} \left(r_0, \sum_{p=1}^n \tau_{s,p} \right)} \quad (18)$$

La fonction $Z_{s,p}^{i(t)}$ est donnée par l'éqn. (14) où l'on a cependant substitué le coefficient D_{A_p} au coefficient D_{A_1} et où $\theta = \sum_{p=1}^n \tau_{s,p}$.

(c) *La décharge d'une substance met en jeu un nombre d'étapes consécutives différent suivant la tension d'électrode, chacune des étapes procédant à des tensions suffisamment distantes entre elles pour permettre la mesure de temps de transition distincts.* On opère de la même façon que dans le cas (b). Néanmoins la condition limite à l'électrode (17) est remplacée pour le système (4) par la relation

$$i(t) = (n_1 + n_2) F D_{A_1} \left(\frac{\partial a_1(r, t, i(t))}{\partial r} \right)_{r=r_0} + n_2 F D_{B_1} \left(\frac{\partial b_1(r, t, i(t))}{\partial r} \right)_{r=r_0} \quad (19)$$

avec D_{B_1} et $b_1(r, t, i(t))$ respectivement le coefficient de diffusion et la concentration instantanée à la distance r de l'espèce B_1 . Il vient dès lors

$$\frac{n_1 + n_2}{n_1} = \frac{Z_{s,1}^{i(t)}(r_0, \tau_{s,1} + \tau_{s,2})}{Z_{s,1}^{i(t)}(r_0, \tau_{s,1})} \quad (20)$$

où $Z_{s,1}^{i(t)}(r_0, \tau_{s,1} + \tau_{s,2})$ est donné par l'éqn. (14) avec $\theta = \tau_{s,1} + \tau_{s,2}$.

3. RÉGIME DE DIFFUSION CYLINDRIQUE

RIUS, POLO ET LLOPIS¹⁴ ont obtenu l'expression $[a^0 - a_1(r_0, t, i^0)]$ en régime de diffusion cylindrique lorsqu'une seule substance dépolarisante est présente en solution. Si l'on suppose que l'inégalité $(D_{A_1} t / r_0^2)^{\frac{1}{2}} < 1$ est réalisée^{14,18}, ce qui est le cas généralement, on trouve, en appliquant le théorème de DUHAMEL²² aux relations valables en électrolyse sous courant constant, que

$$a_1^0 n_1 F \sqrt{D_{A_1}} = Z_{c,1}^{i(t)}(r_0, \tau_{c,1}) \quad (21)$$

et

$$Z_{c,1}^{i(t)}(r_0, \tau_{c,1}) \equiv \frac{1}{\sqrt{\pi}} \int_0^{\theta - \tau_{c,1}} i(t') \left\{ \frac{1}{(\theta - t')^{\frac{1}{2}}} - \frac{\sqrt{\pi}}{2} \left(\frac{D_{A_1}}{r_0^2} \right)^{\frac{1}{2}} + \frac{3}{8} \left(\frac{D_{A_1}}{r_0^2} \right) (\theta - t')^{\frac{1}{2}} - \frac{3\sqrt{\pi}}{8} \left(\frac{D_{A_1}}{r_0^2} \right)^{\frac{1}{2}} (\theta - t') \dots \right\} dt' \quad (22)$$

où $\tau_{c,1}$ est le temps de transition mesuré en régime de diffusion cylindrique.

Par un traitement analogue à celui de PETERS ET LINGANE¹⁸ basé sur la définition de la couche de diffusion différentielle, $\delta_{c,1}$ dans un champ de diffusion cylindrique, on obtient des relations semblables à (16), (18) et (20) mais où cependant $\delta_{s,1}$, $Z_{s,p}^{i(t)}$ et $Z_{s,1}^{i(t)}$ sont respectivement remplacés par $\delta_{c,1}$, $Z_{c,p}^{i(t)}(r_0, \sum_{p=1}^n \tau_{c,p})$ et $Z_{c,1}^{i(t)}(r_0, \tau_{c,1} + \tau_{c,2})$.

4. APPLICATIONS

(a) $i(t) = \rho t^P \quad (-1 < P)$

Pour un semblable programme, on trouve en intégrant (14) et (22)

$$Z_{s,1}^{\rho t^P}(r_0, \tau_{s,1}) \equiv \rho P! \tau_{s,1}^{P+\frac{1}{2}} \left\{ \frac{1}{(P + \frac{1}{2})!} - \frac{1}{(P + 1)!} \left(\frac{D_{A1} \tau_{s,1}}{r_0^2} \right)^{\frac{1}{2}} + \frac{1}{(P + \frac{3}{2})!} \left(\frac{D_{A1} \tau_{s,1}}{r_0^2} \right) - \frac{1}{(P + 2)!} \left(\frac{D_{A1} \tau_{s,1}}{r_0^2} \right)^{\frac{3}{2}} \dots \right\} \quad (23a)$$

$$Z_{c,1}^{\rho t^P}(r_0, \tau_{c,1}) \equiv \rho P! \tau_{c,1}^{P+\frac{1}{2}} \left\{ \frac{1}{(P + \frac{1}{2})!} - \frac{1}{2(P + 1)!} \left(\frac{D_{A1} \tau_{c,1}}{r_0^2} \right)^{\frac{1}{2}} + \frac{3}{8(P + \frac{3}{2})!} \left(\frac{D_{A1} \tau_{c,1}}{r_0^2} \right) - \frac{3}{8(P + 2)!} \left(\frac{D_{A1} \tau_{c,1}}{r_0^2} \right)^{\frac{3}{2}} \dots \right\} \quad (23b)$$

Dans le cas où le courant imposé est de la forme $\rho t^{\frac{1}{2}}$, il vient à partir des expressions précédentes que

$$Z_{s,1}^{\rho t^{\frac{1}{2}}}(r_0, \tau_{s,1}) \equiv \frac{\rho \sqrt{\pi}}{2} \tau_{s,1} \left\{ 1 - \frac{4}{3\sqrt{\pi}} \left(\frac{D_{A1} \tau_{s,1}}{r_0^2} \right)^{\frac{1}{2}} + \frac{1}{2} \left(\frac{D_{A1} \tau_{s,1}}{r_0^2} \right) - \frac{8}{15\sqrt{\pi}} \left(\frac{D_{A1} \tau_{s,1}}{r_0^2} \right)^{\frac{3}{2}} \dots \right\} \quad (24a)$$

$$Z_{c,1}^{\rho t^{\frac{1}{2}}}(r_0, \tau_{c,1}) \equiv \frac{\rho \sqrt{\pi}}{2} \tau_{c,1} \left\{ 1 - \frac{2}{3\sqrt{\pi}} \left(\frac{D_{A1} \tau_{c,1}}{r_0^2} \right)^{\frac{1}{2}} + \frac{3}{16} \left(\frac{D_{A1} \tau_{c,1}}{r_0^2} \right) - \frac{1}{5\sqrt{\pi}} \left(\frac{D_{A1} \tau_{c,1}}{r_0^2} \right)^{\frac{3}{2}} \dots \right\} \quad (24b)$$

Ces deux dernières valeurs ont pu être établies ailleurs par une méthode d'application moins générale que celle proposée ici²¹.

(b) $i(t) = i^0(t) \quad (0 \leq t \leq t_1)$
 $i^0(t) + i^1(t - t_1) \quad (t_1 \leq t \leq t_2)$
 \vdots
 $i^0(t) + i^1(t - t_1) \dots + i^q(t - t_q) \dots + i^j(t - t_j) \quad (t_j \leq t \leq t_{j+1})$

Lorsque le programme consiste en impulsions successives de formes variées on peut facilement justifier à partir des expressions (14) et (22) le principe d'additivité admis par MURRAY ET REILLEY¹¹. On montre en effet de façon tout à fait générale que

$$\int_{t_q}^{\theta} i^q(t' - t_q) F(\theta - t') dt' = \int_0^{\theta - t_q} i^q(t'') F(\theta - t_q - t'') dt'' \quad (25)$$

où la valeur de la fonction $F(\theta - t')$ peut être obtenue par comparaison entre la

relation (25) et (14) ou (22). Il en résulte que l'on a aussi bien pour un mode de diffusion sphérique, cylindrique que linéaire

$$Z_1^{i(t)}(r_0, \tau_1) = \sum_{q=0}^j Z_1^{i^q}(r_0, \tau_1 - t_q) \quad (26)$$

avec $t_0 = 0$. L'absence d'indice s ou c affectant les grandeurs $Z_1^{i(t)}$ et τ_1 dans l'éqn. (26) et par la suite indique que les relations concernées sont valables en régime de diffusion cylindrique et sphérique. Il apparaît clairement à partir de ce qui précède que lorsque les impulsions i^q choisies sont d'amplitudes constantes, on est ramené au cas de la fonction en escalier traitée par MURRAY ET REILLEY¹¹.

(c) Notons enfin, comme l'ont fait remarquer MURRAY ET REILLEY¹¹ qu'il est possible de représenter toute fonction analytique par un polynôme du type

$$i(t) = \sum_{n=0}^{\infty} k_n t^{n/2} = k_0 + k_1 t^{1/2} + k_2 t \dots \quad (27)$$

De même tout programme de forme (b) est susceptible par un choix judicieux des amplitudes $i^0, i^1, \dots, i^q, \dots, i^j$ et de chacun des intervalles $t_1, t_2 - t_1, t_{j+1} - t_j$, de reproduire les fonctions $i(t)$ les plus variées, périodiques, continues ou discontinues. Dès lors, selon que l'on se sert d'un train d'impulsions ou d'une série polynomiale en puissance de $t^{1/2}$ on est amené à utiliser les relations (23) ou (26) présentées plus haut.

5. DÉTERMINATION DU COURANT COMPENSANT LES EFFETS LIÉS À LA NON-LINÉARITÉ DU CHAMP DE DIFFUSION

On se limite, dans cette détermination, aux cas usuels où l'inégalité $(D_{A_1} t / r_0^2)^{1/2} < 1$ est satisfaite. Sachant que toute densité de courant $i(t)$ [$i(t)$ étant une fonction analytique en t] peut être représentée par un polynôme de la forme (27), on introduit cette valeur dans les expressions (14) et (22) que l'on intègre ensuite. En partant des formules (23) il apparaît aussitôt que les solutions de (14) et (22) dans les conditions choisies sont des polynômes de puissance croissante en $\tau_1^{1/2}$

$$Z_1^{i(t)}(r_0, \tau_1) = l_1(k_0)\tau_1^{1/2} + l_2(k_0, k_1)\tau_1 + l_3(k_0, k_1, k_2)\tau_1^{3/2} + \dots \quad (28)$$

dont les coefficients $l_n(k_0, k_1, \dots, k_{n-1})$ sont fonction de $k_0, k_1, k_2, \dots, k_{n-1}$ (cf. appendice A 1). Il devient alors possible de résoudre (28) pour les variables k_n dès le moment où l'on s'est fixé à l'avance la fonction $Z_1^{i(t)}$ sous la forme d'un polynôme dont les coefficients l_n appartiennent aux termes d'ordre n en $\tau^{1/2}$ (cf. appendice A 2).

Dans le cas où

$$Z_1^{i(t)}(r_0, \tau_1) = \frac{2i^0\tau_1^{1/2}}{\sqrt{\pi}}$$

on trouve que les programmes $i(t)$ de la forme

$$i_s(t) = i^0 \left[1 + \frac{2}{\sqrt{\pi}} \left(\frac{D_{A_1} t}{r_0^2} \right)^{1/2} \right] \quad (29a)$$

$$i_c(t) = i^0 \left[1 + \frac{1}{\sqrt{\pi}} \left(\frac{D_{A_1} t}{r_0^2} \right)^{1/2} - \frac{1}{8} \left(\frac{D_{A_1} t}{r_0^2} \right) \dots \right] \quad (29b)$$

satisfont respectivement sur l'électrode de géométrie sphérique et cylindrique à la relation de SAND¹⁰,

$$\sqrt{\tau_1} = \frac{n_1 F \sqrt{\pi D_{A_1}} a_1^0}{2i^0} \tag{30}$$

De même les valeurs

$$i_s(t) = \varrho \sqrt{t} \left[1 + \frac{\sqrt{\pi}}{2} \left(\frac{D_{A_1} t}{r_0^2} \right)^{\frac{1}{2}} \right] \tag{31a}$$

$$i_c(t) = \varrho \sqrt{t} \left[1 + \frac{\sqrt{\pi}}{4} \left(\frac{D_{A_1} t}{r_0^2} \right)^{\frac{1}{2}} - \frac{1}{12} \left(\frac{D_{A_1} t}{r_0^2} \right) + \dots \right] \tag{31b}$$

imposées respectivement à l'électrode de forme sphérique et cylindrique satisfont à l'expression

$$\tau_1 = \frac{2n_1 F \sqrt{D_{A_1}} a_1^0}{\varrho \sqrt{\pi}} \tag{32}$$

associée à la fonction réponse

$$Z_1^{i(t)}(r_0, \tau_1) = \varrho \frac{\sqrt{\pi}}{2} \tau_1$$

Par récurrence aux relations (29) (31) et à partir de l'expression (1) on trouve que les densités de courant de la forme suivante

$$i_s(t) = i_l(t) + \frac{1}{\sqrt{\pi}} \sqrt{\frac{D_{A_1}}{r_0^2}} \int_0^t \frac{i_l(t')}{(t-t')^{\frac{1}{2}}} dt' = i_l(t) + \sqrt{\frac{D_{A_1}}{r_0^2}} Z_1^{i(t)}(0, t) \tag{33a}$$

$$i_c(t) = i_l(t) + \frac{1}{2\sqrt{\pi}} \sqrt{\frac{D_{A_1}}{r_0^2}} \int_0^t \frac{i_l(t')}{(t-t')^{\frac{1}{2}}} dt' - \frac{1}{8} \frac{D_{A_1}}{r_0^2} \int_0^t i_l(t') dt' \simeq i_l(t) + \frac{1}{2} \sqrt{\frac{D_{A_1}}{r_0^2}} Z_1^{i(t)}(0, t) \tag{33b}$$

valables respectivement sur électrode sphérique et cylindrique correspondent aux relations générales

$$Z_{s,1}^{i_s(t)}(r_0, t) = Z_1^{i_l(t)}(0, t) = \frac{1}{\sqrt{\pi}} \int_0^{\theta-t} \frac{i_l(t')}{(\theta-t')^{\frac{1}{2}}} dt' = n_1 F \sqrt{D_{A_1}} [a_1^0 - a_1(r_0, t, i_s(t))] \tag{34a}$$

$$Z_{c,1}^{i_c(t)}(r_0, t) = Z_1^{i_l(t)}(0, t) = \frac{1}{\sqrt{\pi}} \int_0^{\theta-t} \frac{i_l(t')}{(\theta-t')^{\frac{1}{2}}} dt' = n_1 F \sqrt{D_{A_1}} [a_1^0 - a_1(r_0, t, i_c(t))] \tag{34b}$$

grâce auxquelles on détermine le temps de transition ($\theta = \tau$ pour $a_1 = 0$) quelle que soit l'allure du programme $i_l(t)$ que l'on aurait appliqué à l'électrode plane.

Qu'advient-il cependant lorsque l'on impose un courant de la forme (33) à un système contenant un dépolarisant X_n dont le coefficient de diffusion D_{X_n} est différent de D_{A_1} . Posons

$$\frac{\sqrt{D_{X_n}} - \sqrt{D_{A_1}}}{\sqrt{D_{X_n}}} = h_n^{(1)}; \quad \frac{D_{X_n} - D_{A_1}}{D_{X_n}} = h_n^{(2)} \dots \tag{35}$$

substituons dans l'expression (14) D_{X_n} à D_{A_1} et introduisons y la valeur $i_s(t)$ donnée par l'éqn. (33a) lorsque $i_l(t) = \varrho t^p$. Grâce à l'expression (6) on trouve, pour un temps d'électrolyse t ,

$$Z_{s,x_n}^{i_s(t)}(r_0, t) = \rho P! t^{P+\frac{1}{2}} \left\{ \frac{1}{(P + \frac{1}{2})!} - \frac{h_n^{(1)}}{(P+1)!} \left(\frac{Dx_n t}{r_0^2} \right)^{\frac{1}{2}} + \frac{h_n^{(1)}}{(P + \frac{3}{2})!} \left(\frac{Dx_n t}{r_0^2} \right) - \dots \right\} \quad (36a)$$

En procédant de la même manière en régime de diffusion cylindrique, compte tenu de (33b) et (22) il vient

$$Z_{c,x_n}^{i_c(t)}(r_0, t) = \rho P! t^{P+\frac{1}{2}} \left\{ \frac{1}{(P + \frac{1}{2})!} - \frac{h_n^{(1)}}{2(P+1)!} \left(\frac{Dx_n t}{r_0^2} \right)^{\frac{1}{2}} + \frac{2h_n^{(1)} + h_n^{(2)}}{8(P + \frac{3}{2})!} \left(\frac{Dx_n t}{r_0^2} \right) \dots \right\} \quad (36b)$$

6. DISCUSSION

La quantité de dépolarisant qui se décharge par unité de surface, diffuse à partir d'un certain volume de solution au voisinage de l'électrode. Ce volume croît d'autant plus vite, avec l'extension de la couche de diffusion, que la courbure moyenne de l'électrode est grande. Il en résulte un apport diffusif de matière vers l'électrode augmentant dans les mêmes proportions et supérieur, dans tous les cas, à la quantité de substance qui diffuserait vers l'électrode plane ($r_0 \rightarrow \infty$) pour la même densité de courant $i(t)$. Les temps de transition, mesurés en régime de diffusion sphérique (éqns. 13, 14) et cylindrique (éqns. 21, 22) sont de ce fait plus grands que ceux que l'on observerait en régime de diffusion linéaire (éqn. 2), toutes autres conditions égales.

Toutefois cet apport massique supplémentaire obtenu à l'électrode non plane pour un système à un seul dépolarisant A_1 peut être entièrement compensé si l'on se fixe des valeurs de la densité de courant de la forme $i_s(t)$ ou $i_c(t)$ (éqns. (33)), supérieures aux valeurs $i_l(t)$ imposées à l'électrode plane. Des relations particulièrement simples existent entre ces nouveaux courant $i_s(t)$ ou $i_c(t)$ et le rayon r_0 ainsi que l'extension $\delta_{l,1}$ de la couche de diffusion en régime linéaire. On trouve en effet, en portant dans (33) l'expression correspondant à (16) pour $\delta_{l,1}$, que

$$i_s(t) = i_l(t) \left(1 + \frac{\delta_{l,1}}{r_0} \right) \quad (37a)$$

$$i_c(t) = i_l(t) \left(1 + \frac{1}{2} \frac{\delta_{l,1}}{r_0} - \dots \right) \quad (37b)$$

Etant donné la condition $(DA_1 t / r_0^2)^{\frac{1}{2}} < 1$ il est généralement permis de se limiter aux deux premiers termes des développements (33b) et (37b) sans commettre une erreur appréciable*.

Les densités de courant $i_s(t)$ sur électrode sphérique, $i_c(t)$ sur électrode cylindrique, et $i_l(t)$ sur électrode plane ont par conséquent la propriété de réaliser dans leurs modes de diffusion respectifs une même concentration superficielle $a_1(r_0$ ou $0, t, i(t))$ du dépolarisant A_1 pour un temps d'électrolyse t identique. Or par définition¹¹ les valeurs $a_1(r_0$ ou $0, t, i(t))$ sont liées aux fonctions réponses $Z_{s,1}^{i_s(t)}$, $Z_{c,1}^{i_c(t)}$, $Z_{l,1}^{i_l(t)}$ dont l'emploi s'avère souvent utile dans le traitement des systèmes relativement compliqués^{9,11} (programmes à impulsions multiples, réactions de décharge successives, etc.). Il ressort de ce

* En négligeant les termes du troisième rang et de rang supérieur dans les éqns. (29b), (31b) et (33b) on commet une erreur relative sur la valeur de la fonction réponse $Z_{c,1}^{i_c(t)}$ ($= Z_{l,1}^{i_l(t)}$) inférieure à 5% pour $(DA_1 t / r_0^2)^{\frac{1}{2}} \leq 0.80$ et inférieure ou égale à 1% pour $(DA_1 t / r_0^2)^{\frac{1}{2}} \leq 0.35$.

fait qu'une même valeur de la fonction réponse est conservée dans les trois régimes diffusifs considérés (éqns. 34). C'est d'ailleurs en partant d'une telle condition que la forme des programmes $i_s(t)$ et $i_c(t)$ a été calculée.

Les densités de courant $i_s(t)$ et $i_c(t)$ jouissent cependant d'une autre propriété particulière. Il peut se produire en effet que D_{A_1} dans les éqns. (33) prenne une valeur différente de celle du coefficient de diffusion D_{X_n} de l'espèce dépolarisante X_n . On montre dans ces conditions que $i_s(t)$ et $i_c(t)$ modifient d'une manière très simple la fonction réponse de X_n . L'examen comparé des relations (23) et (36) prouve effectivement que $Z_{s, X_n}^{i_s(t)}$ et $Z_{c, X_n}^{i_c(t)}$ conservent une forme polynomiale équivalente à celle qui s'obtiendrait pour $i_i(t)$ appliqué à l'électrode sphérique ou cylindrique. Toutefois la somme des termes correctifs d'ordres successifs en $(D_{X_n} t / r_0^2)^{1/2}$ est multipliée par le facteur $h_n^{(1)} = (\sqrt{D_{X_n}} - \sqrt{D_{A_1}}) / \sqrt{D_{X_n}}$. Ceci n'est pas rigoureux pour un mode de diffusion cylindrique (36b) mais peut néanmoins être admis en bonne approximation étant donné les conditions $(D_{X_n} t / r_0^2)^{1/2} < 1$ et $0 \leq h_n^{(1)} \leq 1$ (soit $D_{X_n} > D_{A_1}$).

Considérons les trois cas distincts suivants:

(a) $D_{A_1} \simeq 0$ soit $h_n^{(1)} = 1$: dans ces conditions $i_s(t) = i_c(t) = i_i(t)$ et comme prévu les expressions (36) et (23) sont identiques.

$$(b) 0.90 \leq \frac{D_{A_1}}{D_{X_n}} \leq 1.10 \quad \text{soit} \quad h_n^{(1)} < |0.05|$$

Compte tenu de la précision des mesures on peut admettre que les termes liés à la symétrie non linéaire du mode de diffusion sont totalement compensés dans l'éqn. (36). On est ramené aux égalités (34).

$$(c) D_{A_1} \neq D_{X_n} \quad \text{soit} \quad h_n^{(1)} > |0.05|$$

La somme des termes correctifs dans (36) n'est que partiellement compensée ($D_{X_n} > D_{A_1}$) ou surcompensée ($D_{A_1} > D_{X_n}$).

Des trois cas envisagés ci-dessus, seule la condition $h_n^{(1)} < |0.05|$ possède un certain intérêt pratique. Cependant l'état (c) se présente dans quelques uns des systèmes discutés brièvement ci-après.

(1) *Réaction de décharge isolée irréversible.* L'unique espèce dépolarisante présente en solution est A_1 . Dans ces conditions, bien que $i_s(t)$, $i_c(t)$ ou $i_i(t)$ déterminent respectivement (avec D_{A_1} connu à $\pm 10\%$) une même valeur de la fonction réponse et du temps de transition, la morphologie des courbes tension temps est le plus souvent modifiée. Pour une réaction totalement irréversible, on obtient sur les trois types d'électrode, sphérique, cylindrique et plane du même métal,

$$\frac{i_s(t)}{n_1 F a_1(r_0, t, i_s(t))} = k(E_1) \quad (38a)$$

$$\frac{i_c(t)}{n_1 F a_1(r_0, t, i_c(t))} = k(E_2) \quad (38b)$$

$$\frac{i_i(t)}{n_1 F a_1(o, t, i_i(t))} = k(E_3) \quad (38c)$$

où les fonctions $k(E)$ désignent les valeurs de la constante de vitesse (rapportée aux concentrations) pour une tension E_1 , E_2 ou E_3 mesurée par rapport à une électrode

de comparaison déterminée. Grâce à la connaissance de la fonction $k(E)$ et des relations (1), (34) il est aisé d'établir les équations des courbes tension-temps. Si la relation de Volmer est vérifiée on trouve également à partir de (38) après un temps d'électrolyse t

$$\ln \frac{i_o(t)}{i_i(t)} = \pm \frac{\alpha n_\alpha F}{RT} (E_1 - E_3) \quad (39a)$$

$$\ln \frac{i_c(t)}{i_i(t)} = \pm \frac{\alpha n_\alpha F}{RT} (E_2 - E_3) \quad (39b)$$

où α est le coefficient de transfert, n_α le nombre d'électrons associés à l'étape déterminante, les signes (+) et (-) correspondant respectivement à une réaction d'oxydation et de réduction. Tout écart aux relations (39) implique la non-validité des hypothèses de Volmer ou l'incidence d'un effet de double-couche électrochimique.

Il peut se produire que la décharge du dépolarisant A_1 mette en jeu deux étapes successives du type (4). A chacune de ces étapes correspond un temps de transition dont la valeur n'est pas modifiée selon que l'on soumette le système de géométrie sphérique à $i_s(t)$, de géométrie cylindrique à $i_c(t)$ et linéaire à $i_l(t)$. Ce résultat est facilement déduit des relations (5), (20) et (34).

(2) *Réaction de décharge isolée réversible.* On admet que A_1 et B_1 constituent les partenaires réactionnels du couple oxydo-réducteur électroactif. Si l'on impose dès lors les densités de courant de la forme $i_s(t)$, $i_c(t)$ et $i_l(t)$ et si de plus la condition $0.90 < D_{B_1}/D_{A_1} < 1.10$ est respectée, on trouve dans chacun des régimes diffusifs envisagés une même expression de la fonction réponse de A_1 et de B_1 . De la sorte les temps de transition $\tau_{l,A}$ et $\tau_{l,B}$ ainsi que la morphologie des courbes tension-temps sont conservées. Cependant lorsque l'écart relatif entre D_{B_1} et D_{A_1} est supérieur à 10%, les égalités (34) ne sont valables que pour l'espèce A_1 (D_{A_1} figurant dans $i_s(t)$ et $i_c(t)$). Quant à la fonction réponse de B_1 elle est modifiée de la façon indiquée en (36) et de ce fait le chronopotentiogramme est déformé.

(3) *Cas de plusieurs réactions de décharge successives.* Soit que l'on applique $i_s(t)$ et $i_c(t)$ au système comprenant plusieurs substances $A_1, A_2 \dots A_n \dots$ déchargées successivement à l'électrode. La valeur des densités de courant $i_s(t)$ et $i_c(t)$ est choisie de façon à compenser les termes correctifs dans l'expression de la fonction réponse d'un constituant A_n autre que A_1 . Compte tenu de (18) on observe que la valeur du temps de transition $\tau_{l,n}$ n'est pas conservée dans ces conditions.

Du point de vue pratique, le courant croissant en racine carrée du temps, $k_1 t^{\frac{1}{2}}$, qui se superpose dans (29) à i^0 peut être produit par l'intermédiaire de dispositifs expérimentaux connus. Ceux-ci ont été décrits en détails dans un travail antérieur³. Le courant de forme $k_2 t$ qui s'ajoute dans (31) à la valeur $\rho\sqrt{t}$, s'obtient sans difficultés techniques particulières⁴. Quant aux grandeurs k_1 et k_2 , elles dépendent du facteur d'amplitude (i^0 ou ρ), du coefficient de diffusion et du rayon r_0 de l'électrode. Ces deux dernières valeurs sont généralement déterminées de façon indépendante et connues avec une marge d'erreur inférieure à 10%.

CONCLUSION

Le fait de se fixer d'avance la valeur de la fonction réponse que l'on désire obtenir à l'électrode sphérique ou cylindrique pourrait conduire à un certain nombre d'appli-

cations nouvelles de la méthode chronopotentiométrique dans différents domaines. D'une part en effet, on sait que l'existence d'une fonction réponse de forme peu compliquée conditionne l'emploi de cette méthode en tant qu'instrument d'analyse électrochimique rapide. D'autre part, il apparaît qu'une évolution simple en fonction du temps, imposée aux concentrations à la surface de l'électrode, serait susceptible de faciliter l'interprétation de certains phénomènes superficiels associés à la décharge.

REMERCIEMENTS

Nous remercions ici Monsieur le Professeur L. GIERST dont les conseils nous ont aidé dans l'élaboration du présent travail.

APPENDICE

 (a) *Champ de diffusion sphérique*

Evaluation des coefficients l_n figurant dans l'éqn. (25)

$$l_1(k_0) = \frac{2}{\sqrt{\pi}} k_0$$

$$l_2(k_0, k_1) = \frac{\sqrt{\pi}}{2} k_1 - k_0 \left(\frac{D_{A_1}}{r_0^2} \right)^{\frac{1}{2}}$$

$$l_3(k_0, k_1, k_2) = \frac{4}{3\sqrt{\pi}} \left\{ k_2 - \frac{\sqrt{\pi}}{2} k_1 \left(\frac{D_{A_1}}{r_0^2} \right)^{\frac{1}{2}} + k_0 \left(\frac{D_{A_1}}{r_0^2} \right) \right\}$$

⋮

$$l_n(k_0, k_1 \dots k_{n-1}) = \sum_{m=1}^n \frac{1}{\binom{n}{m}!} \left\{ (-1)^{m-1} k_{n-m} \left(\frac{n-m}{2} \right)! \left(\frac{D_{A_1}}{r_0^2} \right)^{(m-1)/2} \right\} \quad (\text{A1,a})$$

dont il résulte que

$$k_0 = \frac{\sqrt{\pi}}{2} l_1$$

$$k_1 = \frac{2}{\sqrt{\pi}} l_2 + l_1 \left(\frac{D_{A_1}}{r_0^2} \right)^{\frac{1}{2}}$$

$$k_2 = \frac{3\sqrt{\pi}}{4} l_3 + l_2 \left(\frac{D_{A_1}}{r_0^2} \right)^{\frac{1}{2}}$$

⋮

⋮

$$k_n = \frac{\left(\frac{n+1}{2} \right)!}{\binom{n}{2}!} l_{n+1} + l_n \left(\frac{D_{A_1}}{r_0^2} \right)^{\frac{1}{2}} \quad (l_0 = 0) \quad (\text{A2,a})$$

 (b) *Champ de diffusion cylindrique*

Evaluation des coefficients l_n figurant dans l'éqn. (25)

$$l_1(k_0) = \frac{2}{\sqrt{\pi}} k_0$$

$$l_2(k_0, k_1) = \frac{\sqrt{\pi}}{2} k_1 - \frac{1}{2} k_0 \left(\frac{DA_1}{r_0^2} \right)^{\frac{1}{2}}$$

$$l_3(k_0, k_1, k_2) = \frac{4}{3\sqrt{\pi}} \left\{ k_2 - \frac{\sqrt{\pi}}{4} k_1 \left(\frac{DA_1}{r_0^2} \right)^{\frac{1}{2}} + \frac{3}{8} k_0 \left(\frac{DA_1}{r_0^2} \right) \right\}$$

$$l_4(k_0, k_1, k_2, k_3) = \frac{1}{2} \left\{ \frac{3\sqrt{\pi}}{4} k_3 - \frac{1}{2} k_2 \left(\frac{DA_1}{r_0^2} \right)^{\frac{1}{2}} + \frac{3\sqrt{\pi}}{16} k_1 \left(\frac{DA_1}{r_0^2} \right) - \frac{3}{8} k_0 \left(\frac{DA_1}{r_0^2} \right)^{\frac{1}{2}} \right\} \quad (\text{A1,b})$$

dont il résulte que

$$k_0 = \frac{\sqrt{\pi}}{2} l_1$$

$$k_1 = \frac{2}{\sqrt{\pi}} l_2 + \frac{1}{2} l_1 \left(\frac{DA_1}{r_0^2} \right)^{\frac{1}{2}}$$

$$k_2 = \frac{3\sqrt{\pi}}{4} l_3 + \frac{1}{2} l_2 \left(\frac{DA_1}{r_0^2} \right)^{\frac{1}{2}} - \frac{\sqrt{\pi}}{16} l_1 \left(\frac{DA_1}{r_0^2} \right)$$

$$k_4 = \frac{8}{3\sqrt{\pi}} l_4 + \frac{1}{2} l_3 \left(\frac{DA_1}{r_0^2} \right)^{\frac{1}{2}} - \frac{1}{6\sqrt{\pi}} l_2 \left(\frac{DA_1}{r_0^2} \right) + \frac{1}{12} l_1 \left(\frac{DA_1}{r_0^2} \right)^{\frac{1}{2}} \quad (\text{A2,b})$$

RÉSUMÉ

Des relations mathématiques générales ont été dérivées, qui permettent d'obtenir les temps de transition chronopotentiométriques théoriques sur une électrode sphérique ou cylindrique pour un système de décharge contrôlé par la diffusion.

De cette façon, il est possible de déterminer la valeur des densités de courant qu'il faut imposer à ces électrodes afin de compenser en tout ou en partie les différents termes liés au caractère non linéaire du mode de diffusion.

SUMMARY

General mathematical relations are given for theoretical chronopotentiometric transition times on spherical or cylindrical electrodes in the case of diffusion-controlled systems.

In this way, it is possible to obtain current density values which have to be imposed at these electrodes in order to compensate fully or partly the different terms expressing the non-linear character of the diffusion field.

BIBLIOGRAPHIE

- 1 T. BERZINS ET P. DELAHAY, *J. Am. Chem. Soc.*, 75 (1953) 4205.
- 2 M. SENDA, *Rev. Polarog. (Kyoto)*, 4 (1956) 89.
- 3 H. HURWITZ ET L. GIERST, *J. Electroanal. Chem.*, 2 (1961) 128.
- 4 R. C. BOWERS, C. WARD, C. M. WILSON ET D. D. DEFORD, *J. Phys. Chem.*, 65 (1961) 672.
- 5 W. H. REINMUTH, *Anal. Chem.*, 32 (1960) 1509.
- 6 R. W. MURRAY ET C. N. REILLEY, *J. Electroanal. Chem.*, 3 (1962) 64.

- 7 A. C. TESTA ET W. H. REINMUTH, *Anal. Chem.*, 33 (1961) 1324.
- 8 Y. TAKEMORI, T. KAMBARA, M. SENDA ET I. TACHI, *J. Phys. Chem.*, 61 (1957) 968.
- 9 H. B. HERMAN ET A. J. BARD, *Anal. Chem.*, 35 (1963) 1121.
- 10 H. J. S. SAND, *Phil. Mag.*, 1 (1901) 45.
- 11 R. W. MURRAY ET C. N. REILLEY, *J. Electroanal. Chem.*, 3 (1962) 182.
- 12 H. HURWITZ, Abstract nr. 3.8 — 13e Réunion du C.I.T.C.E. (Rome), *Electrochim. Acta*, 7 (1962).
- 13 T. KAMBARA ET I. TACHI, *J. Phys. Chem.*, 61 (1957) 1405.
- 14 A. RIUS, S. POLO ET J. LLOPIS, *Anales Real Soc. Españ. Fis. Quím. (Madrid)*, 45B (1949) 2.
- 15 G. MAMANTOV ET P. DELAHAY, *J. Am. Chem. Soc.*, 76 (1954) 5323.
- 16 J. KOUTECKÝ ET J. CIZEK, *Collection Czech. Chem. Commun.*, 22 (1957) 914.
- 17 D. G. PETERS ET J. J. LINGANE, *J. Electroanal. Chem.*, 2 (1961) 1.
- 18 D. G. PETERS ET J. J. LINGANE, *J. Electroanal. Chem.*, 2 (1961) 249.
- 19 D. H. EVANS ET J. E. PRICE, *J. Electroanal. Chem.*, 5 (1963) 77.
- 20 M. G. MCKEON, *J. Electroanal. Chem.*, 4 (1962) 93.
- 21 H. HURWITZ, *J. Electroanal. Chem.*, 2 (1961) 142.
- 22 H. S. CARSLAW ET J. C. JAEGER, *Conduction of Heat in Solids*, Clarendon Press, London, 1959.
- 23 C. N. REILLEY, G. W. EVERETT ET R. H. JOHNS, *Anal. Chem.*, 27 (1955) 483.
- 24 H. HURWITZ, *J. Electroanal. Chem.*, 2 (1961) 328.
- 25 A. C. TESTA ET W. H. REINMUTH, *Anal. Chem.*, 33 (1961) 1320.
- 26 M. VON STACKELBERG, *Z. Elektrochem.*, 45 (1939) 466.

J. Electroanal. Chem., 7 (1964) 368-381

MEASUREMENT OF HYDROGEN ADSORPTION BY THE MULTIPULSE POTENTIODYNAMIC (MPP) METHOD*

S. GILMAN

General Electric Research Laboratory, Schenectady, New York (U.S.A.)

(Received February 20th, 1964)

INTRODUCTION

The detailed study of electrochemical processes occurring at a solid electrode require establishment of a highly reproducible surface state. In the past, each investigator has usually adopted some type of surface pre-treatment either preceding each individual measurement, or preceding an entire series of experiments (*e.g.*, one day's experimentation). These pre-treatments usually involve a combination of anodic and cathodic pulses of current (or potential) with the electrode in contact with either stirred or unstirred electrolyte. It has been observed, in the study of the hydrogen electrode in particular¹, that it is possible to obtain a variety of results depending on the particular pre-treatment.

One method which has been favored recently for the reproducibility of the data obtained, is the use of a continuous triangular potential-time sweep²⁻⁷. If the amplitude and frequency are carefully controlled, it is possible to set up a *steady state* condition for which the conditions of adsorption and electrochemical reaction are similar during each of the ascending sweeps and each of the descending sweeps (but results obtained for the two different potential directions are not necessarily equal). The approach is limited in that it becomes impossible to define boundary conditions for mass-transport of active species from the solution under these complicated experimental conditions. A second limitation is that at high sweep rates, overlap of reactions involving different rate constants will occur².

GILMAN⁸ has assumed that the active surface produced under the conditions of *cyclic voltammetry* is due to the elimination of contaminants from the electrode surface at the high (≥ 1.6 V) potentials often achieved during the anodic portion of the cycle and that *deactivation* is associated with the subsequent adsorption of impurities from solution. An earlier interpretation was that *deactivation* was due to *surface recrystallization*². Independent of the interpretation, it is possible to establish a reproducible surface state (as demonstrated by the constancy of hydrogen-deposition^{8,9}, *oxygen adsorption*^{8,9} and electrode capacity⁹) by the use of precisely controlled potential

* This work was made possible by the support of the Advanced Research Projects Agency (Order No. 247) through the United States Army Engineer Research and Development Laboratories under Contract Number DA-44-009-ENG-4909.

pulses. It is then possible to preserve the *active* surface (to within a few per cent *deactivation*) for 100 sec or more, depending on solution purity⁸. These principles have been embodied in the MPP method which has been found useful in the study of CO adsorption and electrochemical oxidation^{6,8,10}, of "oxygen adsorption"⁹ and of anion adsorption^{11,12}. It is the purpose of this paper to demonstrate how the method may be applied to studies of the hydrogen-electrode. In particular, this work establishes that linear potential time sweeps of much higher speeds than attained previously² may be employed in the study of the hydrogen-electrode if a repetitive signal is avoided.

EXPERIMENTAL

Equipment and chemicals

The equipment, test vessel, etc., have been described previously⁸. Reagent-grade perchloric acid and permanganate-treated triply-distilled water were used in preparing the stock solution of 1 *N* perchloric acid. Solutions of HCl were prepared by addition of reagent-grade HCl to the 1 *N* perchloric acid stock solution. The platinum wire used as the working electrode was of 0.020 in. diameter and had a geometric area of 0.064 cm².

Procedures

Measurements were made at 30° in a thermostatted water-bath. All potentials are referred to a reversible hydrogen electrode in 1 *N* perchloric acid. The potential sequences impressed on the working electrode appear in Fig. 1. The procedures followed during each step of the sequences are summarized in Table 1.

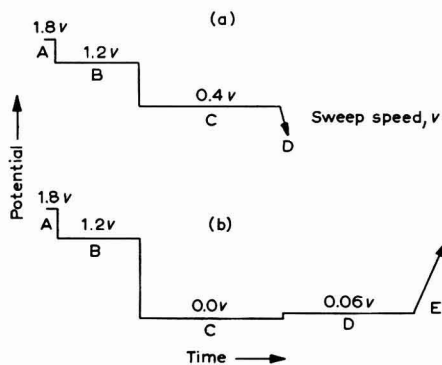


Fig. 1. Potential sequences applied to the working electrode in this study.

RESULTS

I. Hydrogen-deposition during a linear cathodic sweep

Signal sequence I, Table 1, was employed in making these measurements. The trace obtained with a sweep speed, v , of 50 V/sec appears in Fig. 2. The area under such a trace to point (a) will be denoted as sQ_H . The area bounded by the trace, by the dashed horizontal line and the dashed vertical line through point (a) will be denoted as Q_{SH} (the symbol sQ_H was used previously⁵). The quantity Q_{SH} is the charge corresponding to deposition of atomic hydrogen on the surface which precedes large-

TABLE I
PROCEDURES FOLLOWED DURING POTENTIAL SEQUENCES

Sequence	Fig.	Step (refers to Fig.)	Procedure	Purpose
I	1a	A	1) Bubble argon through solution with paddle-stirring for 2 sec.	1) To remove previously adsorbed species from the electrode surface and to deposit a passive "oxygen" film which hinders re-adsorption.
		B	2) Bubbling and stirring continued for 1/2 min. Solution then allowed to become quiescent for 1-1/2 additional min.	2) To retain passive "oxygen" film while sweeping away molecular oxygen and rejected impurities from Step A.
		C	3) The solution is unstirred. T_C is of 10 sec duration.	3) The surface is largely reduced within a few msec, exposing a reproducibly clean surface to the electrolyte.
		D	4) Apply linear cathodic sweep of speed v , and record resulting current-time trace.	4) Obtain the "hydrogen deposition" trace and measure charge under the curve.
II	1b	A	1) Same as step (1) of sequence I.	1) Same as step (1) of sequence I.
		B	2) Same as step (2) of sequence I.	2) Same as step (2) of sequence I.
		C	3) Solution is unstirred. Step C is of 10 sec duration.	3) The passive film is largely reduced within the first few msec. Hydrogen is deposited on the surface at a coverage corresponding to the potential of 0.0 V. The electrode reaches equilibrium with the adjacent solution which then contains dissolved hydrogen having a partial pressure of 1 atm.
		D	4) Solution is unstirred. T_D is chosen as 0 or 10 sec.	4) If T_D is chosen as 10 sec, the surface coverage with hydrogen falls to the proper value for 0.06 V. The electrode comes into equilibrium with the adjacent solution which then contains dissolved hydrogen corresponding to 0.01 atm partial pressure (Nernst equation).
		E	5) Apply linear anodic sweep of speed v and measure corresponding current-time trace.	5) Obtain "hydrogen oxidation" trace and measure area under curve.

scale evolution of molecular hydrogen. The horizontal line is an approximate correction for charging of the double-layer. For the particular working electrode used, Q_{SH} had the value 0.278 mC/cm^2 . It was previously demonstrated⁸ that Q_{SH} has a constant value for values of v as high as 800 V/sec . The limitation imposed by higher values of v is that point (a) of Fig. 2 becomes increasingly more difficult to estimate.

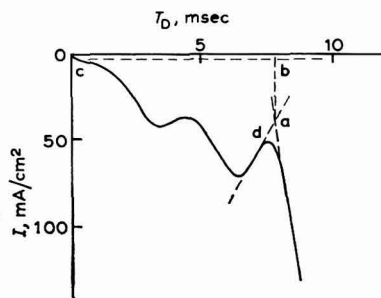


Fig. 2. Trace obtained during application of linear cathodic sweep D of sequence I, Table I; $v = 50 \text{ V/sec}$.

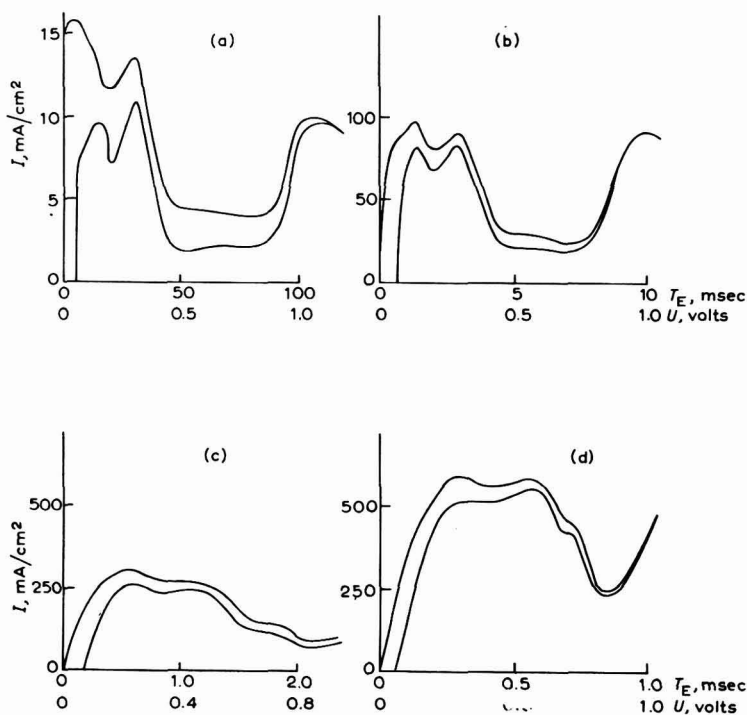


Fig. 3. Current-time traces obtained during application of linear anodic sweep E of sequence II, Table I. The upper and lower traces for any particular value of v correspond to initial potentials, U_0 of 0.0 and 0.06 V , respectively: (a), $v = 10 \text{ V/sec}$; (b), $v = 100 \text{ V/sec}$; (c), $v = 400 \text{ V/sec}$; (d), $v = 1000 \text{ V/sec}$.

II. Hydrogen-oxidation during a linear anodic sweep

Sequence II of Table I was used in making these measurements. After pre-treatment steps A and B, the electrode surface is reduced and allowed to equilibrate with the electrolyte at 0.0 V (step C). At the end of step C, the electrolyte adjacent to the surface contains dissolved hydrogen with a partial pressure of one atmosphere. During step D, the partial pressure of hydrogen is reduced to 0.01 atm (Nernst equation) if T_D is chosen larger than zero. During step E, a linear anodic sweep is applied to the electrode and a current-time trace is recorded. The sweep starts at initial potential $U_0 = 0.0$ V when $T_D = 0$ or at $U_0 = 0.06$ V when $T_D = 10$ sec. Sample traces corresponding to the two different initial potentials and to a range of sweep speeds appear in Fig. 3. The removal of most of the hydrogen adsorbed on the surface is clearly indicated in Fig. 3(a) by the decay of the current to a low plateau between approximately 0.4 V and 0.8 V. In this "double-layer region" the major coulombic processes are charging of the double-layer and oxidation of dissolved hydrogen². This removal of hydrogen by approximately 0.4 V is observed for very slow sweep speeds², and in this work for values of v approaching 200 V/sec. For higher values of v , the overvoltage is much increased as is obvious from Fig. 3(b)–3(d). The voltage drop due to internal resistance can only account for a few millivolts of the overvoltage under these conditions, and the balance must therefore be kinetic in origin. While the kinetics of hydrogen discharge will not be given further attention the amount of hydrogen adsorbed on the electrode surface will be analyzed through integration of the anodic traces.

The charge corresponding to the area under any trace from U_0 to 0.7 V (somewhat higher and into the "double-layer" region for $v = 1000$ and 2000 V/sec) will be referred to as ${}_aQ_H$. This charge contains contributions from oxidation of hydrogen initially

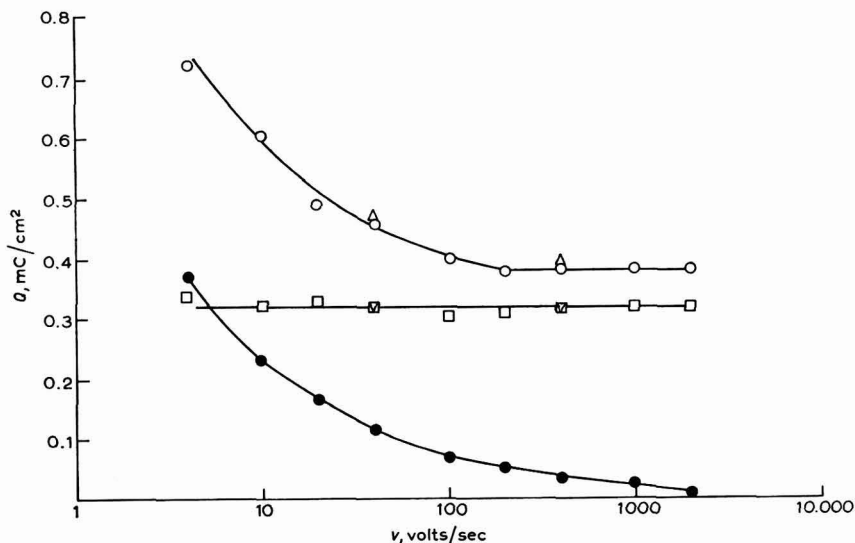


Fig. 4. Variation of ${}_aQ_H$ and of $Q_{D'}$ with the logarithm of sweep speed; \circ and \square , ${}_aQ_H$, $U_0 = 0.0$ V and 0.06 V, absence of dissolved Cl^- ; Δ and ∇ , ${}_aQ_H$, $U_0 = 0.0$ V and 0.06 V, presence of 0.1 M dissolved Cl^- ; \bullet , $Q_{D'}$, $U_0 = 0.0$ V, calculated.

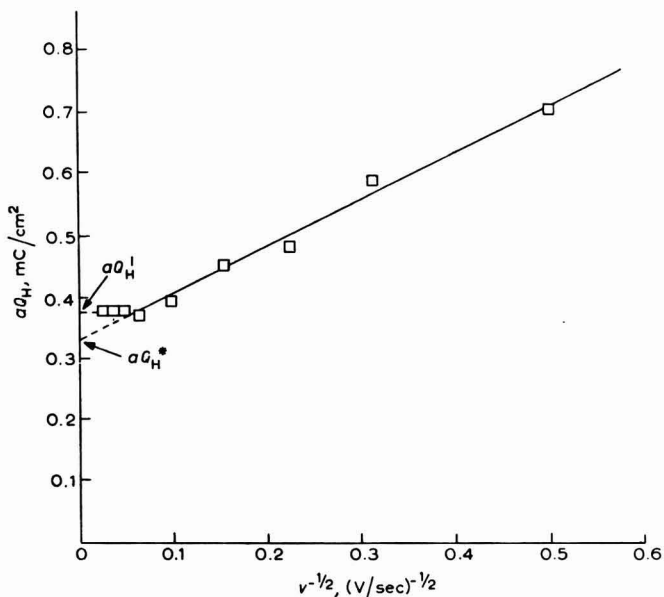


Fig. 5. Variation of aQ_H (for $U_0 = 0.0$ V) with sweep speed.

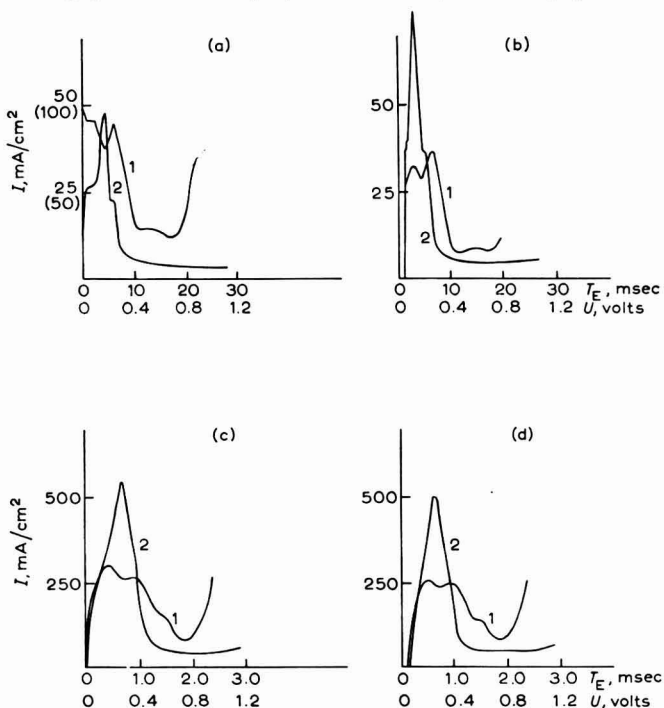


Fig. 6. Current-time traces obtained during application of linear anodic sweep E of sequence II, Table I. Traces marked (1) and (2) were obtained in the absence of dissolved chloride ion, and in the presence of 0.1 M chloride ion, respectively: (a), $v = 40$ V/sec, $U_0 = 0.0$ V (current scale in parenthesis for trace 2); (b), $v = 40$ V/sec, $U_0 = 0.06$ V; (c), $v = 400$ V/sec, $U_0 = 0$ V; (d), $v = 400$ V/sec, $U_0 = 0.06$ V.

adsorbed at U_0 , from molecular hydrogen which diffuses to the electrode during anodic sweep E, and from charging of the ionic double-layer. Values of ${}_aQ_H$ are plotted against $\log v$ in Fig. 4, and against $v^{-1/2}$ in Fig. 5.

When the experiments described above were repeated in the presence of added HCl (0.1 M), the linear anodic traces obtained were considerably different from those obtained in the absence of chloride ion. Sample traces obtained at initial potentials of 0.0 and 0.06 V are displayed in Fig. 6. The main effect, as previously noted^{11,12,13}, is for the hydrogen to be removed at lower potentials during the sweep. The effect is attributed to adsorption of chloride during the linear anodic sweep^{11,12,13}. Values of ${}_aQ_H$ for initial potentials of 0.0 and 0.06 V, and for 0.1 M HCl, 1 N HClO₄ are plotted on Fig. 4.

DISCUSSION

I. Hydrogen-oxidation during a linear anodic sweep

A. Initial potential of 0.06 V. ${}_aQ_H$ may be expressed as the sum of three terms:

$${}_aQ_H = Q_H + Q_D + Q_{dl} \quad (1)$$

where Q_H = charge corresponding to the amount of hydrogen deposited on the surface at the initial potential U_0 (0.06 V, in this case);

Q_D = charge corresponding to the molecular hydrogen which diffuses to the electrode and is oxidized during the linear anodic sweep to 0.7 V;

Q_{dl} = capacitive charge added to the ionic double-layer during the linear anodic sweep to 0.7 V.

If all of the hydrogen deposited at 0.06 V is removed during the anodic sweep, Q_H should be independent of v . Q_{dl} is relatively small and may be assumed approximately constant with v . Then, ideally, variations in ${}_aQ_H$ with sweep speed should reflect corresponding variations in Q_D . The *maximum possible* value of Q_D for any value of v , (Q_D'), may be calculated assuming transport control by semi-infinite linear diffusion. The hydrogen diffusion current is given by¹⁴:

$$I_D' = dQ_D'/dt = nFACD^{1/2}/\pi^{1/2}t \quad (2)$$

Hence

$$Q_D' = 2 nFACD^{1/2}t^{1/2}/\pi^{1/2} \quad (3)$$

where n = number of electrons involved in the oxidation of one hydrogen molecule = 2;

F = Faraday constant;

A = electrode area;

C = initial concentration of dissolved hydrogen;

D = diffusion constant of hydrogen;

t = diffusion time.

Taking $A = 1 \text{ cm}^2$, $C = 6.2 \times 10^{-9} \text{ moles/cm}^3$ (ref. 15, assuming a hydrogen partial pressure of 0.01 atm, and applicability of Henry's Law), $D = 4.1 \times 10^{-5} \text{ cm}^2/\text{sec}$ (ref. 16), and $t = T_E$ (duration of anodic sweep to 0.7 V), we obtain from eqn. (3)

$$Q_D' = 8.8 \times 10^{-6} T_E^{1/2} C/\text{cm}^2. \quad (4)$$

For $v = 4 \text{ V/sec}$, $T_E = 0.18 \text{ sec}$, and $Q_D' = 0.0038 \text{ mC/cm}^2$. This value is just barely significant compared with ${}_aQ_H$ at 4 V/sec. At higher values of v , Q_D' becomes entirely

insignificant, and diffusion of hydrogen to the electrode cannot make any appreciable contribution to ${}_aQ_H$ from $v = 10\text{--}2000$ V/sec. The value of ${}_aQ_H$ over this range is indeed found to be constant to within an average deviation of 2% with an average value of 0.318 mC/cm² (Fig. 4). This result contrasts with the 30% reduction in Q_H observed by WILL AND KNORR² on covering the range, $v = 10\text{--}100$ V/sec, using a continuous triangular sweep. The frequency-independence of our measurements may probably be attributed to a number of experimental conditions:

1. The contribution of diffusion has been made negligible by the choice of an initial potential of 0.06 V which was controlled to within 1 mV.

2. The surface state of the electrode was precisely reproduced by means of the pre-treatment.

3. The amount of hydrogen deposited on the surface at the initial potential was closely reproduced because of (2) and because the initial potential was carefully controlled.

4. "Overlap" of the "hydrogen-adsorption" and "oxygen-adsorption" regions was avoided by use of a single-sweep technique as opposed to the continuous triangular signal².

B. Initial potential of 0.0 V. Unlike the situation for an initial potential of 0.06 V, the values of ${}_aQ_H$ measured for $U_0 = 0.0$ V show a marked variation with sweep speed (see Figs. 4 and 5) up to a value of $v = 200$ V/sec. An average limiting experimental value (${}_aQ_H'$) of 0.38 mC/cm² with an average deviation of 1%, is obtained between $v = 200$ and 2000 V/sec. Referring to eqn. (1) and recalling the constancy of 2% in ${}_aQ_H$ measured for $U_0 = 0.06$ V, we must conclude that it is probably only the term Q_D (corresponding to hydrogen which diffuses to the electrode during the linear anodic sweep) which is responsible for the low-frequency variation in ${}_aQ_H$. As previously, Q_D' (semi-infinite linear diffusion) is taken as the *maximum possible* value of Q_D , and employing eqn. (3) with the appropriate constants, we obtain for one atmosphere of hydrogen:

$$Q_D' = 8.8 \times 10^{-4} T E^{\frac{1}{2}} \text{ C/cm}^2. \quad (5)$$

Values of Q_D' obtained by means of eqn. (5) are plotted in Fig. 4. It can be seen that the variations of ${}_aQ_H$ for $v < 200$ V/sec are paralleled by those of Q_D' . However for $200 < v < 2000$ V/sec, Q_D' remains significantly greater than 0 while ${}_aQ_H$ remains constant. This comparison suggests that Q_D is making no significant contribution to ${}_aQ_H$ at high frequencies.

A second representation of such data has been recently suggested by OSTERYOUNG *et al.*¹⁷. The oxidation of hydrogen not originally adsorbed on the surface is assumed transport-limited and the corresponding current is assumed to be described by the Ševčík equation¹⁸. The charge Q_D is then assumed to be described by the integrated Ševčík equation and hence proportional to $v^{-\frac{1}{2}}$. Since Q_D (by these simple assumptions) must reach a limiting value of zero at $v^{-\frac{1}{2}} = 0$, the y -intercept of the ${}_aQ_H - v^{-\frac{1}{2}}$ plot ought to correspond to terms $Q_H + Q_{ad}$ of eqn. (1). We shall call this extrapolated value ${}_aQ_H^*$ and note that it has the value 0.33 mC/cm² which is not much smaller than the experimental high-frequency value of 0.38 mC/cm². While the difference is not great it is quite significant for the following reasons:

1. The lower value of ${}_aQ_H$ for $U_0 = 0.0$ V (corresponding to 1 atm of hydrogen, obtained by extrapolation, ${}_aQ_H^*$), is almost identical to the value for $U_0 = 0.06$ V

(corresponding to 0.01 atm of hydrogen). This suggests that the surface coverage with hydrogen is identical for both potentials and hydrogen partial pressures.

2. The higher value of aQ_H obtained at high frequencies (aQ_H') is independent of frequency for $200 < \nu < 2000$ V/sec, and suggests that molecular hydrogen oxidation is relatively slow in this frequency range. One possibility is that the rate of re-adsorption of hydrogen may be limiting.

Possibility (1) is in disagreement with the high-frequency data presented here. Also if we take the ratio of experimental values of aQ_H' for $U_0 = 0.0$ and 0.06 V, we obtain the value 1.2, which is exactly the value obtained by taking the ratio of hydrogen surface coverages measured by means of pseudocapacity¹⁹. We therefore tentatively conclude that extrapolation of low-frequency results is not precise for this system simply because the conditions of simple diffusion-control break down. Measurements of adsorption of methanol⁵ and of CO⁸ have been found even less frequency-dependent relative to the concentration of adsorbent. This latter effect has been ascribed to the action of the passive oxygen film in blocking adsorption during the anodic sweep. These situations suggest that direct measurement of adsorption by means of high sweep speeds is, in general, to be preferred over extrapolation methods where a choice is possible.

From the high-frequency values of aQ_H , we may obtain values of Q_H for $U_0 = 0.0$ and 0.06 V if correction is made for charging of the electrical double-layer. Assuming an average capacity of $70 \mu\text{F}/\text{cm}^2$ (ref. 2), and a voltage span from U_0 to 0.7 V, values of 0.27 and 0.33 are obtained for Q_H for $U_0 = 0.06$ V and 0.0 V, respectively.

C. *Initial potential of 0.0 or 0.06 V in presence of dissolved chloride ion.* Figure 4 reveals that at any frequency and for $U_0 = 0.0$ or 0.06 V, the value of aQ_H is virtually identical in the presence or absence of dissolved chloride ion. Intuitively, this is not surprising in view of the observation that chloride ion is rapidly and reversibly adsorbed and desorbed and that the equilibrium value of surface coverage with chloride ion at potentials lower than 0.125 V is zero under our conditions^{11,12}. It is therefore reasonable to expect, in the absence of adsorbed chloride ion, that similar quantities of hydrogen will be deposited at $U_0 = 0.0$ or 0.06 V. The chloride might be expected only to influence the removal of the hydrogen during the subsequent anodic sweep in which potential range chloride does adsorb¹². This it does do — the effect is to cause the removal of hydrogen at *lower* potentials (Fig. 6) than occurs in the absence of adsorbed chloride.

II. Hydrogen-deposition during a linear cathodic sweep

It has been shown that the charge corresponding to hydrogen deposited before large-scale evolution of molecular hydrogen is a quantity which is highly reproducible and constant with frequency up to 800 V/sec⁸. The charge, Q_{SH} , after correction for charging of the double-layer is 0.28 mC/cm². If the value of Q_H obtained for $U_0 = 0.0$ V is taken as corresponding to a mono-layer of hydrogen, Q_{SH} corresponds to approximately 85% of a mono-layer.

SUMMARY

By means of the MPP method, it is possible to study hydrogen adsorption on an extremely reproducible platinum surface under well-defined conditions of mass-transport. Non-repetitive linear potential-time sweeps of speeds up to 2000 V/sec result in

readily-interpretable current-time traces. The addition of chloride ion to the solution is shown quantitatively not to affect the amount of hydrogen deposited at 0.0 or 0.06 V.

REFERENCES

- 1 A. N. FRUMKIN, *Advances in Electrochemistry and Electrochemical Engineering*, Vol. 3., Interscience Publishers, New York, 1963, chapter V.
- 2 F. G. WILL AND C. A. KNORR, *Z. Elektrochem.*, 64, (1960) 258.
- 3 W. VIELSTICH, *Z. Instrumentenk.*, 71 (1963) 29.
- 4 M. W. BREITER, *J. Elektrochem. Soc.*, 109 (1962) 425.
- 5 M. W. BREITER AND S. GILMAN, *J. Elektrochem. Soc.*, 109 (1956) 622.
- 6 S. GILMAN, *J. Phys. Chem.*, 66 (1962) 2657.
- 7 Z. GALUS, H. Y. LEE AND R. N. ADAMS, *J. Electroanal. Chem.*, 5 (1963) 17.
- 8 S. GILMAN, *J. Phys. Chem.*, 67 (1963) 78.
- 9 S. GILMAN, *Electrochim. Acta*, in press.
- 10 S. GILMAN, *J. Phys. Chem.*, 67 (1963) 1898.
- 11 S. GILMAN, *Studies of Anion Adsorption by the MPP Method, Part I*, submitted to *J. Phys. Chem.*
- 12 S. GILMAN, *Studies of Anion Adsorption by the MPP Method, Part II*, submitted to *J. Phys. Chem.*
- 13 M. W. BREITER, G. E. Research Lab. Report 63-RL-3310M, April 1963.
- 14 H. A. LAITINEN AND I. M. KOLTHOFF, *J. Am. Chem. Soc.*, 61 (1939) 3344.
- 15 N. A. LANGE, *Handbook of Chemistry*, McGraw-Hill, New York, 10th ed., 1961.
- 16 G. TAMMANN AND V. JESSEN, *Z. Anorg. Allgem. Chem.*, 179 (1929) 135.
- 17 R. A. OSTERYOUNG, G. LAUER AND F. C. ANSON, *J. Electrochem. Soc.*, 110 (1963) 926.
- 18 A. ŠEVČIK, *Collection Czech. Chem. Commun.*, 13 (1948) 349.
- 19 M. W. BREITER, H. KAMMERMAIER AND C. KNORR, *Z. Elektrochem.*, 60(1956) 37.

J. Electroanal. Chem., 7 (1964) 382-391

COMPARISON OF ALTERNATING VOLTAGE POLAROGRAPHY WITH
ALTERNATING CURRENT POLAROGRAPHY

HENRY H. BAUER AND DAVID C. S. FOO

Section of Agricultural Chemistry, The University of Sydney (Australia)

(Received February 3rd, 1964)

INTRODUCTION

In alternating current polarography the impedance of the measuring circuit exerts undesirable effects: *i.e.*, a.c. polarographic waves are reduced in height as compared with the base-current¹, calibration curves for quantitative analysis are made non-linear², and the frequency-dependence of the wave height can be misleading³. For these reasons, the observed wave-height cannot be directly compared with the theoretical value in studies of the mechanism of an electrode process. Even when care is taken to make the circuit impedance small — *e.g.*, using condensers to act as low-impedance paths for the alternating current⁴ — the results are not really satisfactory. For quantitative work, it is necessary to monitor the alternating voltage at the polarographic cell¹ and this makes measurements considerably more time-consuming and laborious, apart from the additional apparatus required.

It was recently suggested^{5,6} that these difficulties could be avoided by using a technique (alternating voltage (a.v.) polarography) in which the cell is subjected to an alternating current of controlled value and the resulting alternating voltage measured, the obverse of the procedure adopted in a.c. polarography. Whereas in the latter case the circuit impedance makes it impossible to control satisfactorily the alternating voltage, in the former it is a simple matter to control the magnitude of the alternating current. The present communication illustrates some of the advantages obtained with the new arrangement. Superior calibration curves are obtained, so that analysis becomes feasible over a wider range of concentrations, and the results obtained agree well with the theoretical values for the faradaic impedance.

EXPERIMENTAL

The a.c. polarograph used was of the conventional type fully described elsewhere⁷. The requirements for alternating voltage polarography have been previously discussed⁵ and details given of the instruments actually used⁶ in the present work.

RESULTS AND DISCUSSION

(1) Calibration curves for quantitative analysis

The height of an a.c. polarographic wave is by definition⁸ the difference between the total current at the summit potential and the base-current. In analytical work, there is no advantage to be gained by preparing calibration curves in terms of a.c.

wave-height rather than in terms of the total current (i_T) at the summit potential; the sensitivity and accuracy of the method depend on the relative magnitude of i_T and of the base-current i_B in either case. In the first case, where $(i_T - i_B)$ is plotted as a function of concentration, the curve is theoretically linear at low concentrations, but the accuracy of determination of $(i_T - i_B)$ is poor as i_T and i_B are similar in magnitude. In the second case, where i_T is recorded as a function of concentration, the curve is non-linear at low concentrations and has a smaller slope than in the former case, but the precision with which i_T can be measured is greatly superior to that obtainable for $(i_T - i_B)$. Therefore, since these two procedures do not differ in the overall accuracy obtainable, it is advantageous in terms of time and convenience to measure merely i_T . The calibration curves shown in the following figures were obtained in this way.

A.v. polarography gives a measure of V , the alternating voltage across the cell, obtained by the imposition of the alternating current I . It is necessary for the present purpose to compare these values with conventional a.c. polarograms, using a comparable scale. Now, the a.c. polarogram gives a value of I' obtained when alternating voltage V' is superposed; for comparison, we have computed for a.v. polarography the magnitude of the current required if the voltage is to equal V' . This *equivalent*

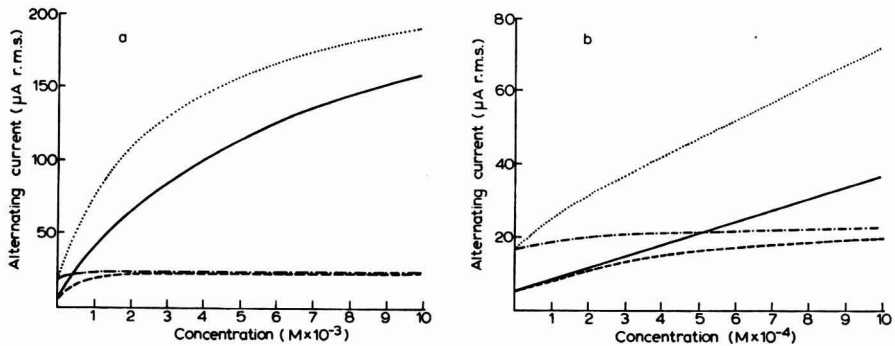


Fig. 1a,b. Calibration curves for Tl(I) in 0.5 M H_2SO_4 : \cdots , a.v. polarography, 250 c/sec; $---$, a.c. polarography, 250 c/sec; $—$, a.v. polarography, 60 c/sec; $- - -$, a.c. polarography, 60 c/sec.

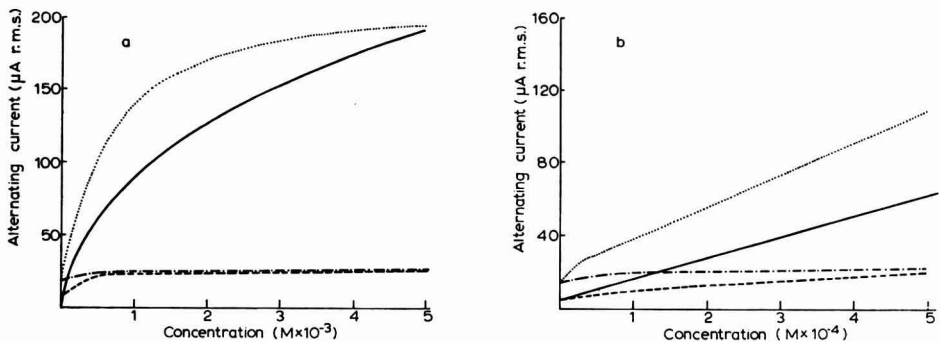


Fig. 2a,b. Calibration curves for Cd(II) in 1 M HCl: \cdots , a.v. polarography, 250 c/sec; $---$, a.c. polarography, 250 c/sec; $—$, a.v. polarography, 60 c/sec; $- - -$, a.c. polarography, 60 c/sec.

current $I(V'/V)$ is the quantity shown in the calibration curves obtained with the a.v. polarograph.

Figures 1 and 2 show calibration curves obtained by a.c. and by a.v. polarography, at frequencies of 60 and 250 c/sec for Tl(I) in 0.5 *M* H₂SO₄ and Cd(II) in 1 *M* HCl respectively; Figs. 1a and 2a show the whole concentration range studied, Figs. 1b and 2b show in more detail these curves at lower concentrations. It is necessary to emphasize that the comparison of the two techniques by means of figures such as these is illustrative, and not quantitative. The a.v. polarograph eliminates the effects exerted by circuit impedance in a.c. polarography, and the degree of improvement shown, *e.g.*, in calibration curves, depends entirely on the actual circuit-impedance of the particular a.c. polarograph used. In the present case, the a.c. polarograph employed was one which has been in use in these laboratories for routine work over several years, and has been hitherto regarded as a satisfactory compromise between accuracy and convenience; for detailed studies of particular systems, this instrument was always modified to incorporate a vacuum-tube millivoltmeter monitoring the cell voltage and an arrangement for phase-angle measurements.

With the above proviso, inspection of Figs. 1 and 2 demonstrates the superiority of the a.v. polarograph which, it should be noted, is as convenient and rapid in use as the simple a.c. polarograph. The a.c. polarograph gave curves that were useful for analytical purposes at concentrations up to *ca.* 10^{-3} *M* at 60 c/sec, but the curves at 250 c/sec were quite unsatisfactory. The a.v. polarograph gave much better curves in all cases, permitting accurate analysis at concentrations greater by a factor of 10 at 60 c/sec, and even at 250 c/sec analysis was readily possible.

Accepting the qualitative nature of this comparison (see above), it is nevertheless apparent that the a.v. polarograph is clearly a superior instrument for analysis, and appreciably extends the concentration range over which analysis is feasible.

(2) *Absolute test of the performance of the a.v. polarograph*

The performance of the a.v. polarograph can be assessed in absolute terms by comparing the measured voltages with those calculated on the basis of the equation for a fast electron-transfer process

$$I = \frac{n^2 F^2 A C V (\omega D)^{1/2}}{4RT}$$

where I and V have already been defined, ω is the angular frequency of the alternating signal, D the diffusion coefficient of the depolarizer, C the concentration of the latter in the bulk of the solution, and n , F , R , and T have their usual significance.

Table 1 reports values of I for the reduction of Tl(I) on the basis of theory and from the results obtained with the a.c. and a.v. polarographs; the experimental results were corrected for base-current contribution by assuming a faradaic phase-angle of $\pi/4$ which is known⁷ to be a reasonable postulate for this system at the frequencies employed. No correction was made for series resistances, since this would vitiate the comparison of the two techniques; consequently, agreement between theory and experiment can only be expected at low concentrations. It is clear from Table 1 that the a.v. polarograph gives results that are in reasonable agreement with theory, whereas the a.c. polarographic measurements deviate considerably. It is worth noting that, whereas in a.c. polarography a poor performance of the circuit

TABLE I
REDUCTION OF Tl(I) IN 0.5 M H₂SO₄

Concentration (M)	Faradaic alternating current					
	at 60 c/sec			at 250 c/sec		
	A.v. polarography (μ A r.m.s.)	A.c. polarography (μ A r.m.s.)	Theoretical (μ A r.m.s.)	A.v. polarography (μ A r.m.s.)	A.c. polarography (μ A r.m.s.)	Theoretical (μ A r.m.s.)
4×10^{-5}	1.69	—	1.53	3.55	—	3.12
1×10^{-4}	4.17	2.13	3.82	7.1	—	7.8
1.5×10^{-4}	6.16	2.48	5.73	10.2	—	11.7
2×10^{-4}	8.5	3.79	7.64	14.8	—	15.6
4×10^{-4}	14.4	9.42	15.3	25.7	3.7	31.2
1×10^{-3}	33	14.5	38.2	55.5	6.03	78
1.5×10^{-3}	47.8	16.3	57.3	75.4	6.48	117
2×10^{-3}	63.4	16.6	76.4	92.9	6.96	156
4×10^{-3}	95.4	18.3	153	125	7.26	312
1×10^{-2}	155	20.1	382	175	7.98	780

(high impedance) is reflected in currents that are too small, in a.v. polarography the equivalent current may be too high — for instance, if the voltage-measuring device across the cell, or the choke in the d.c. polarizing circuit, has too low an impedance compared to that of the cell^{5,6}. The results indicate such an effect, since the experimental results show more deviation from the theoretical ones at 60 c/sec, than at 250 c/sec where the cell impedance is lower.

(3) Control of the alternating current in a.v. polarography

The magnitude of the alternating current is controlled by a large resistance in series with the cell. This resistance should be much greater than the cell impedance, as should the impedance of the voltage-measuring device across the cell, and the choke in the d.c. polarizing circuit. For work involving measurement of the base-current at low frequencies, these impedances must be of the order of megohms since the cell

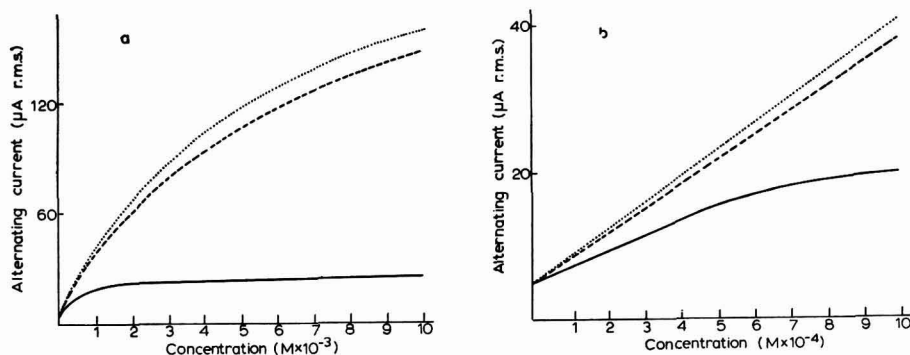


Fig. 3a,b. Calibration curves for Tl(I) in 0.5 M H₂SO₄: ···, a.v. polarography, current-controlling resistance, 1 MΩ; — — —, idem, 0.05 MΩ; —, a.c. polarography.

impedance can be of the order of tens of thousands of ohms. At the summit potential, however, the cell impedance is lowered by the presence of the faradaic admittance, so that lower values of the relevant impedances can be used in analytical work. Figure 3 illustrates this situation; it is clear that the deviations observed need not be important in analytical work.

ACKNOWLEDGEMENT

This work was made possible by a grant from the Australian Atomic Energy Commission whose support is gratefully acknowledged.

SUMMARY

It has been shown that the a.v. polarograph provides much better calibration curves than does the a.c. polarograph. The concentration range amenable to analysis is greatly extended, and useful results are obtainable at higher frequencies. The convenience and rapidity of a.v. polarography are the same as with the simplest type of a.c. polarograph.

The circuit arrangement in a.v. polarography is not particularly critical. While for absolute precision, various parts of the circuit need to have impedances so high that the cell impedance is by comparison negligible, the results are not greatly affected if this condition is not rigorously met. By contrast, the impedance of the measuring circuit in a.c. polarography is a critical matter — for instance, it is necessary to use as small a voltage-dropping resistance as possible, and even a decrease from 100 to 10 Ω in this value improves the performance considerably; this makes necessary higher amplification, and it is one illustration of the advantage of a.v. polarography that no amplification at all is required when using readily available vacuum-tube millivoltmeters.

Comparison of the results with theory demonstrated that the a.v. polarograph gives information that can be quantitatively interpreted in terms of the electrode processes occurring. In a.c. polarography, this can be done only with a more elaborate arrangement in which the cell voltage is continuously monitored, making the investigation considerably more time-consuming and laborious.

REFERENCES

- 1 H. H. BAUER AND P. J. ELVING, *Anal. Chem.*, 30 (1958) 334.
- 2 B. BREYER, F. GUTMANN AND S. HACOBIAN, *Australian J. Sci. Res.*, A3 (1950) 567.
- 3 A. KALYANASUNDARAM, *Proc. Indian Acad. Sci.*, 33A (1951) 316.
- 4 B. BREYER, F. GUTMANN AND S. HACOBIAN, *Australian J. Sci. Res.*, A4 (1951) 595.
- 5 H. H. BAUER, *Rev. Polarog. (Kyoto)*, 11 (1963) 58.
- 6 H. H. BAUER, *Australian Conference on Electrochemistry, 1963*, Pergamon Press, London, to be published.
- 7 B. BREYER AND H. H. BAUER, *Alternating Current Polarography and Tensammetry*, Wiley/Interscience Publishers Inc., New York, 1963.
- 8 B. BREYER, T. BIEGLER AND H. H. BAUER, *Rev. Polarog. (Kyoto)*, 11 (1963) 50.

J. Electroanal. Chem., 7 (1964) 392-397

AN AUTOMATIC AMPEROMETRIC METHOD FOR THE SPECIFIC ENZYMATIC DETERMINATION OF GALACTOSE

HARRY L. PARDUE AND CHRISTOPHER S. FRINGS

Department of Chemistry, Purdue University, Lafayette, Indiana (U.S.A.)

(Received February 14th, 1964)

INTRODUCTION

Conventional methods for the quantitative determination of galactose are based on the reducing power of the sugar. As such, the methods are not specific and specialized procedures have been developed for galactose in the presence of other reducing agents⁸. These procedures usually depend upon separation steps or selective conversion of the interfering substances to inactive products. For example, galactose can be determined in samples containing glucose by selective oxidation of the latter prior to the determination of galactose. The accuracy of such procedures is limited by the selectivity of reagents or by the completeness of separations. At best, the methods are quite time-consuming. Improved methodology is needed when galactose is to be determined in the presence of other reducing materials.

COOPER *et al.*³ have described an enzyme, galactose oxidase, which catalyzes the oxidation of galactose by oxygen. Work by these authors and by AVIGAD *et al.*¹ has demonstrated that the enzyme exhibits selectivity for galactose over a wide variety of other sugars. In addition, they showed that hydrogen peroxide is a product of the enzyme reaction. They suggested selective quantitative procedures for galactose based on the measurement of the hydrogen peroxide produced using a coupled enzyme reaction. ROREM AND LEWIS⁷ have described a test-paper for the qualitative identification of galactose based on the same reaction. These reports do not provide sufficient information for an evaluation of the reliability of the methods for galactose and in addition the quantitative procedures are tedious and time-consuming.

In a recent paper a reaction sequence employing the iodine-iodide redox system was described for detecting the hydrogen peroxide produced in the enzymatic oxidation of glucose⁴. In the present work, aspects of this reaction pertinent to its use for the determination of galactose have been studied extensively. Optimum conditions for the determination of galactose in the concentration range 50-500 p.p.m. have been established. In addition automatic measurement equipment described earlier^{4,5} has been adapted to the determination of the rate of oxidation of galactose.

The enzyme reaction takes place in the presence of an excess of iodide and catalytic amounts of Mo(VI). Hydrogen peroxide formed, rapidly oxidizes iodide to iodine. The formation of iodine is detected continuously using a pair of polarized platinum electrodes. Automatic control equipment measures the time required for a small

predetermined amount of iodine to be produced. The measured time is related to the galactose concentration. Under the suggested conditions the reciprocal of the measured time is a linear function of galactose concentration.

The resulting procedure for galactose is simple. Results reported demonstrate the relative standard deviations and accuracy of the method to be within 2%. The analysis time is strongly dependent upon galactose concentration; it ranges from a few seconds for high concentrations to about ten minutes for the lowest concentrations for which data are reported.

EXPERIMENTAL

Reagents

All solutions are prepared in water which has been passed through a mixed cation-anion exchange resin bed. Potassium iodide solutions are stored at 4°.

Galactose standards. Standard galactose solutions are prepared by diluting a 1000 p.p.m. solution prepared by dissolving 1.000 g of glucose-free D(+) galactose (Sigma Chemical Company, St. Louis, Mo.) in water and diluting to 1 l.

Phosphate buffer. Potassium dihydrogen phosphate (1.4 g) is dissolved in 900 ml of water. The solution is adjusted to pH 7.0 with NaOH and diluted to 1 l with water.

Galactose oxidase. 2 mg of galactose oxidase dry powder (Worthington Biochemical Corporation, Freehold, New Jersey) is triturated in a mortar and diluted to 50 ml with the buffer solution and filtered through a Whatman No. 1 filter paper. Three drops of a 1000 p.p.m. galactose solution is added to the enzyme solution and the solution is mixed thoroughly.

Molybdate catalyst. 3.2 g of ammonium molybdate $[(\text{NH}_4)_6\text{Mo}_7\text{O}_{24}\cdot 4\text{H}_2\text{O}]$ and 1.4 g of potassium dihydrogen phosphate are dissolved in 900 ml of water. The solution is adjusted to pH 7.0 with sodium hydroxide and diluted to 1 l with water.

Potassium iodide. Potassium iodide (16.5 g) is dissolved in water and diluted to 100 ml.

Apparatus

The apparatus used is similar to that described originally for the amperometric determination of glucose⁵. The auxiliary relay and timer used in the original work are replaced by the commercially available reaction rate adapter for the Concentration Comparator (Model QRR Reaction Rate Adapter, E. H. Sargent and Co., Chicago, Ill.) which performs the same function. The polarizing voltage is 300 mV and the current is measured across a 4000 Ω precision resistor (R in Fig. 1 of ref. 5). The pre-measurement bias is 8 mV and the measurement bias is 2 mV. Other components of the apparatus are the same as those described previously.

All samples and reagents are handled with tuberculine-type hypodermic syringes.

Procedure

All samples and reagents are adjusted to the working temperature of 35.0° by immersion in a water bath. The sample compartment is rinsed with deionized water before and after each run.

Exactly 1 ml of galactose sample and 0.50 ml of galactose oxidase solution are added to the sample cell and the stirrer is started. Then 0.25 ml of Mo(VI) and 0.25 ml

of potassium iodide solution are added rapidly. The starter switch on the reaction rate adapter is closed momentarily. From this point the measurement is completed automatically.

When the measurement is complete the reaction time in seconds is read from the timer. The sample concentration is then read from a plot of reciprocal time *vs.* galactose concentration.

RESULTS AND DISCUSSION

Quantitative data

Plots of reaction rate (reciprocal time) *vs.* galactose concentration between 50 and 500 p.p.m. approach linearity. Therefore, a calibration curve can be constructed from two standards. Typical quantitative data for aqueous galactose solutions are given in Table I. Experimentally-determined values of galactose concentration are obtained

TABLE I
AUTOMATIC RESULTS FOR AQUEOUS GALACTOSE SOLUTIONS

Galactose in 2-ml sample (μg)		Reciprocal time ($\text{sec}^{-1} \cdot 10^3$)	Rel. S.D. (%)	Error (%)
Taken	Found			
100	90	4.90	—	-10
200	202	8.24	1.7	+ 1.0
300	296	10.9	0.43	- 1.3
400	—	14.2	1.2	—
500	502	17.1	1.3	+ 0.4
600	596	19.4	1.4	- 2.3
700	—	23.0	0.13	—
1000	966	30.7	1.4	- 3.4

from a calibration curve constructed from the 200 and 350 p.p.m. standards. Between 100 and 350 p.p.m., errors are within about 2%. At the ends of the range, a curve drawn through all the points is concave toward the concentration axis. This is the reason for the large negative error at 50 p.p.m. and the moderate error at 500 p.p.m. The relative standard deviation of the method is within 2% throughout this concentration range. Accuracies of this order are obtained throughout the range by using one more standard near each end of the plot.

Amperometric response curve

Although the measurement times for the data in Table I are all within about 200 sec, actual analysis times range from 100 sec for the 500 p.p.m. sample to about 10 min for the 50 p.p.m. sample. This results from the fact that there is a lag between the time when substrate and enzyme are mixed and the time when the reaction rate reaches the maximum value limited by the galactose concentration. This induction period increases with decreasing galactose concentration. Under the conditions of this work, it ranges from a few seconds at 500 p.p.m. galactose to about 10 min at 50 p.p.m. galactose.

Because of this induction period the amperometric response curves are concave upward from the time axis only becoming linear after the induction period is ex-

ceeded. Rate measurements are made on the linear portion of the response curve. Otherwise the linear relationship between galactose concentration and measured reaction rate demonstrated in Table 1 does not hold. To automate the measurement step it is necessary to program the instrument so that all measurements will be made on the linear portion of the curve regardless of the galactose concentration.

It is observed experimentally that the absolute value of the indicator electrolysis current at which the curves become linear decreases with decreasing galactose concentration. Therefore, the magnitude of the pre-measurement current which provides reliable data for the highest galactose concentration of interest is satisfactory for all lower concentrations. The recommended pre-measurement current for the concentration range for which data are given is $2 \mu\text{A}$.

It is observed that a small amount of galactose added to the enzyme solution before measurements are to be made, reduces the length of the induction period. The quantity added in the procedure described above provides faster analyses and does not contribute significant errors.

Enzyme concentration

The effect of enzyme concentration on the procedure was investigated. As the enzyme concentration is increased above the 0.04 mg/ml level recommended, the curve becomes increasingly non-linear and the simple calibration procedure described above is not valid for the concentration range discussed here. This low enzyme concentration increases the induction period slightly. However, the advantage of a linear working curve far outweighs the slight disadvantage of the increased measurement time. For galactose concentrations below 50 p.p.m. it is desirable to work at higher enzyme concentrations to avoid excessively long measurement times.

Optimum pH

The effect of pH on the reaction was examined. The optimum range of 7.0-7.3 reported by COOPER *et al.*³ was confirmed.

Temperature dependence

The rate of reaction increases linearly with temperature between 20° and 50°. The slope of the plot is about 5% per degree at 30°. The temperature of 35° suggested above provides increased sensitivity for galactose. Also it is observed that at 35°, for a given galactose concentration, the induction period is only about two-fifths of that at 25°.

Comparison of methods

The measurement method described here has several important advantages when compared to other methods which could be applied to this reaction. It has two important advantages when compared to the conventional procedure in which the reaction is permitted to proceed for a predetermined time interval, and then is quenched and the extent of reaction measured. The method described here is both simpler and faster. Also the conventional method includes measurements during the induction period when the reaction rate has not reached the limiting rate imposed by the galactose concentration. The result is a non-linear working curve, concave toward the rate axis. In the present method the instrument is programmed to make the

rate measurement only after the reaction has reached its limiting value, and working curves are linear.

The method of BLAEDEL AND HICKS² should be applicable to this reaction so long as the downstream time is sufficient for the induction period of the lowest galactose concentration encountered to be overcome. The disadvantage is that the downstream time would be the same for all samples, both high and low. As a result, the more concentrated solutions with shorter induction periods would approach completion before the rate measurement was made and measured rates would be likely to give low results for galactose concentration. Also, the analysis times would be the same for all samples and would be limited by the most dilute one. In the present method the results for high concentrations are obtained within a few seconds.

The potentiometric method described by MALMSTADT AND PARDUE⁴ should be applicable to this system. However, the non-linearity of the potentiometric response combined with the initial non-linearity in reaction rate caused by the induction period would give a complex response curve. The choice of the proper point at which to begin the rate measurement to avoid the induction period would be one of trial and error and would be difficult at best. However, after measurement conditions are established the method should be perfectly satisfactory.

The slope method described recently⁶ should also be applicable to this reaction since the instrument is easily programmed to read the slope at a pre-selected point on the curve. The advantage of this method would be direct read-out of concentration data. This latter possibility is being investigated.

ACKNOWLEDGEMENT

This work was supported in part by a grant from the Indiana Elks.

SUMMARY

An automatic enzymatic method is described for the determination of galactose. The method is based on the catalysis by galactose oxidase of the oxidation of galactose. Hydrogen peroxide produced by the enzymatic reaction rapidly oxidizes iodide to iodine in the presence of Mo(VI).

The formation of iodine is detected amperometrically. Automatic control equipment provides direct read-out of the time required for a definite amount of iodine to be produced. The reciprocal of the measured time interval when plotted against the galactose concentration provides a linear working curve.

Automatic results for samples show relative standard deviations of about 2% over a range of 50–500 p.p.m. galactose.

REFERENCES

- 1 G. AVIGAD, C. ASENSIO, D. AMARAL AND B. L. HORECKER, *Biochem. Biophys. Res. Commun.*, 4 (1961) 474.
- 2 W. J. BLAEDEL AND G. P. HICKS, *Anal. Chem.*, 34 (1962) 388.
- 3 J. A. D. COOPER, W. SMITH, M. BACILA AND H. MEDINA, *J. Biol. Chem.*, 234 (1959) 445.
- 4 H. V. MALMSTADT AND H. L. PARDUE, *Anal. Chem.*, 33 (1961) 1040.
- 5 H. L. PARDUE, *Anal. Chem.*, 35 (1963) 1240.
- 6 H. L. PARDUE, *Anal. Chem.*, in press.
- 7 E. S. ROREM AND J. C. LEWIS, *Anal. Biochem.*, 3 (1962) 230.
- 8 H. SABOTKA AND C. P. STEWART, *Advances in Clinical Chemistry*, Vol. 5, Academic Press, New York, (1962), p. 28.

KINETIC PARAMETERS FROM IRREVERSIBLE POLAROGRAPHIC WAVES
IN PRESENCE OF MASS TRANSFER POLARIZATION

S. SATHYANARAYANA

Electrochemical Technology Laboratory, Department of Chemical Engineering, Indian Institute of Technology, Bombay-76 (India)

(Received February 22nd, 1964)

INTRODUCTION

A number of rigorous methods are available at the present time for the theoretical analysis of irreversible polarographic waves. Such an analysis is required to calculate the formal kinetic parameters (the standard rate constant, K_s , and the transfer coefficient, α) of an electrochemical reaction taking into account the slow rates of mass-transfer and charge-transfer phenomena. Among these methods may be mentioned those of MEIMAN¹, DELAHAY², KOUTECKÝ³ and more recently, RANGLES⁴, who has also reviewed the topic.

The analysis of irreversible polarographic waves as proposed by RANGLES merits further discussion and application, because in this form it seems to be the easiest of all available rigorous methods for calculating the kinetic parameters for the general case when the rate of the backward reaction is significant, *i.e.*, for a quasi-reversible (or partially irreversible) polarographic wave.

An approximate equation, simpler in form, for the irreversible polarographic wave has been developed by STROMBERG⁵; this is based on an earlier derivation by FRUMKIN⁶ of a similar equation for the totally irreversible polarographic wave.

The rigorous equation given by RANGLES for instantaneous current-potential curves⁴ as well as STROMBERG's approximate equation are applicable only for composite polarographic waves (*i.e.*, anodic-cathodic waves) and in the form given, are inapplicable for single waves (*i.e.* purely cathodic or anodic). The latter case, however, is more common in practice.

The present paper is an attempt to modify the equations given by RANGLES and by STROMBERG so that they are applicable for single waves (purely anodic or cathodic) and to compare the values of kinetic parameters obtained by the two modified equations when applied to experimental data.

THEORETICAL

The rigorous method

According to RANGLES⁴, for a reaction $O + n e \rightleftharpoons R$ which is of the first order in both directions, (either both O and R are soluble in the electrolyte or R is an amalgam-forming metal) the instantaneous current at the end of the drop life of a dropping

mercury electrode may be expressed as

$$\frac{i_t}{i_a} = \frac{1 - \exp nf\eta}{1 + r \exp nf\eta} \varphi(\chi) \quad (1)$$

where, i_t = instantaneous current at the end of the drop life, t being the drop time;

$r = i_a / i_a^{\leftarrow}$, where i_a and i_a^{\leftarrow} are the limiting-diffusion currents for the reduction of the substance O and oxidation of the substance R , respectively, the instantaneous value of the current at the end of the drop life being taken in both cases.

η = total polarization = $E - E_{\text{rev}}$, where E is the electrode potential corresponding to i_t , and E_{rev} is the reversible (equilibrium) potential of the electrode corresponding to the bulk concentrations of $O (= C_O^\circ)$ and $R (= C_R^\circ)$;

n = number of electrons involved in the rate determining step;

$f = F/RT$, where F is the Faraday.

The function $\varphi(\chi)$ has been tabulated by KOUTECKÝ (reproduced by DELAHAY in Table 4-1 of his book⁷) for various values of $\chi = 2Q\sqrt{t}$ where

$$Q = \sqrt{\frac{3}{7}} \left(\frac{K_f}{\sqrt{D_O}} + \frac{K_b}{\sqrt{D_R}} \right)$$

K_f and K_b being rate constants for the forward and backward directions, respectively, of the reaction $O + n e = R$.

It may be noted that K_f and K_b are related to the apparent standard rate constant, K_s (*i.e.*, neglecting the double-layer effect) and the apparent energy transfer coefficient, α , according to the following equations:

$$K_f = K_s \exp[-\alpha n f (E - E_f^\circ)]$$

$$K_b = K_s \exp[(1 - \alpha) n f (E - E_f^\circ)]$$

where E_f° is the formal standard potential of the couple O/R , which is, therefore, dependent on the nature and ionic strength of the supporting electrolyte also.

Let us now consider the case of a purely cathodic wave, *i.e.*, when $C_R^\circ = 0$. In other words, the substance R is initially absent in the solution. In this case, since i_a^{\leftarrow} is proportional to C_R° , the term r in eqn. (1) becomes infinite and hence the equation appears to be inapplicable.

However, since by the Nernst equation

$$C_O^\circ = C_R^\circ \exp [n f (E_{\text{rev.}} - E_f^\circ)]$$

and by the Ilkovič equation

$$|i_a^{\leftarrow}| = n F A C_R^\circ \sqrt{\frac{7 D_R}{3 \pi t}}$$

where t is the drop time, we get

$$r \exp nf\eta = \sqrt{\frac{D_O}{D_R}} \exp [n f (E - E_f^\circ)]$$

Hence, eqn. (1) may be written as

$$\frac{i_t}{i_a} = \frac{(1 - \exp nf\eta)\varphi(\chi)}{1 + \sqrt{\frac{D_o}{D_R}} \exp[nf(E - E_f^\circ)]} \quad (2)$$

The problem of analysis of a purely cathodic wave has been discussed also by HALE AND PARSONS¹⁴. However, in their equation for i_t/i_a , the term, $[\exp(nf\eta)]$, in the right-hand side of eqn. (2) is absent. It may be noted that since the activity coefficients of the species O and R are not inserted above, the quantities calculated using eqn. (2) are thus formal only.

Since the formal standard potential, E_f° , is often known, or can be calculated from the polarogram itself¹⁴, eqn. (2) is easily applied to calculate $\varphi(\chi)$ and hence (χ) from the polarographic instantaneous current, i_t -electrode potential, E , data.

As given by RANDES⁴, K_f is next determined from (χ) using the equation

$$\chi = \sqrt{\frac{12t}{7}} K_f \left(1 + \sqrt{\frac{D_o}{D_R}} \exp[nf(E - E_f^\circ)] \right) \quad (3)$$

Then a plot of $\log K_f$ vs. E is drawn, from which K_s and α can be determined even when one of the participants of the reaction is not present in the solution.

The reversible potential, $E_{rev.}$, for such systems, which obviously cannot be calculated by the Nernst equation (because $C_R^\circ = 0$) can, however, be obtained experimentally as the value of the potential at the point of intersection of the polarographic wave with the residual current curve⁸, particular care being taken to eliminate electro-reducible or electro-oxidisable trace impurities from the solution (otherwise these would set up a mixed potential at the electrode). A finite value of $E_{rev.}$ in such a case, with $C_R^\circ = 0$, corresponds to a minute amount of R produced at the electrode surface by an initial double-layer exchange process according to $O + ne = R$.

The approximate method

Let us now consider the equation for the irreversible polarographic wave as proposed by STROMBERG⁵ which is admittedly approximate since its derivation assumes that the non-stationary current flow at a dropping mercury electrode is equivalent to a stationary current governed by a constant diffusion-layer thickness. The equation is

$$\frac{i}{Ai_o} = \left(1 - \frac{i}{i_a} \right) \exp[-\alpha nf\eta] - \left(1 + \frac{i}{|i_a|} \right) \exp[\overleftarrow{1} - \alpha nf\eta] \quad (4)$$

where i is the average value of the current during drop life corresponding to the electrode potential E ; i_o is the exchange current density for the reaction $O + ne = R$ at the reversible potential ($\eta = 0$); and A is the average area of the dropping mercury electrode. It should be noted that the currents i_a and $\overleftarrow{i_a}$ refer to the average values of the current during drop life.

For the case of a purely cathodic wave, since $C_R^\circ = 0$, $\overleftarrow{i_a} = 0$ and hence eqn. (4) is invalid if the rate of the backward reaction is significant, *i.e.*, in the case of partially irreversible polarographic waves.

Such a limitation of eqn. (4) can be avoided by modification according to the following method.

The general rate equation for a first order reaction⁹ excluding the double-layer effects of FRUMKIN is

$$\frac{i_t}{A i_o} = \frac{C_o(o, t)}{C_o^\circ} \exp(-\alpha n f \eta) - \frac{C_R(o, t)}{C_R^\circ} \exp[(1 - \alpha) n f \eta] \quad (5)$$

This can also be expressed as

$$\frac{i_t}{n F A K_S} = C_o(o, t) \exp[-\alpha n f (E - E_f^\circ)] - C_R(o, t) \exp[(1 - \alpha) n f (E - E_f^\circ)] \quad (6)$$

since the exchange current density is given by

$$i_o = n F K_S C_o^{\circ(1-\alpha)} C_R^{\circ\alpha}$$

In eqns. (5) and (6), i_t is the instantaneous current at time, t , of electrolysis; $C_o(o, t)$ and $C_R(o, t)$ are the concentrations of O and R , respectively, at the electrode surface at time, t , of electrolysis.

If the non-stationary current at the dropping mercury electrode be equated to the stationary current of eqn. (4), it follows from eqns. (4) and (5) that

$$C_o(o, t) = C_o^\circ \left(1 - \frac{i}{i_a} \right) \quad (7)$$

and

$$C_R(o, t) = C_R^\circ \left(1 + \frac{i}{|i_a|} \right) \quad (8)$$

Now

$$\frac{i}{|i_a|} = \frac{i}{i_a} \cdot \frac{i_a}{|i_a|} = \frac{i}{i_a} \sqrt{\frac{D_o}{D_R}} \cdot \frac{C_o^\circ}{C_R^\circ} \quad (9)$$

From eqns. (8) and (9)

$$C_R(o, t) = C_R^\circ + C_o^\circ \frac{i}{i_a} \sqrt{\frac{D_o}{D_R}} \quad (10)$$

Using this and eqn. (7) in eqn. (6), and writing i in place of i_t because of stationary conditions we get

$$\frac{i}{n F A K_S} = C_o^\circ \left(1 - \frac{i}{i_a} \right) \exp[-\alpha n f (E - E_f^\circ)] - \left(C_R^\circ + C_o^\circ \frac{i}{i_a} \sqrt{\frac{D_o}{D_R}} \right) \times \exp[(1 - \alpha) n f (E - E_f^\circ)] \quad (11)$$

This is an exact equation for a stationary regime of electrolysis (the solution is stirred, or the electrode rotated so that a steady convective transport of ions takes place) and an approximate one when applied to irreversible polarographic waves. The magnitude of the error involved in the latter application will be evaluated below with reference to experimental data,

In particular, for a purely cathodic polarographic wave, eqn. (11) yields, with $C_R^\circ = 0$,

$$\frac{i}{nFAK_s C_o^\circ} = \left(1 - \frac{i}{i_a}\right) \exp[-\alpha n f (E - E_f^\circ)] - \frac{i}{i_a} \sqrt{\frac{D_o}{D_R}} \exp[(1 - \alpha) n f (E - E_f^\circ)] \quad (12)$$

Thus eqn. (11) is amenable for calculation of K_s in the case of purely cathodic waves without neglecting the rate of the backward reaction, *i.e.*, even in the case of partially irreversible single waves. In order to calculate K_s and α from the experimental current-potential data using eqn. (12), it is expedient to write this equation as

$$\log_{10} \frac{i}{i_a B} = \log_{10} K_s + \left(\frac{1}{2} - \alpha\right) \frac{n f}{2.303} (E - E_f^\circ) \quad (13)$$

where

$$B = \sqrt{\frac{3\pi t}{7D_o}} \left[\left(1 - \frac{i}{i_a}\right) \exp\left\{\frac{-n f}{2} (E - E_f^\circ)\right\} - \sqrt{\frac{D_o}{D_R}} \cdot \frac{i}{i_a} \exp\left\{\frac{n f}{2} (E - E_f^\circ)\right\} \right]$$

where t is the drop time, and i and i_a correspond to the instantaneous values at the end of the drop life. It is assumed here that the ratio of the currents, i/i_a , is the same with either the average or the instantaneous values for both. For a totally irreversible reaction (for example, $\text{Ni}^{2+} - \text{Ni}$) the second term in the right-hand side of eqn. (12) is equal to zero and the resulting equation analogous to eqn. (13) is now

$$\log_{10} \frac{i}{i_a B'} = \log_{10} K_s - \frac{\alpha n f}{2.303} (E - E_f^\circ) \quad (13a)$$

where

$$B' = \sqrt{\frac{3\pi t}{7D_o}} \left(1 - \frac{i}{i_a}\right)$$

Starting with eqn. (6) and proceeding along similar lines, it is possible to arrive at an equation, analogous to eqn. (11), which is amenable for calculation of K_s in the case of partially irreversible purely anodic waves. The result for the oxidation reaction $R - n e = O$ is

$$\frac{i}{nFAK_s} = C_R^\circ \left(1 - \frac{i}{i_a}\right) \exp[\beta n f (E - E_f^\circ)] - \left(C_o^\circ + C_R^\circ \frac{i}{i_a} \sqrt{\frac{D_R}{D_o}}\right) \times \exp[-(1 - \beta) n f (E - E_f^\circ)] \quad (14)$$

where β , ($= 1 - \alpha$), is the energy transfer coefficient for the anodic reaction. Here, i and i_a refer to the net anodic reaction of oxidation of R .

It should be noted that the expressions (7) and (10) for $C_o(0, t)$ and $C_R(0, t)$ obtained from the Nernst diffusion-layer concept are identical with those obtained by a rigorous solution of the diffusion equation for a plane electrode with a reversible electrochemical reaction¹⁰, (modified for the case when $C_R^\circ \neq 0$). It is, therefore, to be expected that STROMBERG's eqn. (4) for the irreversible composite (anodic and cathodic) polarographic wave or the modified forms [eqns. (11) and (14)] applicable also

for single (purely cathodic or anodic) polarographic waves, give more accurately the kinetic parameters, the larger the value of K_s . In other words, the error involved in calculating the kinetic parameters by the approximate method should be less for a quasi-reversible (or partially irreversible) polarographic wave than for a totally irreversible polarographic wave.

EXPERIMENTAL

In order to test the validity of eqns. (2) and (11) and to compare the values of K_s and α calculated with the aid of these equations, two cathodic reactions at a dropping mercury electrode have been chosen:



The vanadic-vanadous reaction is known to be quasi-reversible when studied by d.c. polarography and therefore, the rate of the backward reaction is significant; on the other hand, the reaction Ni^{2+} -Ni is totally irreversible and therefore, the rate of the backward reaction is negligible in this case.

It is generally more accurate to measure the instantaneous currents at the end of the drop-life than average currents and hence, only such data are used below.

For the Ni^{2+} -Ni reaction, the polarographic maximum current-potential curve given by GIERST¹¹ ($10^{-3} M \text{Ni}^{2+}$ in $0.25 M \text{NaClO}_4$ solution) was interpolated to get the i/i_d data, reproduced below under the headings RESULTS and DISCUSSION.

Since accurate values of instantaneous current-potential data in the absence of surface active substances and with $[\text{V}^{2+}] = 0$ have not been obtained so far for the V^{3+} - V^{2+} reaction at the dropping mercury electrode, experiments were conducted in order to obtain the required data.

Pure ammonium vanadate was ignited at 550° to get vanadium pentoxide which was then dissolved in hot concentrated H_2SO_4 . On passing SO_2 gas through this solution, a blue solution of VOSO_4 was obtained. Excess of SO_2 was expelled by prolonged boiling. The solution was diluted with twice-distilled water to give $1.0 M \text{H}_2\text{SO}_4$ (titration against alkali using glass electrode). Before use, the solution was shaken with purified activated charcoal for a day and filtered through a sintered-glass funnel.

Mercury, purified by aeration under hot dilute HNO_3 , was distilled under vacuum. Twice-distilled water, the second distillation over alkaline permanganate in all-glass Pyrex assembly, was used throughout. H_2SO_4 was distilled under reduced pressure from A.R. grade H_2SO_4 . Activated charcoal was boiled with $1 M \text{H}_2\text{SO}_4$ and then repeatedly washed with twice-distilled water prior to use. For de-aerating the solutions, hydrogen from an all-glass electrolysis unit was used; it was passed over heated platinum-black (catalyst), then through alkaline plumbite solution and finally silica gel.

The polarographic cell was set up in an air thermostat the temperature of which was maintained at $25^\circ \pm 0.2^\circ$. The vanadyl sulphate solution in the cell was de-aerated by passing hydrogen for 2 h. The solution was then subjected to electrolytic reduction using a mercury pool cathode (which served also as the auxiliary electrode for polarizing the dropping mercury electrode) in the cell and a platinum strip anode

isolated from the solution in the cell by a sintered-glass plug. When all vanadyl sulphate was reduced to the vanadous stage (indicated by a faint violet colour of the solution), electrolysis was discontinued, but bubbling of hydrogen was continued. The polarographic cell contained a large platinum cylinder above the mercury pool, and surrounding the dropping mercury electrode. In about 4 h, because of the catalytic action of this large platinum surface, all the vanadous ion was found to be oxidized to the vanadic state (checked by limiting-diffusion current). The solution contained at this stage pure vanadic sulphate, $V_2(SO_4)_3$, at a concentration of 8.31×10^{-3} mole/l (as determined by the limiting-diffusion current later) in 1 *M* H_2SO_4 . The concentration of the vanadous ion was virtually zero.

Potential measurements were carried out with an accuracy of ± 0.5 mV using a Cambridge Vernier Potentiometer. The reference electrode used was a hydrogen electrode in 1 *M* H_2SO_4 (pressure of hydrogen, 1 atm) connected to the polarographic cell through a closed, ungreased, stopcock which terminated in a Luggin capillary close to the dropping mercury electrode; liquid-junction potentials were thus practically eliminated.

Instantaneous current measurements at the end of drop life were carried out by choosing a dropping mercury electrode with a period of 10–11 sec and a mirror galvanometer with a period of 4 sec and a sensitivity of 1.73×10^{-9} A/mm. Hence, when the galvanometer was slightly under-damped, the instantaneous currents at the fall of a drop of the dropping mercury electrode could be accurately measured without any significant lag. Since the half-wave potential for the $V^{3+}-V^{2+}$ system is close to the null-point of mercury, variations in the drop time with the electrode potential over the rising portion of the polarographic wave could not be large enough to vitiate the measurement of maximum currents at the end of the drop life. The total resistance of the polarising circuit was such that the non-uniformity of polarization of the dropping mercury electrode at any shunt-setting of the galvanometer was not more than 0.3 mV.

The capillary characteristics were:

$$\left. \begin{array}{l} h = 105 \text{ cm of mercury} \\ m = 0.41 \text{ mg/sec} \\ t = 10.9 \text{ sec} \end{array} \right\} \text{ in 1 } M \text{ } H_2SO_4 \text{ at the null-point of mercury.}$$

The current–potential measurements were made manually at 5–10 mV potential intervals.

RESULTS AND DISCUSSION

The polarographic maximum current–potential curve for the $V^{3+}-V^{2+}$ reaction is shown in Fig. 1. The reversible potential for the solution from Fig. 2 is -0.143 V vs. a hydrogen electrode in the same solution. The value of $E_{\frac{1}{2}}$ obtained (this could be reproduced to within 2 mV) is about 55 mV more negative than the value reported in the literature, possibly because in the present work, a hydrogen electrode in the same solution as that in the polarographic cell has been used as a reference electrode thus avoiding liquid-junction potentials. It was also found, subsequently, that when a saturated calomel electrode is used as the reference electrode, $E_{\frac{1}{2}}$ obtained was within 15 mV of the literature value.

The standard rate constant, K_s , and the transfer coefficient, α , were then determined using eqns. (2) and (11). The value given by Randles for E_f° of the $V^{3+}-V^{2+}$

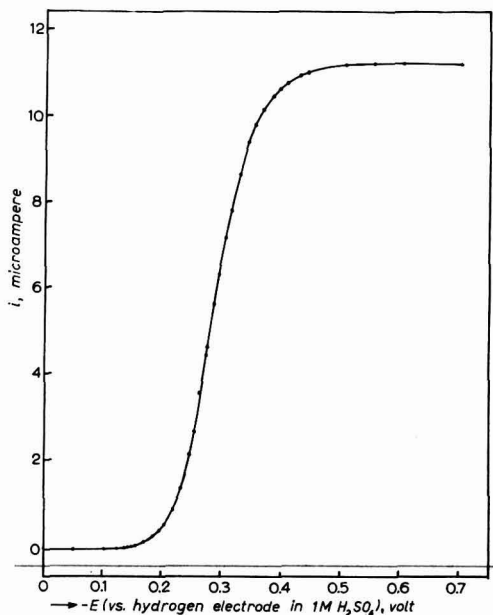


Fig. 1. Polarographic maximum current-potential curve for the reduction of V^{3+} ion in 1 M H_2SO_4 at 25° .

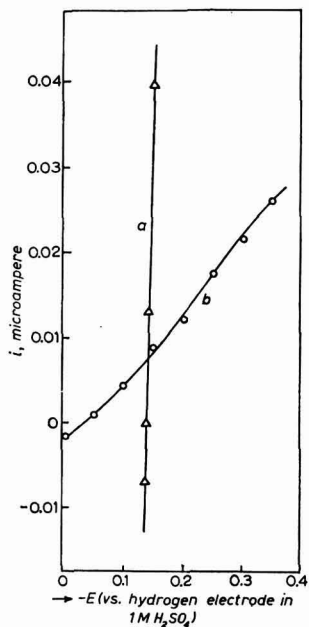


Fig. 2. Polarographic determination of the reversible potential for $V^{3+}-V^{2+}$ system. Polarographic current (a) and residual current (b) curves for the reduction of 8.31×10^{-3} mole/l V^{3+} ion in 1 M H_2SO_4 at 25° . ($-E$ in volt.)

reaction in strong acid supporting electrolyte (-0.30 V vs. N.H.E.) was used in order to facilitate comparison with the values of K_S and α obtained in the latter's work. D_O and D_R were calculated from the values of diffusion-current constants given by LINGANE AND MEITES¹². Thus,

$$D_{V^{3+}} = 5.4 \times 10^{-6} \text{ cm}^2\text{sec}^{-1}; \quad D_{V^{2+}} = 8.2 \times 10^{-6} \text{ cm}^2\text{sec}^{-1}.$$

The values of $\varphi(\chi)$ were obtained for various values of i/i_a ranging from 0.6 to 0.9 (for greater accuracy) using eqn. (2). The corresponding values of χ were then read out from the curve drawn with the help of Table 4-1 of DELAHAY⁷. The plot of $\log K_f$ [calculated from eqn. (3)] vs. $(E - E_f^\circ)$ is shown in Fig. 3, line a.

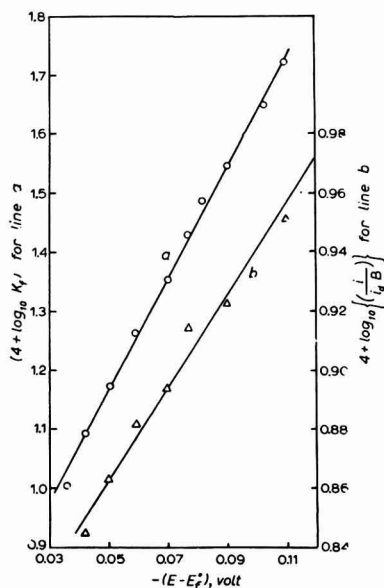


Fig. 3. Rate constant-potential plot for the polarographic reduction of V^{3+} in $1 M H_2SO_4$ at 25° : (a), according to eqn. (2); (b), according to eqn. (11).

The plot of $\log (i/i_a B)$ against $(E - E_f^\circ)$ obtained according to eqn. (11) is shown in Fig. 3, line b.

From Fig. 3, the kinetic parameters of the V^{3+} - V^{2+} reaction in $1 M H_2SO_4$ when the V^{2+} concentration in the solution is zero are found to have the following values:

Equation used	Logarithmic plot	$K_S(\text{cm/sec})$	α
2	Fig. 3, line a	0.51×10^{-3}	0.55
11	Fig. 3, line b	0.61×10^{-3}	0.59

For comparison, the values of the kinetic parameters obtained by RANDES from a composite polarogram (anodic and cathodic, temp. 15.3°) are

$$K_S = 1.03 \times 10^{-3} \text{ cm sec}^{-1}; \quad \alpha = 0.455.$$

For the reaction $\text{Ni}^{2+} + 2e \rightarrow \text{Ni}$ at a dropping mercury electrode, the polarographic curve for the instantaneous current at the end of the drop life—electrode potential, E , in 0.25 M NaClO_4 (data of GIERST¹¹) gave on interpolation the following values for i/i_a .

i/i_a	0.1	0.2	0.3	0.4	0.5	0.6
E , (V vs. N.H.E.)	-0.672	-0.708	-0.730	-0.746	-0.761	-0.777

Taking $E_f^\circ = -0.245$ V (vs. N.H.E.), the plots of $\log K_f$ against $(E - E_f^\circ)$, [Fig. 4, line a; eqns. (2) and (3)] and $\log (i/i_a B')$ against $(E - E_f^\circ)$ [Fig. 4, line b; eqn. (13a)] were then determined. The kinetic parameters were found to be as follows:

Equation used	Logarithm plot	$K_S(\text{cm/sec})$	αn
2	Fig. 4, line a	4.0×10^{-9}	0.62
11	Fig. 4, line b	2.4×10^{-9}	0.66

For comparison, the kinetic parameters for Ni^{2+} - $\text{Ni}(\text{Hg})$ from 1 M KCl solution at 30° as obtained by DELAHAY AND MATTAX¹³ are

$$K_S = 2.6 \times 10^{-10} \text{ cm sec}^{-1}; \quad \alpha n = 0.70$$

These values for K_S and α show that eqns. (2) and (11) can be applied to the irreversible polarographic wave of purely cathodic (or the corresponding equations for anodic) reactions to yield formal kinetic parameters. The approximate eqn. (11) gives K_S and

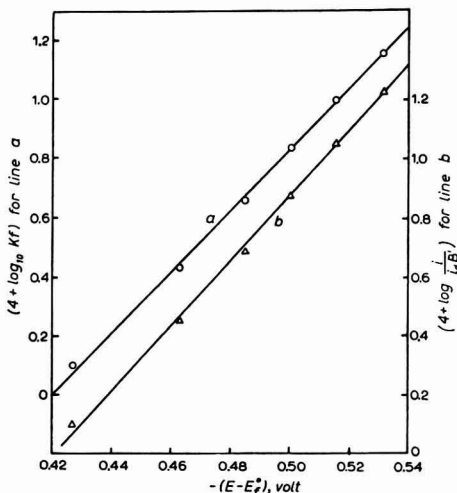


Fig. 4. Rate constant-potential plot for the polarographic reduction of Ni^{2+} in 0.25 M sodium perchlorate solution: (a), according to eqn. (2); (b), according to eqn. (11).

α in greater accord with those obtained by the rigorous eqn. (2) in the case of quasi-reversible (*i.e.*, V^{3+} - V^{2+} reaction) polarographic waves than when applied to totally irreversible (*i.e.*, Ni^{2+} - Ni reaction) polarographic waves. It has been shown under the heading THEORETICAL, that this should indeed be so.

The somewhat different values of K_S and α obtained in the present work for the $V^{3+}-V^{2+}$ reaction as compared with the values of K_S and α given in the literature may be due to the fact that in the present work the bulk concentration of the vanadous ion was zero which was not the case in the earlier work on the same reaction. Since the possibility of contamination of the solution by surfactant impurities in the work described here appears unlikely, it seems that there is perhaps a double-layer or adsorption effect connected with the presence of vanadous ion in solution, thereby influencing the apparent values of K_S and α ; however, further work is necessary to confirm this view.

CONCLUSIONS

The modified general rate eqns. (2) and (II) for irreversible polarographic waves can be applied to the calculation of kinetic parameters from experimental current-voltage curves. In particular, the more common practical case of single, *i.e.*, purely cathodic or anodic, polarographic waves can be analysed with the help of these modified equations. The approximate eqn. (II) which is simpler in form than the rigorous eqn. (2) gives more correct results for quasi-reversible (partially irreversible) polarographic waves than for totally irreversible waves. The kinetic parameters calculated for the $V^{3+}-V^{2+}$ and $Ni^{2+}-Ni$ reactions from instantaneous current-potential curves at a dropping mercury electrode confirm the above conclusions.

ACKNOWLEDGEMENT

The author is grateful to Prof. N. R. KAMATH for his encouragement and is also indebted to T. V. PADMA for assistance in the course of this work.

SUMMARY

Modified forms of general rate equations applicable for quasi-reversible (partially irreversible) polarographic single waves (purely cathodic or anodic) have been derived. These equations have been applied to calculate the formal kinetic parameters, using experimental data for $V^{3+}-V^{2+}$ reaction obtained by polarography. The application of the above equations to totally irreversible polarographic waves has also been shown using polarographic data for the $Ni^{2+}-Ni$ reaction.

REFERENCES

- 1 N. N. MEIMAN, *Zh. Fiz. Khim.*, 22 (1948) 1454.
- 2 P. DELAHAY, *J. Am. Chem. Soc.*, 75 (1953) 1430.
- 3 J. KOUTECKÝ, *Collection Czech. Chem. Commun.*, 18 (1953) 597.
- 4 J. E. B. RANGLES, *Can. J. Chem.*, 37 (1959) 238.
- 5 A. G. STROMBERG, *Zh. Fiz. Khim.*, 36 (1962) 2714.
- 6 A. N. FRUMKIN AND G. FLORIANOVICH, *Dokl. Akad. Nauk. SSSR*, 80 (1951) 907.
- 7 P. DELAHAY, *New Instrumental Methods in Electrochemistry*, Interscience Publishers Inc., New York, 1954, p. 79.
- 8 A. G. STROMBERG, *Proceedings, CITCE Meeting (1963) Moscow*, preprint.
- 9 T. BERZINS AND P. DELAHAY, *J. Am. Chem. Soc.*, 77 (1955) 6448.
- 10 P. DELAHAY, *New Instrumental Methods in Electrochemistry*, Interscience Publishers Inc., New York, 1954, p. 57.
- 11 L. GIERST, *Transactions of the Symposium on Electrode Processes*, edited by E. YEAGER, John Wiley and Sons, Inc., New York, 1961, p. 127.
- 12 J. J. LINGANE AND L. MEITES, *J. Am. Chem. Soc.*, 70 (1948) 2525.
- 13 P. DELAHAY AND C. C. MATTAX, *J. Am. Chem. Soc.*, 76 (1954) 874.
- 14 J. M. HALE AND R. PARSONS, *Collection Czech. Chem. Commun.*, 27 (1962) 2444.

REPORTGORDON RESEARCH CONFERENCE ON ELECTROCHEMISTRY,
SANTA BARBARA, CALIFORNIA

The first Gordon Research Conference on Electrochemistry, subtitled *Electrode Reactions*, was held in Santa Barbara, California during the week February 3rd–7th, 1964. In keeping with the spirit of the Gordon Research Conferences, an atmosphere of informality was established by the efforts of the Director, Dr. W. PARKS and the Conference Chairman, Professor R. ADAMS, and also by the cordiality of the participants, the extraordinarily beautiful seaside location and the clear, balmy weather.

The scope of the program was intentionally broad. It was apparent to the program planners that the study of electrode processes involves a variety of disciplines; but more important, electrode processes are the common threads between fundamental and applied fields which connect the various parts of electrochemistry *viz.*, electrode kinetics, electroanalysis, electrochemical synthesis, corrosion, electroplating, electropolishing, and fuel cell technology. The material presented was mostly new and perhaps incomplete, but it was always stimulating and provided plentiful material for discussion. Because of the variety of topics, part of the discussions was devoted to review and a clarification of electrode process studies.

Professor L. GIERST presented new results on specific salt effects on adsorption involving both a *psi*-effect and a salting-out effect. Professor P. DELAHAY reported on new work in progress, from which kinetic parameters may be deduced from overpotential change by systematic variation in electrode area through intermediate change in the state of double-layer charge. Professor W. REINMUTH described advanced coulometric relaxation techniques using multiple impulses.

Current research on the rates of homogeneous exchange reactions of transition-metal complexes was described by Professor H. TAUBE and Dr. N. SUTIN. A lively discussion involving Professor R. MARCUS brought out the relation between specific homogeneous rate constants and the corresponding standard electrochemical heterogeneous rate constants. A theoretical basis for variable transfer coefficients was suggested.

A study of the Volmer reduction of hydrogen and deuterium ions using a potentiostatic sweep with superimposed a.c. galvanostatic current was presented by Dr. M. BREITER. The course of the reduction of dissolved oxygen on carbon and nickel oxide electrodes as determined by isotopic measurements, product analysis, and rotating disk electrode limiting current measurements, was elaborated by Professor E. YEAGER. The design of rotating disk electrodes and comparison of actual limiting-current behavior with theory was discussed by Professor A. RIDDIFORD. This was followed by an experimental study of iodine adsorption on platinum by Professor S. BRUCKENSTEIN using the ring-disk technique. New results on the adsorption of iodide and iodine determined by integration of current–time curves after a potential step and radio tracer studies were given by Dr. R. OSTERYOUNG.

Experimental evidence for solvated electrons in aqueous and alcoholic solutions together with reaction identification and measurement of reaction rates of solvated electrons with solvent and various dissolved species was presented by Dr. L. DORFMAN. An invited paper by Dr. G. BARKER, read by Professor R. MARCUS, provided evidence for the production of solvated electrons during mercury arc irradiation of a negatively-polarized mercury pool.

Experimental anodic current-potential behavior of Ge, Si, InSb, and GaAs single crystals of various orientations was described by Professor H. GERISCHER. Interpretation of this behavior was extended to a general theory of transfer of charge between valence or conduction bands of electrodes and soluble redox couples. Extensive double-layer capacitance measurements on polarized germanium electrodes were described and interpreted by Dr. P. BODDY.

Professor D. SMITH presented new a.c. polarographic results on the phase angle between faradaic current and applied potential for various kinetic schemes involving alternation of homogeneous reaction and electron-transfer reaction steps. Professor A. BARD described a number of applications of controlled-potential coulometry for the determination of overall reaction schemes and the measurement of homogeneous rate constants of intervening steps which cause apparent deviation from stoichiometry. Informal presentations in the Gordon Research Conference tradition, were given by Drs. B. BRUMMER, J. BUTLER, and Professor P. VAN RYSSELBERGHE.

A second conference on Electrode Processes will be held in the winter of 1965 at the same location with Dr. R. BUCK as Chairman and Professor E. YEAGER as Co-Chairman.

*Bell Howell Research Center,
Pasadena, California (U.S.A.)*

RICHARD P. BUCK

Received February 21st, 1964

Book Review

Lead 62, published by the Lead Development Association, London, 1962, 253 pages, 45s.

This book, which is a collection of papers read at the First International Conference on Lead held in London in 1962, is divided into four sections: cable sheathing, batteries, radiation shielding and special contributions. The Conference was organized by the Lead Development Association and its sister associations in Europe. One of the declared objects of these associations is "to extend the knowledge of lead in its manifold uses" and, perhaps for this reason, the papers are of a practical rather than a fundamental nature.

The section on batteries, which consists of 6 papers, is no exception. In Chapters 10, 12, 13 and 14 (by M. BARAK, R. ZIEGFELD, G. GENNIN and E. VARADY) accounts are given of recent developments over the whole field of battery technology. Most of the developments described are improvements in choice of materials, design and methods of assembly. For example, Dr. BARAK demonstrates the increase in properties obtained by replacing the slotted ebonite tubes in tubular batteries with a woven terylene gauntlet and Mr. ZIEGFELD shows the advantages of a new design and production method for intercell connectors.

In Chapter 9, A. HARDY considers the competitive position of the lead-acid battery comparing it with other types of storage battery and fuel cells. Again, the emphasis is on the technical improvements which have enabled lead-acid batteries to retain their advantages over other batteries for most applications.

The only chapter devoted to a specific subject is that by C. REUTEL (Chapter 11), who considers the use of lead dust (or grey oxide, as it is known in the industry) in battery manufacture. Dr. REUTEL surveys the properties of grey oxide which can be measured and gives details of tests which can be carried out on grey oxide. He finds, however, that these properties bear little relation to the characteristics of paste in battery plates. His practical conclusions are that grey oxide quality and paste processing methods should be adapted to each other and that the properties of grey oxide should be kept as constant as possible.

Although the section on batteries contains excellent reviews of recent technical developments and an up-to-date practical picture of the battery industry, a more balanced view would have been given if at least one chapter had been devoted to the electrochemical research which is being carried out. Perhaps at future Conferences on Lead this omission will be corrected.

N. E. BAGSHAW, Chloride Technical Services, Ltd.

CONTENTS

Original papers

- Effects of working-electrode potential on the rates and extents of controlled-potential electrolyses
L. MEITES (Brooklyn, N.Y., U.S.A.) 337
- The adsorption of hydroxyl ions at the mercury-solution interface and the anodic double-layer capacity in fluoride solutions
R. PAYNE (Bristol, England) 343
- Polarography of hydrogen peroxide in lanthanum nitrate solutions
M. T. HENNE AND J. W. COLLAT (Columbus, Ohio, U.S.A.) 359
- Propriétés générales des méthodes chronopotentiométriques en régime de diffusion cylindrique et sphérique. Détermination du courant compensant les effets liés au caractère non linéaire du mode de diffusion
H. D. HURWITZ (Bruxelles, Belgique) 368
- Measurement of hydrogen adsorption by the multipulse potentiodynamic (MPP) method
S. GILMAN (Schenectady, N.Y., U.S.A.) 382
- Comparison of alternating voltage polarography with alternating current polarography
H. H. BAUER AND D. C. S. FOO (Sydney, Australia) 392
- An automatic amperometric method for the specific enzymatic determination of galactose
H. L. PARDUE AND C. S. FRINGS (Lafayette, Ind., U.S.A.) 398
- Kinetic parameters from irreversible polarographic waves in presence of mass transfer polarization
S. SATHYANARAYANA (Bombay, India) 403
- Report*
- Gordon Research Conference on Electrochemistry, Santa Barbara, California
R. P. BUCK (Pasadena, Calif., U.S.A.) 414
- Book Review* 416

All rights reserved

ELSEVIER PUBLISHING COMPANY, AMSTERDAM

Printed in The Netherlands by

NEDERLANDSE BOEKDRUK INRICHTING N.V., 'S-HERTOGENBOSCH

New Elsevier books for

SPECTROSCOPISTS

Infra-red Spectroscopy and Molecular Structure

An outline of the principles

edited by Mansel Davies

x + 468 pages, 70 tables, 171 illus., 800 refs., 1963, 75s.

Physical Aids to the Organic Chemist

by M. St. C. Flett

xii + 388 pages, 38 tables, 109 illus., 430 refs., 1962, 45s.

Characteristic Frequencies of Chemical Groups in the Infra-red

by M. St. C. Flett

viii + 94 pages, 15 tables, 181 refs., 1963, 25s.

Line Interference in Emission Spectrographic Analysis

A general emission spectrographic method, including sensitivities of analytical lines and interfering lines

by J. Kroonen and D. Vader

viii + 213 pages, 1963, 60s.

as a companion volume to Beynon's very successful

MASS SPECTROMETRY AND ITS APPLICATIONS TO ORGANIC CHEMISTRY

we have published

Mass and Abundance Tables for Use in Mass Spectrometry

by J. H. Beynon and A. E. Williams

with an introduction in English, German, French and Russian

xxii + 570 pages, 1963, 80s.



ELSEVIER PUBLISHING COMPANY
AMSTERDAM LONDON NEW YORK